NUREG/CR-XXXX
SAND2002-0447P

Cable Insulation Resistance Measurements Made During Cable Fire Tests

Manuscript Completed: April 2002
Date Published:

Prepared by

Francis J. Wyant, Steven P. Nowlen

Sandia National Laboratories
Albuquerque, NM 87185 USA

Prepared for
Probabilistic Risk Assessment Branch
Office of Nuclear Regulatory Research
U.S. Nuclear Regulatory Commission
Washington, DC 20555

NRC Job Code Y6037
NRC Project Manager: H. W. Woods

Page intentionally left blank.

Abstract

An insulation resistance diagnostic system was recently developed and exercised during a series of cable fire tests sponsored by the commercial U.S. nuclear industry. This insulation resistance measurement system was able to identify and quantify the changes in insulation resistance occurring between the separate conductors and the conductors to ground in cable bundles as they were being exposed to fires. Eighteen separate fire tests were conducted during the period January through May 2001 and included a variety of cable and fire exposure conditions. The insulation resistance measurement system was operated at a 120 VAC input to the conductors for 14 of those test runs and at 100 VDC input for three of the runs. One test was run with the insulation resistance measurement system providing 24 VDC to two separate instrument cables being exposed to the fire. The results obtained by the insulation resistance measurement system during these tests showed that cables will fail during a fire in one of three ways: by internal shorting of the conductors in a multiconductor cable, by shorting of the conductors in different cables bundled together, or by individual conductors shorting to ground. No incidents of fire-induced open circuits were found to have occurred during any of these tests. A mockup of a simple 4 to 20 mA DC current loop instrument circuit was included in six of the later tests. The intent was to investigate the potential of misleading or loss of instrument indication from fire damage to the signal cable. This report provides an analysis of the insulation resistance data and current loop results for the 18 tests run in the industry test program.

Page intentionally left blank.

Contents

ABSTRACT iii

ACKNOWLEDGMENTS ix

ACRONYMS AND INITIALISMS x

1. INTRODUCTION 1
   1.1 Background 1
   1.2 Report Structure 2

2. INSULATION RESISTANCE MEASUREMENT TECHNIQUES 3
   2.1 Overview 3
   2.2 Insulation Resistance Measurement Techniques 3

3. THE SANDIA NATIONAL LABORATORIES INSULATION RESISTANCE MEASUREMENT SYSTEM 9
   3.1 Concept 9
   3.2 Design 12
      3.2.1 Power Input Panel 13
      3.2.2 Switching Relay Panels 13
      3.2.3 Voltmeters 13
      3.2.4 Relay Controller 13
      3.2.5 Computer 14
      3.2.6 Interface Patch Panel 14
      3.2.7 Wiring Harness 14
      3.2.8 Insulation Resistance Cable Bundle 14
   3.3 An Unplanned System Anomaly 14
   3.4 Operation 17

4. CABLE FIRE TESTS 20
   4.1 Description 20
   4.2 Test Matrix 23
   4.3 IR Measurement Interfaces 28

5. INSULATION RESISTANCE MEASUREMENT RESULTS 30
   5.1 Tests 1 through 3 30
      5.1.1 Test 1 30
      5.1.2 Test 2 33
      5.1.3 Test 3 36
   5.2 Tests 4 through 8 39
      5.2.1 Test 4 39
      5.2.2 Test 5 42
      5.2.3 Test 6 46
      5.2.4 Test 7 49
      5.2.5 Test 8 51
   5.3 Tests 9 through 12 57
      5.3.1 Test 9 57
      5.3.2 Test 10 59
      5.3.3 Test 11 61
      5.3.4 Test 12 63
   5.4 Tests 13 through 18 66

5.4.1 Test 13 67
5.4.2 Test 14 69
5.4.3 Test 15 70
5.4.4 Test 16 73
5.4.5 Test 17 75
5.4.6 Test 18 78

6. CURRENT LOOP DATA AND RESULTS 81
6.1 Test Data and Results 81
6.1.1 Test 13 81
6.1.2 Test 14 82
6.1.3 Test 15 82
6.1.4 Test 16 84
6.1.5 Test 17 84
6.1.6 Test 18 85
6.2 Observations 85

7. CONCLUSIONS 87
7.1 Insulation Resistance-Based Cable Failure Mode Results 87
7.2 Insulation Resistance Measurement Results Compared to SNL Influence Factors 89
7.2.1 Cable Physical Properties and Configuration Factors 90
7.2.2 Routing Factors 92
7.2.3 Fire Exposure Condition Factors 93

8. REFERENCES 94

List of Figures

Figure 2-1. A simple cable functionality monitoring circuit using a single voltage potential applied to a single conductor cable. 4
Figure 2-2. Electrical schematic of a single voltage potential monitoring system applied to a multiconductor cable. 6
Figure 2-3. A single voltage source system applied to a multiconductor cable without a switching system.. 7
Figure 2-4. An example of a cable monitoring circuit using two energizing voltage potentials. 8
Figure 3-1. Simple IR measuring circuit. 9
Figure 3-2. Circuit for measuring IR between any conductor pair in a cable. 10
Figure 3-3. Resistive leakage paths for each conductor with a ground present. 11
Figure 3-4. IR measuring circuit with ground paths. 11
Figure 3-5. Complementary IR measuring circuit with respect to the circuit shown in Figure 3-4. 11
Figure 3-6. IR measurement system block diagram of functional areas. 12
Figure 3-7. Schematic diagram of the IR measurement system. 13
Figure 3-8. Cross-sectional views of the various cable bundle configurations tested using the IR measurement system. 15
Figure 3-9. Front view of the IR measurement system instrument rack. 16
Figure 3-10. Rear view of the IR measurement system instrument rack. 16
Figure 3-11. IR measurement system "in" wiring harness connection to the test cable bundle. 18
Figure 3-12. IR measurement system control program flow chart. 18
Figure 3-13. Example of data file format. 19
Figure 4-1. Fire test cell. 20
Figure 4-2. Diffusion burner—30 cm × 30 cm (12 in. × 12 in.). 20
Figure 4-3. Cable arrangement near corner of tray. 21
Figure 4-4. Tray, with cables, installed in fire test cell. 21
Figure 4-5. Overhead view of tray and burner arrangement inside test cell. 22
Figure 4-6. Vertical tray and cables installed in test cell. 22
Figure 4-7. Water sprinkler head inside fire test cell. 23
Figure 4-8. Cable arrangements in tray for the various tests. 29
Figure 5-1. Representative tray and TC-4 cable temperatures recorded during Test 1. 31
Figure 5-2. Representative conductor-to-conductor IRs obtained during Test 1. 32
Figure 5-3. Conductor-to-ground IRs obtained during Test 1. 32
Figure 5-4. Leakage currents resulting from IR changes in Conductors 1 and 2 during Test 1. 33
Figure 5-5. Representative tray and TC-4 cable temperatures recorded during Test 2. 34
Figure 5-6. Representative conductor-to-conductor IRs obtained during Test 2. 34
Figure 5-7. Conductor-to-ground IRs obtained during Test 2. 35
Figure 5-8. Leakage currents resulting from IR changes in Conductors 1 and 2 during Test 2. 35
Figure 5-9. Representative tray and TC-4 cable temperatures recorded during Test 3. 37
Figure 5-10. Representative conductor-to-conductor IRs obtained during Test 3. 37
Figure 5-11. Conductor-to-ground IRs obtained during Test 3. 38
Figure 5-12. Leakage currents resulting from IR changes in Conductors 1 and 6 during Test 3. 38
Figure 5-13. Representative tray and TC-4 cable temperatures recorded during Test 4. 40
Figure 5-14. Representative conductor-to-conductor IRs obtained during Test 4. 41
Figure 5-15. Conductor-to-ground IRs obtained during Test 4. 41
Figure 5-16. Leakage currents resulting from IR changes between Conductors 5 and 10 during Test 4. 43
Figure 5-17. Representative tray and TC-4 cable temperatures recorded during Test 5. 43
Figure 5-18. Representative conductor-to-conductor IRs obtained during Test 5. 44
Figure 5-19. Conductor-to-ground IRs obtained during Test 5. 45
Figure 5-20. Leakage currents resulting from IR changes between Conductors 1 and 2 during Test 5. 45
Figure 5-21. Representative tray and TC-3 cable temperatures recorded during Test 6. 46
Figure 5-22. Representative conductor-to-conductor IRs obtained during Test 6. 47
Figure 5-23. Conductor-to-ground IRs obtained during Test 6. 48

Figure 5-24. Leakage currents resulting from IR changes between Conductors 4 and 9 during Test 6. 48
Figure 5-25. Representative tray and TC-4 cable temperatures recorded during Test 7. 49
Figure 5-26. Representative conductor-to-conductor IRs obtained during Test 7. 50
Figure 5-27. Conductor-to-ground IRs obtained during Test 7. 51
Figure 5-28. Leakage currents resulting from IR changes between Conductors 4 and 5 during Test 7. 52
Figure 5-29. Overhead sketch of the tray and conduit locations in the fire test cell during Test 8. 52
Figure 5-30. Representative temperatures for the tray, conduit, TC-1, and TC-4 cables recorded during Test 8. 53
Figure 5-31. Representative conductor-to-conductor IRs for cable IR1 in the cable tray during Test 8. 54
Figure 5-32. Representative conductor-to-conductor IRs for cable IR2 in the conduit during Test 8. 54
Figure 5-33. Conductor-to-ground IRs obtained during Test 8. 55
Figure 5-34. Leakage currents resulting from IR changes between Conductors 1 and 2 in the cable tray cable during Test 8. 56
Figure 5-35. Leakage currents resulting from IR changes between Conductors 7 and 8 in the conduit cable during Test 8. 56
Figure 5-36. Representative tray and TC-4 cable temperatures recorded during Test 9. 57
Figure 5-37. Representative conductor-to-conductor IRs obtained during Test 9. 58
Figure 5-38. Leakage current resulting from IR changes between Conductors 1 and 2 during Test 9. 59
Figure 5-39. Representative tray and TC-4 cable temperatures recorded during Test 10. 60
Figure 5-40. Representative conductor-to-conductor IRs obtained during Test 10. 60
Figure 5-41. Leakage current resulting from IR changes between Conductors 1 and 2 during Test 10. 61
Figure 5-42. Representative tray and cable (TC-1 and TC-4) temperatures recorded during Test 11. 62
Figure 5-43. IR between Conductor 1 and 2 obtained during Test 11. 62
Figure 5-44. IRs between Conductor 3 and Conductors 4 through 8 obtained during Test 11. 63
Figure 5-45. Leakage currents resulting from IR changes between Conductors 1 and 2 and between Conductors 3 and 4 during Test 11. 64
Figure 5-46. Representative tray and TC-3 cable temperatures recorded during Test 12 65
Figure 5-47. Representative conductor-to-conductor IRs obtained during Test 12. 65
Figure 5-48. Conductor-to-ground IRs obtained during Test 12. 66
Figure 5-49. Leakage currents resulting from IR changes between Conductors 1 and 2 during Test 12. 67
Figure 5-50. Representative tray and TC-4 cable temperatures recorded during Test 13. 68
Figure 5-51. Total IR of each conductor recorded during Test 13. 68
Figure 5-52. Total leakage currents resulting from IR changes for each conductor during Test 13. 69
Figure 5-53. Representative conductor-to-conductor IRs obtained during Test 14. 70
Figure 5-54. Conductor-to-ground IRs obtained during Test 14. 71
Figure 5-55. Leakage currents resulting from IR changes in Conductors 1 and 2 during Test 14. 71
Figure 5-56. Representative tray and TC-3 cable temperatures recorded during Test 15. 72
Figure 5-57. Total IR of each conductor recorded during Test 15. 72
Figure 5-58. Total leakage currents resulting from IR changes for each Conductor during Test 15. 74
Figure 5-59. Representative tray and TC-4 cable temperatures recorded during Test 16. 74
Figure 5-60. Total IR of each conductor recorded during Test 16. 75
Figure 5-61. Total leakage currents resulting from IR changes for each conductor during Test 16. 76
Figure 5-62. Representative tray and TC-4 cable temperatures recorded during Test 17. 76
Figure 5-63. Total IR of each conductor recorded during Test 17. 77
Figure 5-64. Total leakage currents resulting from IR changes for each conductor during Test 17. 77
Figure 5-65. Representative conductor-to-conductor IRs obtained during Test 18. 79
Figure 5-66. Conductor-to-ground IRs obtained during Test 18. 79
Figure 5-67. Leakage currents resulting from IR changes in Conductors 1 and 2 during Test 18. 80
Figure 6-1. Instrument loop circuit. 81
Figure 6-2. Current loop data obtained during Test 13. 82
Figure 6-3. Current loop data obtained during Test 14. 83
Figure 6-4. Current loop data obtained during Test 15. 83
Figure 6-5. Current loop data obtained during Test 16. 84
Figure 6-6. Current loop data obtained during Test 17. 85
Figure 6-7. Current loop data obtained during Test 18. 86

List of Tables

Table 5-1. Approximate Conductor Failure Times and Modes in Test 3 39
Table 5-2. Summary of Cable Failure Times and Modes during Test 4 42
Table 5-3. Summary of Cable Failure Times and Modes during Test 6 47
Table 5-4. Summary of Cable Failure Times and Modes during Test 7 51
Table 5-5. Summary of Cable Failure Times and Modes during Test 9 58
Table 5-6. Summary of Cable Failure Times and Modes during Test 12 66
Table 5-7. Summary of Cable Behavior during Test 15 73
Table 5-8. Summary of Cable Behavior during Test 16 73
Table 5-9. Summary of Cable Behavior during Test 17 78
Table 5-10. Summary of Cable Failure Times and Modes during Test 18 78
Table 6-1. Current Loop Test Data 86
Table 7-1. Summary of Observed Initial Failure Modes for Conductors in the Multiconductor Cables and the Single-Conductor Cables.. 88
Table 7-2. Composition of Cables Tested Using the IR Measurement System 91

Acknowledgments

The authors wish to thank the following people for their contributions to this work: Nathan O. Siu of the U.S. Nuclear Regulatory Commission for his support and approval to construct the prototype insulation resistance (IR) measurement system and use it in the cable fire tests with industry; H.W. 'Roy' Woods of the U.S. Nuclear Regulatory Commission for his direct help with the conduct and completion of the testing program; Spencer M. 'Mike' Luker of Sandia National Laboratories for developing, writing, and troubleshooting the control software and suggesting improvements to the IR system design; and D. Michael Ramirez of Sandia National Laboratories for his technical support in procuring and assembling the IR system hardware. The authors also thank Fred Emerson of the Nuclear Energy Institute and Robert 'Bob' Kassawara of EPRI for allowing Sandia to participate in the industry-initiated testing program. We also thank Omega Point Laboratories for allowing Sandia to bring our equipment into their facilities and to participate in the testing program.

Acronyms and Initialisms

DOE	U.S. Department of Energy
EP	ethylene propylene
EPR	ethylene propylene rubber
EPRI	Electric Power Research Institute
GPIB	general-purpose interface bus
HRR	heat release rate
IR	insulation resistance
MOV	motor-operated valve
NEI	Nuclear Energy Institute
NIST	National Institute of Standards and Technology
NRC	U.S. Nuclear Regulatory Commission
PE	polyethylene
PVC	polyvinyl chloride
RES	Nuclear Regulatory Research
SNL	Sandia National Laboratories
TC	thermocouple
U.S.	United States
XLPE	cross-linked polyethylene

Page intentionally left blank.

1. INTRODUCTION

1.1 Background

Sandia National Laboratories (SNL) has been working under contract to the United States (U.S.) Nuclear Regulatory Commission (NRC) Office of Nuclear Regulatory Research (RES) to help develop improved fire risk analysis methods, data, and tools. One particular task activity is providing improved circuit analysis tools, techniques, and data. The results of an initial investigation into cable failure modes and circuit fault effects have been documented in a SNL Letter Report (Ref. 1) (hereafter referred to as the SNL Letter Report).

As a part of this preliminary study, SNL reviewed the then-existing cable fire tests in an attempt to identify data that would support an assessment of the relative likelihood that a particular cable failure mode might be observed given the fire-induced failure of a cable. The failure modes of interest included open circuits, shorts to ground, and conductor-to-conductor hot shorts involving either intracable (conductors within a single multiconductor cable) or intercable (conductors of different cables) interactions. While some substantive data of relevance was identified, a definitive answer to the question of relative likelihood, however, was not obtained.

The commercial nuclear power industry (as represented by the Nuclear Energy Institute (NEI) and the Electric Power Research Institute (EPRI), and hereafter referred to as "industry") is also developing methods to address the regulatory issues related to circuit analysis and, in particular, the question of fire-induced spurious equipment actuation. As a part of their efforts, industry proposed to conduct a series of cable fire tests designed to address specific aspects of the cable failure–circuit fault issues of concern to the NRC. In particular, the industry proposed a series of tests to assess the potential for spurious actuation in a surrogate motor-operated valve (MOV) circuit.

Industry developed a test plan[1] based in part on proposals and recommendations contained in the SNL Letter Report. In particular, SNL had recommended a "base case - modifier" approach for quantifying the likelihood of spurious actuation or other circuit faults given cable failure. The industry test plan focused on two base cases (cable in a tray and cable in conduit) and a subset of the factors identified by SNL that would likely have a substantial impact on the cable failure modes and resulting circuit fault behavior. The NRC (and SNL) was invited to observe and participate in the industry tests.

NRC/RES participation in the test program was pursued and, as a result, SNL fielded supplemental cable performance monitoring equipment during the industry tests. The SNL equipment was designed to monitor cable degradation through the measurement of insulation resistance (IR). The SNL approach was designed to both augment and complement the information gathered by industry through their surrogate MOV circuit implementation.

The NRC/SNL-fielded equipment monitors the condition of each conductor's insulation integrity (as indicated by IR) in real-time (see Section 3 for a complete description of the system). The system is capable of determining the conductor-to-conductor IR for individual conductor pairs in all possible pair combinations, as well as the total conductor-to-ground IR for each conductor independently.

The system works by energizing each conductor sequentially. While a particular conductor is energized, the system sequentially measures and records the amount of leakage current being shunted through each of the other (non-energized) conductors. The combined data are used to determine the level of IR between any two conductors, as well as the amount of electrical isolation existing between each conductor and electrical ground. The system is equally effective in assessing conductor-to-conductor breakdown versus conductor-to-ground breakdown both within one multiconductor cable (an intracable breakdown) and between two separate cables (an intercable breakdown).

In addition to the IR tests, a separate surrogate instrument circuit was fielded by NRC/SNL in six of the burn tests. This circuit simulated a 4 to 20 mA instrument circuit current loop. To simulate an instrument signal, a constant current source set to 15 mA was used. The instrument wire transmitting the signal was exposed to the fire environ-

[1] A series of NEI generated test plans was distributed to participants in the test program for review and comment.

ments, and the output signal was monitored for degradation of the transmitted signal. The tested instrument cables were generally two-conductor shielded pairs and included both thermoplastic and thermoset types.

The industry cable tests took place at Omega Point Laboratories, located in Elmendorf, Texas, during the weeks of January 8 through 12, January 22 through 25, and April 2 through 6; the final two tests were conducted on May 31 and June 1, 2001. This report discusses the cable fire test conditions and the results obtained using the SNL IR measurement system during the tests. The results obtained from the instrument loop circuit are also discussed.

1.2 Report Structure

Section 2 of this report discusses IR measurement techniques that were employed in past cable tests. This discussion is intended to provide a background against which the system fielded during these tests can be compared. A description of the SNL IR measurement system is provided in Section 3. The conditions of each test conducted during the industry cable fire tests are summarized in Section 4. A more complete description of the test conditions, including measured temperatures, will be available from an anticipated industry test report; hence, this report covers the test conditions in limited detail. Section 5 presents the results from the IR measurements made by NRC/SNL. Section 6 describes the instrumentation current loop circuit in detail, and presents the results obtained from this circuit during the tests in which it was employed. Section 7 discusses the conclusions drawn from the test results and offers some assessments regarding the importance of the influence factors, identified in the SNL Letter Report, on the likelihood of a particular cable failure mode occurring. References are provided in Section 8.

2. INSULATION RESISTANCE MEASUREMENT TECHNIQUES

2.1 Overview

This section provides background information regarding the measurement of cable performance during exposure to adverse environmental conditions. In particular, the section focuses on past practices regarding the measurement of cable IR during harsh environment exposure testing. Much of the material presented here is based on the information provided in Reference 2.

The typical methods of assessing cable performance in a test environment involve measuring the cable conductor's IR. Such techniques have been widely employed in equipment qualification testing and, to a lesser extent, in fire testing. The approach typically involves energizing a conductor and monitoring that conductor for current leakage. This provides a direct measurement of cable electrical performance during the test. An intact or undegraded cable will have virtually no leakage current. As the cable degrades, the leakage current increases, reflecting a loss in the IR value of the insulation material designed to electrically isolate each conductor.

This approach has the advantage of being a direct measurement of performance, rather than an inferred assessment of performance based on secondary measurements (e.g., estimating IR changes by extrapolating published data to the measured cable temperature response). Furthermore, the methods of measurement can be relatively simple in nature, are not particularly difficult to implement in practice, and the results are easily interpreted.

The only disadvantages of the direct measurement approach are that these measurements require the subject cables to be energized during the test, and the energizing voltage must be nontrivial (generally at least 50 V and preferably somewhat higher). Typical concerns center on the potential personnel safety implications of having energized cables in a fire test, on the potential to introduce "noise" into other data streams (such as thermocouples), and on the potential impact that short circuits involving the energized cables might have on other data gathering systems. In general, these issues can be addressed. Indeed, over the past 25 years, many equipment qualification tests and fire tests have been performed that included energized cables and that monitored for cable electrical failures without compromising either personnel safety or other data streams.

2.2 Insulation Resistance Measurement Techniques

As noted above, the techniques associated with direct measurement of cable functionality typically focus on the cable conductor's IR. This value reflects the electrical resistance of the insulation layer surrounding each conductor and is a direct reflection of the cable's electrical condition and integrity. As the IR degrades, a cable begins to "leak" current. As the leakage current increases, the cable is ultimately unable to perform its design function—ensuring the electrical integrity of the associated circuit. The actual point at which the design function is no longer considered to be fulfilled will depend on the specific circuit of interest. For example, the criteria for functional failure of a 4 kV power circuit may be quite different from the criteria associated with failure of a 4 to 20 mA instrument circuit. One significant advantage of the IR approach is that the results are not circuit-specific. Rather, they are directly representative of the cable performance and can therefore be applied to various circuit types and designs using appropriate failure criteria.

This section provides a general discussion of the measurement methods that were employed in past harsh environment cable electrical performance tests. The reader should recognize, however, that there are no standardized or generally accepted methods of practice in this area. Hence, the discussions presented in this section can be viewed as both historical and speculative in nature. They are intended to provide the reader with some background knowledge of the techniques that have been or may be employed in cable tests based on past testing techniques used in both fire testing and other fields (such as equipment qualification testing). The test objectives from such programs are similar and highlight the associated technical issues that impacted the NRC/RES objectives in the industry fire tests described in this report: to monitor the electrical integrity of the exposed cables, to discern the failure modes observed when the cable insulation failed, and to assess the potential for spurious actuation in a surrogate MOV circuit.

One commonly used means of assessing cable performance in past fire testing efforts is monitoring for gross failure (short-circuiting) of the exposed cable. Detection of gross failure can be accomplished using very simple instrumentation circuitry, and yields correspondingly little or no information on cable degradation behavior, short of gross failure. The cable energizing circuits are typically quite similar to those implemented for an IR measurement; the primary difference lies in the monitoring circuits. An IR measurement requires quantification of the leakage currents versus time. Gross failure monitoring can be based on detecting when leakage currents exceed a preset value. For example, detection of failure is often based on tripping a protective fuse in the cable energizing circuit or illumination of a light in the circuit. Under this approach, what constitutes gross failure is defined based on the energizing circuit and the failure indication means employed. That is, the fuse trip value or the minimum current flow required to illuminate the light inherently defines the failure thresholds reported.

The discussions that follow illustrate both the gross failure and IR techniques, but generally focus on the more informative IR approach. Points relevant to gross failure detection are cited as appropriate and typically involve simplifications of an illustrated IR measurement approach.

The IR value is obtained by applying Ohm's law – the relationship between voltage, current, and resistance (i.e., $V = IR$). To illustrate this approach in its simplest form, consider a single conductor cable, such as that shown in Figure 2-1. The conductor of the subject cable is energized to a pre-determined voltage level (V_{Source}, either DC or AC) and cable integrity is assessed by monitoring the leakage current as a function of time. Often a ballast resistor ($R_{Ballast}$) is placed in the energizing circuit to serve two purposes. First, the resistor can be sized to limit the short-circuit fault currents, which protects the energizing and monitoring circuits and limits the potential electrical hazards. Second, the ballast resistor acts as a current-to-voltage transducer, allowing current to be monitored based on the voltage drop across the resistor. The latter is desirable because voltage is more easily monitored than current. In general, the ballast resistor should have a small resistance in comparison to the anticipated failure resistance, and use of resistors on the order of 10 to 100 Ω is common.

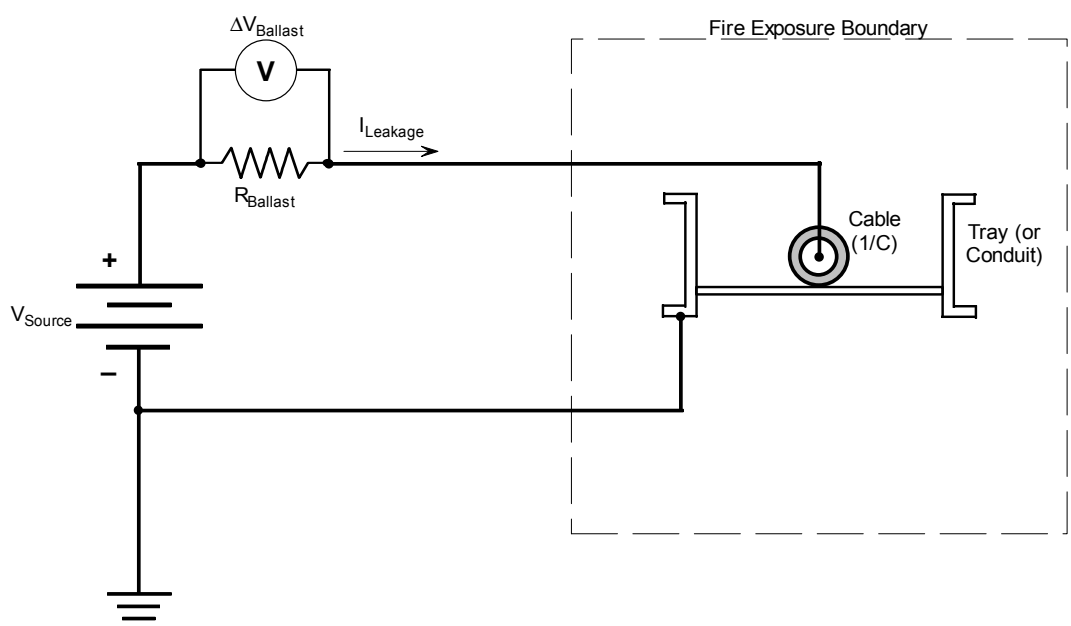

Figure 2-1. A simple cable functionality monitoring circuit using a single voltage potential applied to a single conductor cable. The circuit is capable of estimating the cable IR based on the measured voltage drop across the ballast resistor.

Ohm's law for the ballast resistor yields the leakage current ($I_{Leakage}$) based on the measured voltage drop ($\Delta V_{Ballast}$) and resistance ($R_{Ballast}$) as follows:

$$I_{Leakage} = \frac{\Delta V_{Ballast}}{R_{Ballast}}$$

Using Ohm's law a second time, based on the cable's voltage potential (V_{Source}-$\Delta V_{Ballast}$) and the determined leakage current, the IR ($IR_{Exposed}$) between a conductor and ground ($V_{Reference}$) can be calculated:

$$IR_{Exposed} = \frac{\left(V_{Source} - \Delta V_{Ballast}\right) - V_{\text{Reference}}}{I_{Leakage}}$$

where the $V_{Reference}$ for the case illustrated in Figure 2-1 would be zero. That is, in this simple case, the reference voltage is the local ground.

As shown by this example, with sufficient forethought, a single voltage potential versus ground is sufficient to monitor the performance of a cable during testing. As illustrated, this approach has the distinct advantage of introducing only one current path; namely, the path between the high potential side of the power source and the low potential side (typically ground if a grounded source is used). This makes it a trivial matter to estimate the IR of the energized conductor.

It should be noted that the same approach could also be modified to work as a threshold detection or gross failure detection scheme as well. For example, a fuse can replace the ballast resistor and voltage monitor. Cable insulation breakdown would still lead to leakage currents through the circuit, and the fuse would open when the current reached the rating of the fuse. Failure is thereby defined based on the fuse's amperage rating. Using Ohm's law, the equivalent IR failure threshold can easily be determined using the previous equation and setting ($\Delta V_{Ballast} = 0$). This approach is simpler to implement because it eliminates the need to actually monitor the leakage current over time – one need only monitor the integrity of the fuse and record the time of failure. However, the information gained is much more limited, as no time history of the cable performance is obtained and the failure criteria cannot be generalized.

In many cases, it may be desirable to test multiple cables or a multiconductor cable, rather than one single-conductor cable. This objective complicates the process of detecting cable failures, because conductor-to-conductor failures, in addition to conductor-to-ground failures, are of interest. A single voltage potential can also monitor multiple cables or conductors, but care must be exercised to ensure that all potential cable failure modes are detected (see below). For example, if one conductor were arbitrarily chosen to be continuously energized while the others are permanently grounded, faults between the grounded conductors or between a grounded conductor and the raceway would not be detected. If all of the conductors are continuously energized using the same voltage potential, conductor-to-conductor failures cannot be detected.

One approach to resolving this problem is to use a switching system that can sequentially energize individual conductors while grounding all others. This technique is illustrated in Figure 2-2 and allows one to monitor the performance of each individual conductor over time. However, while the system will detect a failure due to either a conductor-to-conductor or conductor-to-ground short, the results are nonspecific. That is, if a failure occurs, one will only know that a given conductor has shorted. One will not know whether the short was directly to ground or to one of the other conductors, because all of the nonenergized conductors are grounded at the time of the measurement.

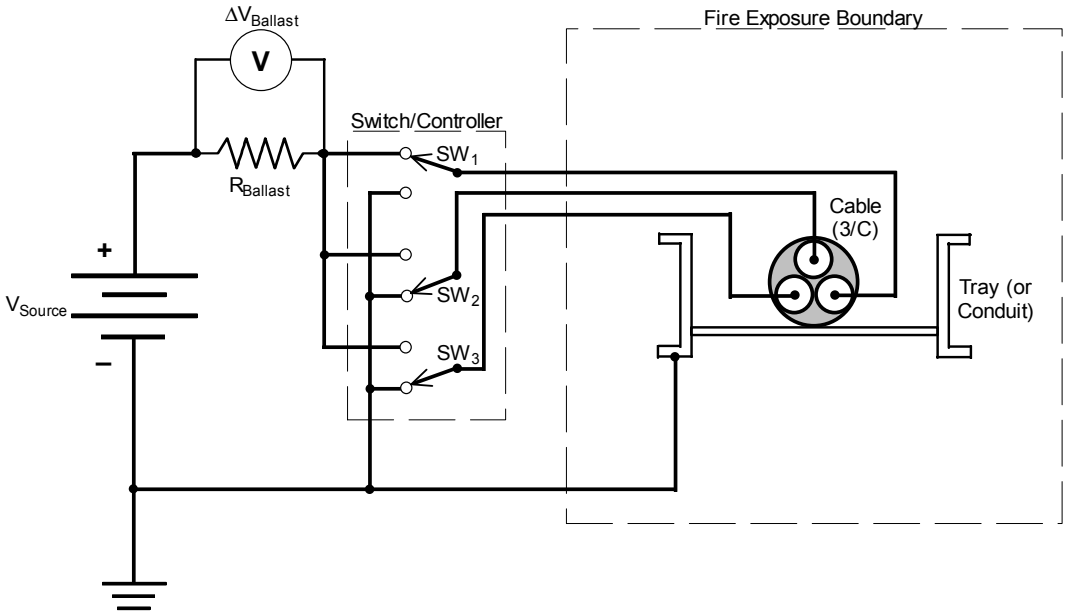

Figure 2-2. Electrical schematic of a single voltage potential monitoring system applied to a multiconductor cable. Note the switching controller is designed to select one conductor at a time to be energized while all others are grounded. A full measurement cycle sequentially energizes each conductor and measures leakage current. This approach can theoretically handle any number of individual conductors.

In practice, the switching task can be accomplished with relative ease using computerized data acquisition and control units. The switching system is then periodically cycled through the full set of conductors to obtain the leakage current as a function of time for each conductor, all under the control of a computer. As with a single conductor cable, the analysis of IR for each conductor is trivial. Because the switching system may energize a conductor that has shorted, the power supply system is commonly designed with a ballast resistor to limit the fault currents. This design allows the system to continue monitoring other conductors that have not failed, even after initial failures are observed, without compromising the power supply system. This approach is common in equipment qualification testing.

The system can also incorporate a complimentary threshold detection scheme to enhance circuit safety. For example, a fuse can be placed on the energizing side of each conductor's powering circuit. If this fuse fails, the conductor has failed and will not be energized during the next switching cycle. If each conductor is provided with an individual fuse and the ballast resistor and voltage-monitoring circuit is eliminated, the system is again reduced to a threshold failure approach.

A slight variation on this general approach is to energize a subset of conductors while grounding the rest. That is, in a seven-conductor cable, one might choose to energize three conductors while grounding the other four. In this case, the leakage current path would be from any of the conductors in the energized set directly to ground or to any one of the grounded conductors. Typically, the selection of the energized conductors would be based on the physical configuration of conductors within the cable. The energized conductors would be selected so that, to the extent possible, each physically adjacent conductor pair would involve one energized and one grounded conductor. This approach was used in a number of past cable fire testing programs and is illustrated in Figure 2-3 for a seven-conductor cable.

This approach has one distinct disadvantage; namely, the IR obtained reflects a composite condition for all of the energized conductors as a group, rather than individual conductor IR values. This is because the conductors are, in effect, wired in a common parallel resistance circuit. One mitigating fact is that the lowest individual conductor IR will dominate the composite IR. Hence, a failing conductor cannot be "masked" by the others in the circuit. However, in analyzing the data, it is not possible to "back out" the individual conductor IR values because many different resistor combinations could yield the same composite resistance.

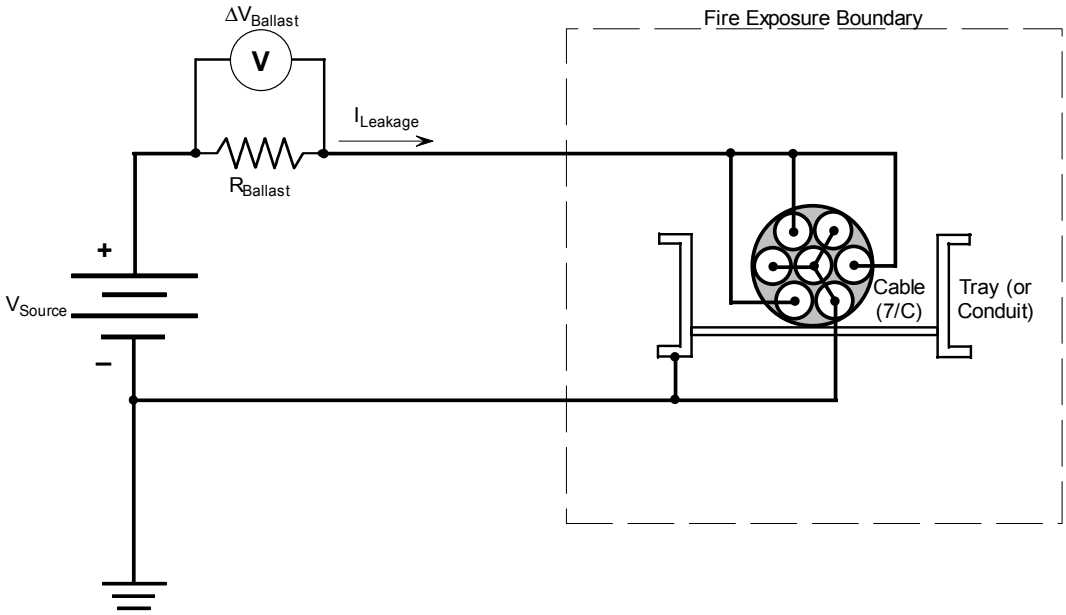

Figure 2-3. A single voltage source system applied to a multiconductor cable without a switching system. Note that the individual conductors are ganged into two groups, one energized and the second grounded. IR is determined for the energized conductors only, and then only as a group.

When testing multiconductor cables, using two or more independent voltage potentials can simplify the instrumentation setup (as compared to a switching system, described above), but can also lead to more difficulty in interpretation of the data and estimating the actual individual cable IR values. The multiple voltage source potentials can eliminate the need for switching systems and yet still allow for the monitoring of both conductor-to-conductor and cable-to-ground breakdown. However, this approach also increases the number of potential leakage paths. For example, with a two-conductor cable energized using two distinct voltage potentials, there are three leakage paths (conductor-to-conductor and each conductor-to-ground). The number of leakage paths quickly increases as the number of conductors, and hence required voltage potentials, increases.

Such a circuit is illustrated in Figure 2-4. Given the increased number of leakage paths, the circuit and data analyses are more complex. In particular, one necessary element to determine individual conductor IR values is the measurement of fault currents on the ground path, requiring that the cable raceway be isolated from the general ground plane. This isolation can lead to additional personnel hazards that must be addressed. Multiple voltage potential methods are quite effective at detecting the general development of IR breakdown, as well as the onset of gross failures and cable failure mode. However, even with just two voltage potentials, the data analysis requires that a set of three equations (all Ohm's law relationships) with three unknowns (two conductor-to-ground and one conductor-to-conductor IR values) be solved. As the number of energizing potentials increases, the number of potential circuit paths, and hence the number of unknowns, increases geometrically.

In more practical terms, the energizing power source is commonly taken from available line power sources. One common approach is to utilize a ±/neutral-110/220 VAC line source, commonly available in household and commercial settings throughout the U.S. In single potential mode, one can simply impose a 110 VAC potential on the energized conductor(s) and connect the rest of the conductor and raceway to the neutral/ground. This simple and readily available configuration is, for example, sufficient to meet the needs of a fire-barrier fire endurance test, where the focus is placed on the barrier performance rather than the cable failure modes. Such a source can also be used in the multiple-potential mode to independently energize two groups of conductors (allowing for detection of conductor-to-conductor IR breakdown) and the neutral/ground plane (allowing for detection of cable-to-ground IR breakdown). Other potential energizing sources include banks of batteries or independent power supplies.

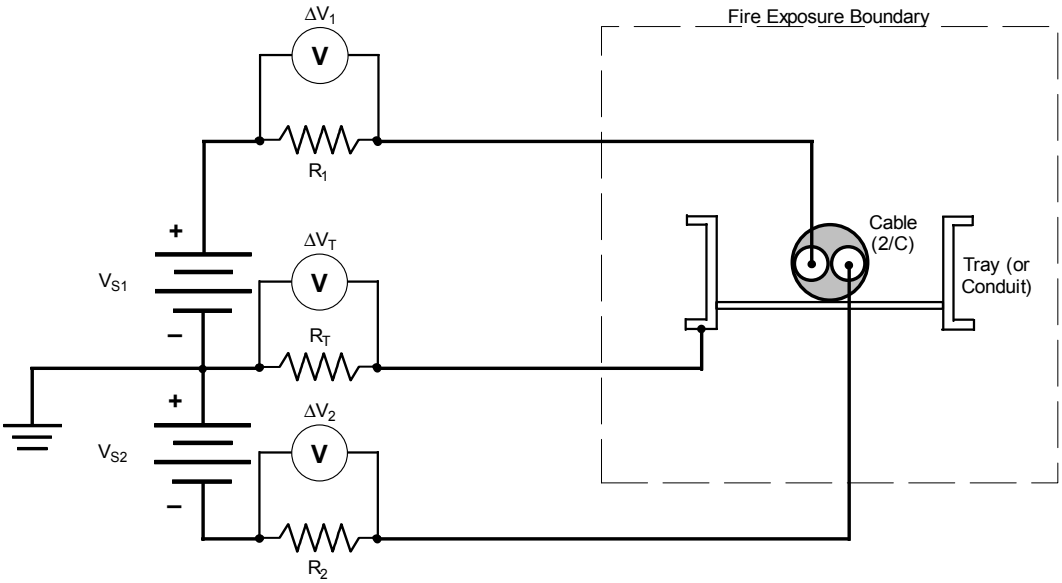

Figure 2-4. An example of a cable monitoring circuit using two energizing voltage potentials. Note the isolation of the raceway from ground by a ballast resistor and monitoring of the leakage current to ground.

Safety concerns during cable failure experiments are commonly addressed through a combination of circuit features and test protocols. Circuit features typically include fuses, switches, interlocks, and ballast resistors in the cable energizing circuits, and provisions for an appropriate ground plane. Switches in the energizing circuit allow for manual activation and isolation of the energizing power source, typically to each energized cable individually. Ballast resistors usually provide an easy means for making the fault current measurement, as noted above, and also limit the fault currents under "bolted" or "dead" short conditions. Fuses can also be used to cut out the energizing voltage upon a cable failure. More elaborate schemes may also use interlocks to isolate energizing voltages to all cable conductors upon an initial failure in any single conductor, to the conductors upon opening of the test chamber, or to isolate energizing voltages for all cables simultaneously by manual actions. None of these features, if properly implemented, compromises the ability to achieve the measurement goals in any way.

The four circuits described above were those most commonly applied during past testing of cable performance in fire and equipment qualification environments. Many possible variations on these circuits might also be employed.

3. THE SANDIA NATIONAL LABORATORIES INSULATION RESISTANCE MEASUREMENT SYSTEM

3.1 Concept

The concept of the SNL IR measurement system is based on the assumption that if one were to impress a unique signature voltage on each conductor in a cable (or cable bundle), then by systematically allowing for and monitoring known current leakage paths, it should be possible to determine if leakage from one conductor to another, or to ground, is in fact occurring. That is, part or the entire voltage signature may be detected on any of the other conductors in the cable (or in an adjacent cable), or may leak to ground directly.

To illustrate, consider a three-conductor (3/C) cable, as illustrated in Figure 3-1. If 100 V are applied to Conductor 1, the degree of isolation of Conductors 2 and 3 from Conductor 1 can be determined by systematically opening a potential conductor-to-conductor current leakage path and then reading the voltages of each conductor in turn while Conductor 1 is energized (see Figure 3-1). Determining the IR between Conductors 1 and 2 at the time of voltage measurement on Conductor 2 is a simple calculation employing Ohm's law:

$$I_{1-2} = \frac{V_2}{R}$$

and

$$R_{1-2} = \frac{V_1}{I_{1-2}} - R \, .$$

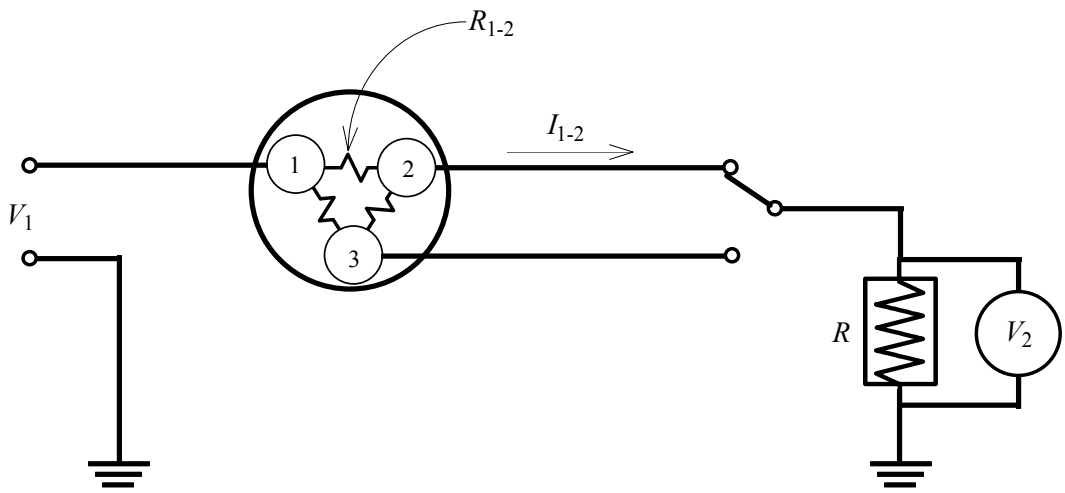

Figure 3-1. Simple IR measuring circuit.

In the same way, the IR existing between Conductors 1 and 3 can be determined at the time V_3 is measured. A time-dependent history of $R_{1\text{-}2}$ and $R_{1\text{-}3}$ can be obtained by continuously switching between the two conductors and recording the voltage drop across R at each switch position. (Of course, an alternate method would be to connect a resistor/voltmeter assembly to both Conductors 2 and 3 simultaneously and keep a continuous record of the two voltages. However, this approach quickly becomes unwieldy as the number of conductors increases.)

The above method alone does not describe the isolation existing between Conductors 2 and 3 (because Conductor 1 is always the energized conductor). However, by sequentially energizing each conductor and reading the impressed voltages on the remaining conductors, one can determine the relative resistance existing between any conductor pair (see Figure 3-2).

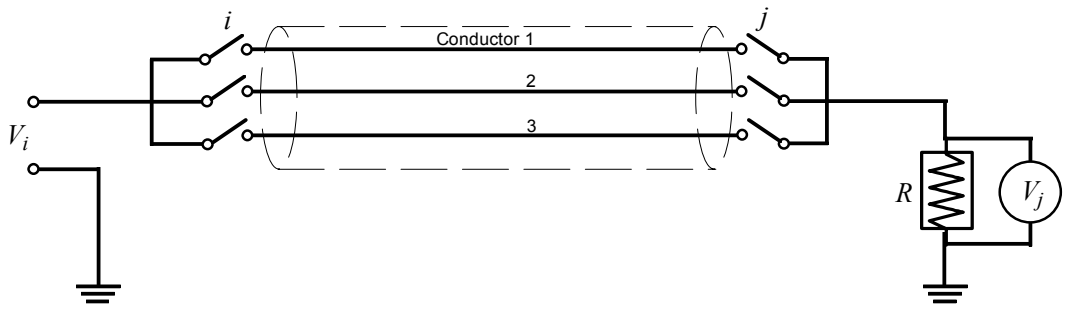

Figure 3-2. Circuit for measuring IR between any conductor pair in a cable.

This concept evolved to include the two sets of controlled switches--one set on the input side (*i*) and one on the output side (*j*) of the circuit. One switch on the voltage input side is closed (thereby energizing one conductor), followed by the sequential closing-measurement-opening of each measurement-side switch. Each sequential switching configuration measures leakage currents between one energized "source" conductor and one nonenergized "target" conductor, and the various pairs are systematically evaluated in sequence.

The IRs between pairs of conductors can be determined in the same manner. Note that when the input- and measurement-side switches are connected to the same conductor ($i = j$), the full input voltage will be measured across R. Since this provides no useful information about the isolation existing between any of the conductor pairs, these measurements can be ignored for the purpose of determining IR. (The presence of the full voltage, $V_j = V_i$, does, however, indicate conductor continuity and otherwise could be useful in identifying an open circuit condition.)

This approach is fine as long as the cable can be kept electrically isolated from ground. If that is not possible (or not desirable, e.g., because short to ground failures are of interest), changes to the design (simple ones) and resistance calculations (significant) are required.

Figure 3-3 shows how the number of possible leakage paths for each of the three conductors in the previous example changes when a ground path is considered. By adding a path to ground for each conductor, the complexity of determining the IR between pairs of conductors grows from one resistance determination to determining three resistances for each pair of conductors. A circuit change is required to enhance the number of independent measurements so as to retain a solvable problem. The revised circuit is shown in Figure 3-4, and includes a ballast/load resistor on the input side, in addition to the output side ballast/load resistor.

The calculation of the three resistances for each conductor pair (one conductor-to-conductor path and each of the two conductor-to-ground paths) requires the measured voltages (V_i and V_j) for two complementary switching configurations. For example, the complement for the case illustrated in Figure 3-4 is shown in Figure 3-5. As illustrated in Figure 3-4, Conductor 2 is connected to the input side and conductor 3 is connected to the measurement side. The complementary case shows Conductor 3 on the input side and Conductor 2 on the measurement side, as shown in Figure 3-5. This complementary pair provides four separate voltage readings that can be used to determine the three resistance paths affecting these two conductors; namely, R_{2-3}, R_{2-G}, and R_{3-G}.

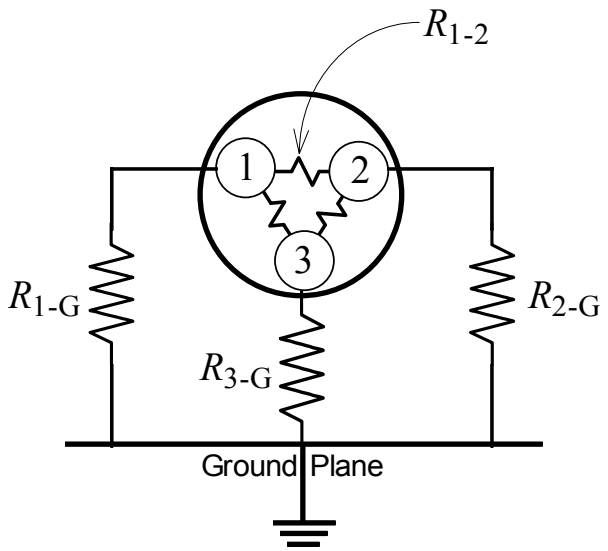

Figure 3-3. Resistive leakage paths for each conductor with a ground present.

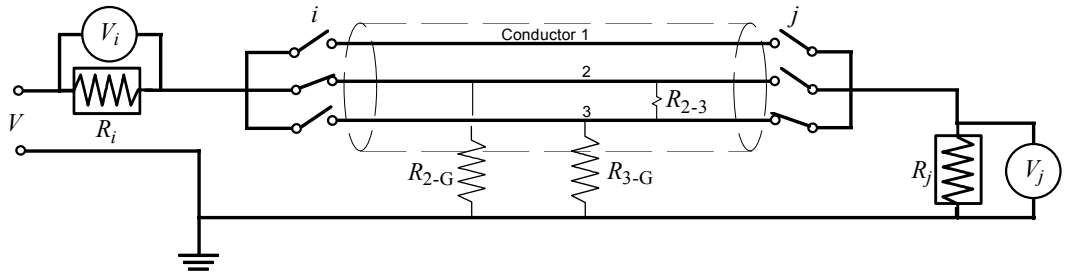

Figure 3-4. IR measuring circuit with ground paths.

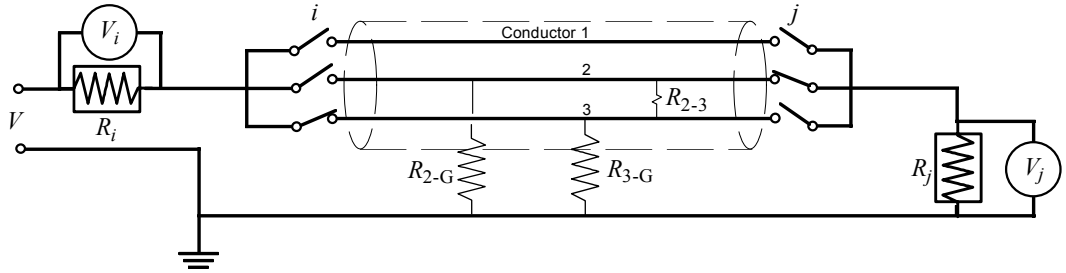

Figure 3-5. Complementary IR measuring circuit with respect to the circuit shown in Figure 3-4.

The equations for determining the three resistances for this case are as follows:

$$R_{2-G} = \frac{\left[V_{j2}V_{j3} - \left(V - V_{i2}\right)\left(V - V_{i3}\right)\right]}{\left[\left(\frac{V_{i3}}{R_i} - \frac{V_{j2}}{R_j}\right)V_{j3} - \left(\frac{V_{i2}}{R_i} - \frac{V_{j3}}{R_j}\right)\left(V - V_{i3}\right)\right]}$$

$$R_{3-G} = \frac{V_{j3}}{\left[\left(\frac{V_{i2}}{R_i} - \frac{V_{j3}}{R_j}\right) - \frac{\left(V - V_{i2}\right)}{R_{2-G}}\right]}$$

$$R_{2-3} = \frac{\left[\left(V - V_{i2}\right) - V_{j3}\right]}{\left[\left(\frac{V_{j3}}{R_{3-G}}\right) + \left(\frac{V_{j3}}{R_j}\right)\right]}$$

This concept is scalable for virtually any number of conductors in a cable or bundle of cables. Another advantage is that only the two voltage measurements for each switching configuration need to be recorded in real time; determining the resistances can be deferred until after the test is completed. This is the basic concept utilized in the design and application of the IR measurement system to generate the results described in this report.

3.2 Design

The SNL IR measurement system as fielded during the industry tests can monitor the IR of up to 10 separate conductors in the AC-energizing mode and eight in the DC-energizing mode. The choice of a maximum of ten conductors was based on the proposed cable configurations to be tested; namely, each test sample would be comprised of one seven-conductor multiconductor cable bundled with three single conductor cables. The capability to test with either an AC or DC power source was added at the request of the NRC. In the DC mode, the total conductor count was limited to eight simply because of limitations on the readily available hardware (DC power relays).

Figure 3-6 provides a block diagram identifying the principal functional areas of the IR measurement system. A schematic diagram of the complete system is provided in Figure 3-7. Each of the functional areas is described in some detail in the following sections.

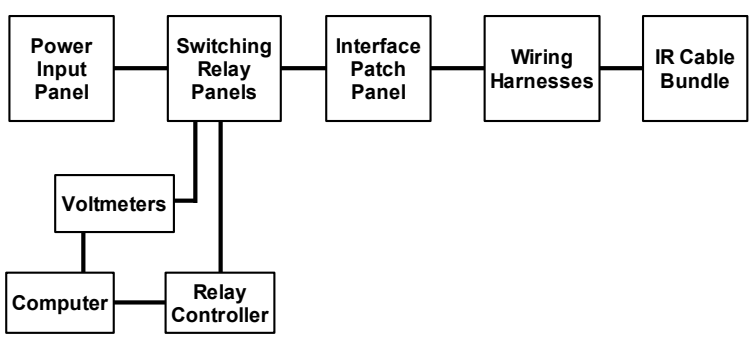

Figure 3-6. IR measurement system block diagram of functional areas.

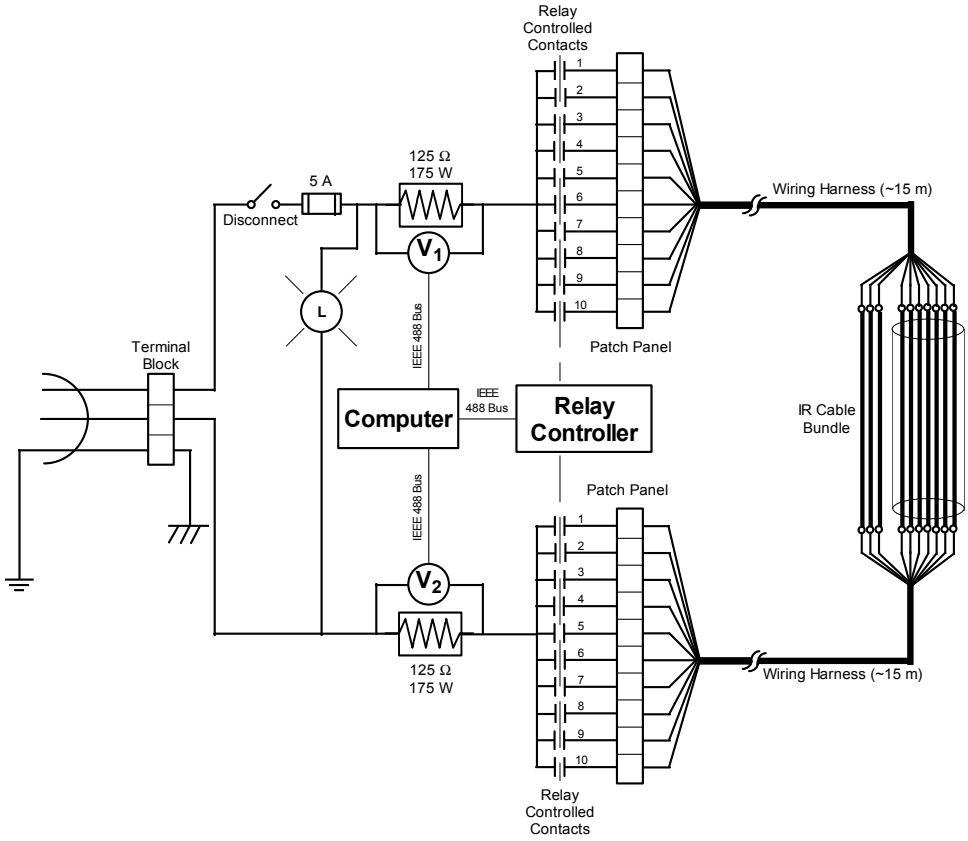

Figure 3-7. Schematic diagram of the IR measurement system.

3.2.1 Power Input Panel

The power input panel consists of a small terminal block for connecting the input power cables, a master disconnect switch to isolate the system from the power input, a 5-A fuse, and a power indication light. Changing the power connection to the system via the terminal block is one of the few manual modifications that needed to be made to reconfigure the system from AC operations to DC.

3.2.2 Switching Relay Panels

Each of the two switching relay panels consists of a 125-Ω ballast resistor, across which a voltmeter is connected, and 10 relays that are separately controlled by the relay controller. Two connections on each relay panel must be changed to convert from AC to DC operation.

3.2.3 Voltmeters

Two HP 34401A digital multimeters are used to measure the voltage drops across the two current-limiting ballast resistors in the IR measurement circuit. Both meters used in this program were subject to regular calibration via the SNL internal calibration program. This calibration program is compliant with all applicable calibration standards and guidelines of the National Institute of Standards and Technology (NIST) and the U.S. Department of Energy (DOE).

3.2.4 Relay Controller

A HP 3497A Data Acquisition/Control Unit is used to control the closing and opening of the relays to connect specific conductors to the voltage source and the measurement side of the circuit. The data logger used in testing is also

subject to the SNL calibration process, although the unit's built-in voltmeter was not utilized in these tests. The data logger was used only as a controller.

3.2.5 Computer

A standard personal computer running Microsoft Windows NT™ was used as the master control unit and data recorder. A general-purpose interface bus (GPIB) was installed and used for device communication between the computer, the relay controller, and the two voltmeters. Control was exercised using a program under LabView™. Data from the voltmeters was logged directly to the computer's hard drive.

3.2.6 Interface Patch Panel

The interface patch panel is composed of a number of jacks compatible with banana plugs to make connection of the wiring harnesses to the output sides of the individual relays a simple matter.

3.2.7 Wiring Harness

Two 15.2 m (50-ft) 10-conductor cables are used to interface the IR measurement system with the test cable.

3.2.8 Insulation Resistance Cable Bundle

For nine of the 18 tests conducted, the IR measurement system was connected to a 10-conductor test bundle, as described above (see also Figure 3-8). For the other tests, the test cable consisted of one of the following cable designs: two tests monitored a single eight-conductor armored cable, one test monitored two five-conductor cables (not collocated in the same raceway), one test monitored an eight-conductor cable, one test monitored IR for two separate instrument cables (one two-conductor cable and one six-conductor), two tests monitored a 12-conductor bundle, and two tests monitored a bundle of three three-conductor cables (a 9/C bundle).

Figures 3-9 and 3-10 show the IR measurement system instrument rack front and rear views, respectively. Part of the computer for the system can be seen through the doorway to the right of the instrument rack in Figure 3-9.

3.3 An Unplanned System Anomaly

One unanticipated effect was noted during the post-test analysis of data from the first set of tests. This effect was strictly an artifact of the solid-state relays used in the AC switching system. (This anomaly did not impact the DC energizing mode of the system because a set of secondary mechanical relays was used in the DC system.)

Each of the solid-state relays used in the AC power source switching system allowed a significant leakage current to pass through the system even when they were supposedly "open." The observed behavior was discussed with the relay manufacturer and this discussion revealed that the relays did not provide a perfect disconnect even when open (i.e., the open contact resistance was not infinite). Rather, each open relay acted more like a 24 kΩ resistor.

Consequently, even with all of the switches open, the effective resistance of this series-parallel network would be approximately 4.8 kΩ (10 48-kΩ resistance circuit paths in parallel). With one relay closed on the input side and a second relay for a different conductor closed on the output side, the circuit resistance would be approximately 4 kΩ (eight 48-kΩ paths and two 24-kΩ paths in parallel). Indeed, the net resistance for this configuration was measured at ~4 kΩ. Hence, with one conductor powered and a second conductor connected to the output side of the circuit, a background leakage current of ~28 mA would be observed during the AC input tests.

So long as all of the conductors retain substantial IR to ground, this artifact of the relays has no impact on the data or data analysis. The behavior becomes more important once any one (or more) conductors short to ground. One conductor shorting to ground will result in an apparent, but artificial, drop in the IRs to ground for all conductors to about 24 kΩ. This artificial impact caused by leakage through the "open" relay to the shorted conductor and then to ground would bypass the output side measurement resistor. Hence, the data analysis will record a discrepancy be-

tween the input and output current and interpret this as an indication of a leakage to ground path associated with the energized conductor.

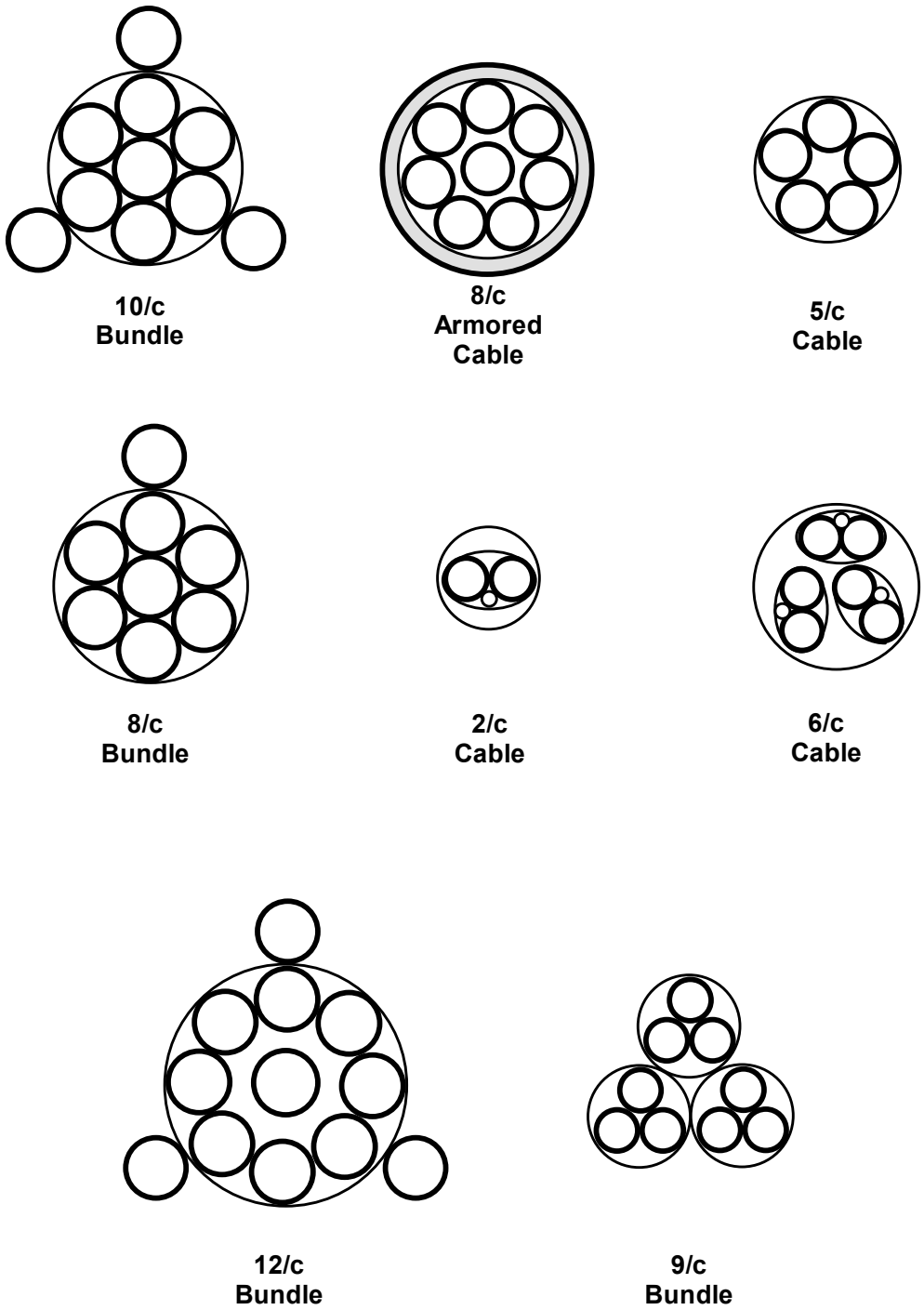

Figure 3-8. Cross-sectional views of the various cable bundle configurations tested using the IR measurement system.

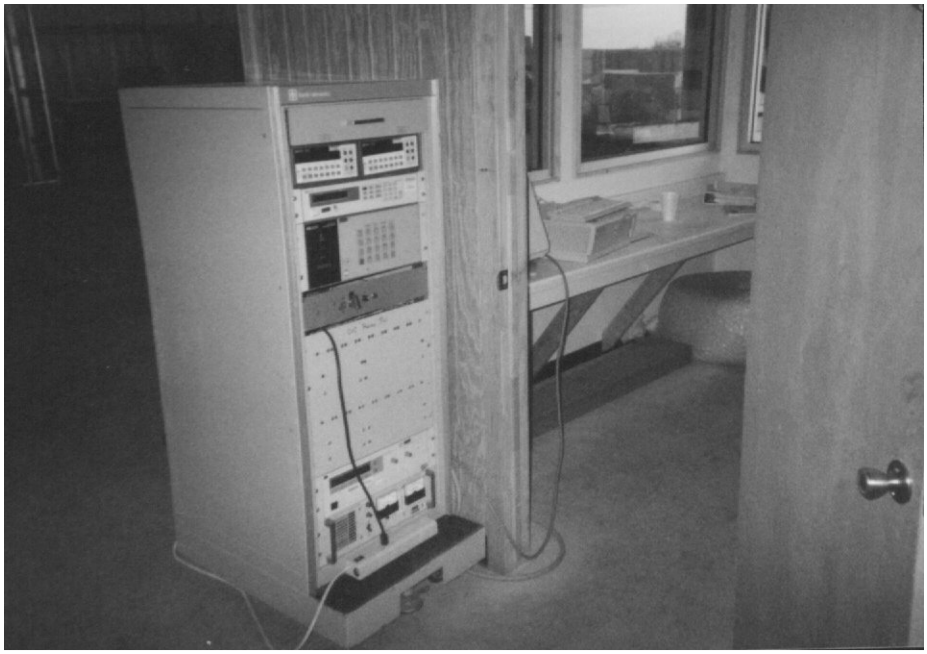

Figure 3-9. Front view of the IR measurement system instrument rack.

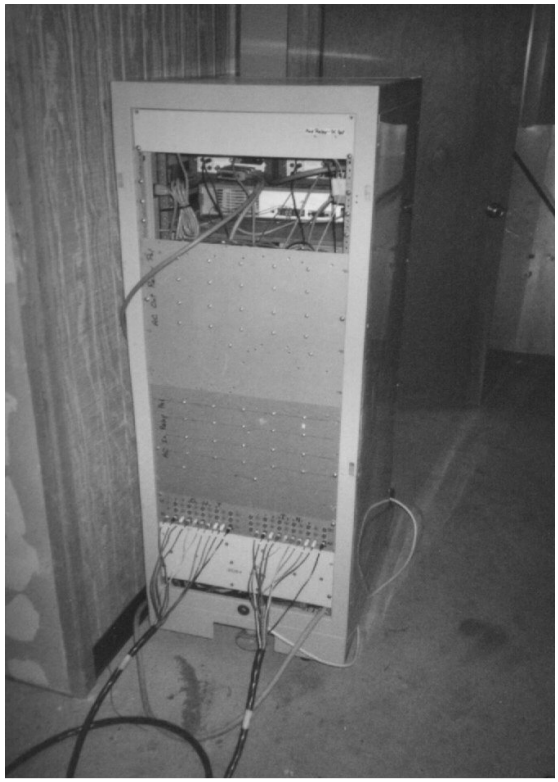

Figure 3-10. Rear view of the IR measurement system instrument rack.

An attempt has been made to correct the data to account for this behavior; however, some residual effects may be noticed in the data plots for a few of the tests. The corrections were made manually in the data analysis spreadsheets. Whenever this anomaly impacted a given test, a note was made in the corresponding discussion of test results (refer to Section 5).

3.4 Operation

Operation of the SNL IR measurement system is a relatively simple matter of connecting the two wiring harnesses to each end of the test cable bundle, turning on power to the two voltmeters and the relay controller, closing the main disconnect switch, and finally, starting the IR measurement program on the computer.

Connection of the wiring harnesses to the test cable was accomplished using commercially-available wire nuts (see Figure 3-11). It is important that each end of a specific conductor in the test cable be connected to the corresponding conductors in both wiring harnesses. For example, the conductors marked "1" in each wiring harness needed to be connected to the ends of the same conductor in the test cable. This also applied to the conductors marked "2" through "10" in the harnesses. Proper connections are checked by performing a continuity check of the pairs of harness conductors at the patch panel ends of the wiring harnesses.

The LabView™ program flow chart is shown in Figure 3-12. The program begins by reading the date and time from the computer's internal clock and the user-defined file name and comments from the associated block on the front screen. It then rewrites this information to the data file (file name), communicates with the GPIB devices (two voltmeters and relay controller) to initialize them, and then begins commanding the closing of the appropriate relays in sequence. For each switch configuration, the voltmeters send their readings back to the computer, which logs the information to the data file and configures the relay switches for the next measurement. This process continues until the user has changed the state of the "SCAN" switch on the front panel to "STOP SCAN," using the mouse. At this time, the program closes the data file and stops running. Figure 3-13 shows a sample from one of the data files generated using this program.

Post-test data analysis was accomplished by importing the data files into an Excel™ spreadsheet and performing the necessary IR calculations. A final manual pass through the resulting IR data was made to determine the nature (e.g., conductor-to-conductor versus conductor-to-ground) and order (i.e., which conductors shorted and when) of observed short-circuit failure. The data analysis also included the generation of IR versus time plots for each conductor in each test. Representative plots for each test are presented in Section 5.

Figure 3-11. IR measurement system "in" wiring harness connection to the test cable bundle.

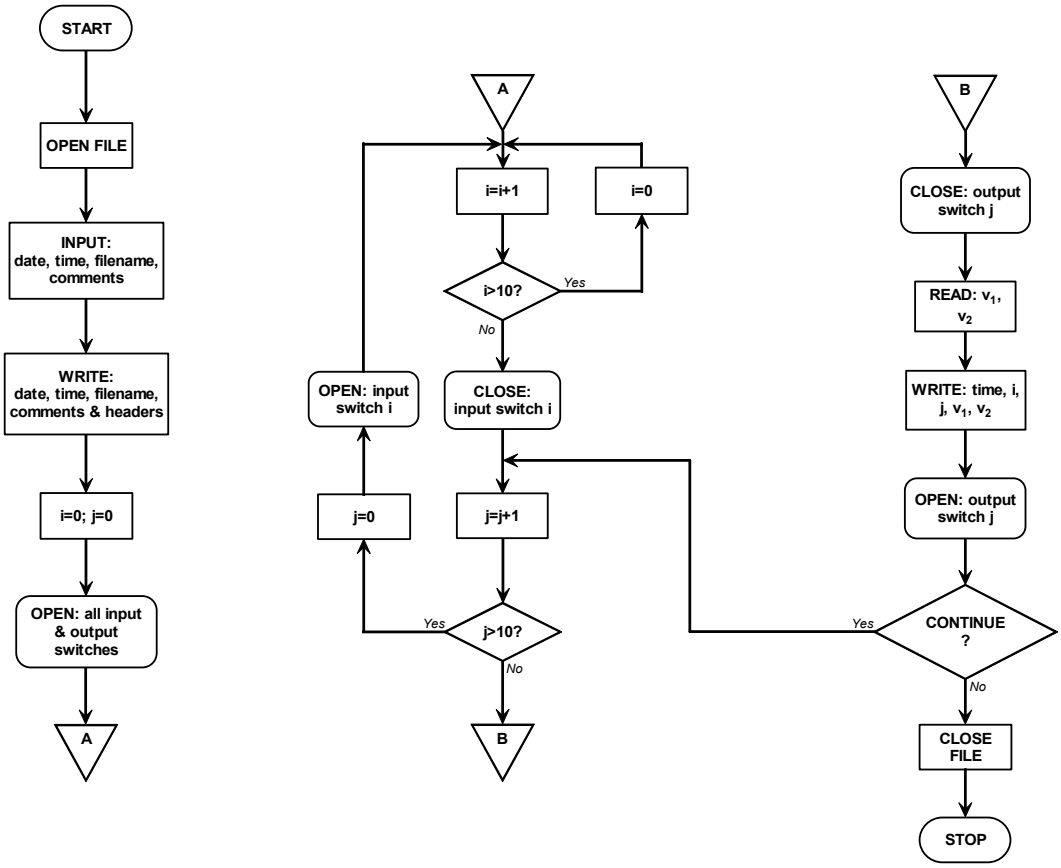

Figure 3-12. IR measurement system control program flow chart.

```
01/12/2001  11:52 AM
Filename:   Cable Fire Test #6.txt
200kW HRR, Thermoplastic cables, tray at 7', flame offset
from tray
Time  Switch i    Switch j    V1    V2

0.000000    1.000000    1.000000    59.865000   60.412000
1.544000    2.000000    1.000000    3.661200    3.809400
0.560000    4.000000    1.000000    3.846600    3.859200
0.562000    8.000000    1.000000    3.620200    3.626700
0.562000    16.000000   1.000000    3.652800    3.648600
0.558000    32.000000   1.000000    3.863000    3.848400
0.559000    64.000000   1.000000    3.782100    3.848400
0.563000    128.000000  1.000000    3.555500    3.534700
0.560000    256.000000  1.000000    3.863000    3.870000
0.566000    512.000000  1.000000    3.566300    3.556400
0.587000    1.000000    2.000000    3.631200    3.740100
1.543000    2.000000    2.000000    61.065000   61.139000
1.541000    4.000000    2.000000    3.727100    3.775300
0.561000    8.000000    2.000000    3.609600    3.556200
0.562000    16.000000   2.000000    3.782300    3.750700
0.562000    32.000000   2.000000    3.588100    3.637300
0.560000    64.000000   2.000000    3.539300    3.523900
0.560000    128.000000  2.000000    3.787500    3.621500
0.562000    256.000000  2.000000    3.755300    3.875400
0.560000    512.000000  2.000000    3.631000    3.615900
0.584000    1.000000    4.000000    3.566500    3.551000
0.560000    2.000000    4.000000    3.793100    3.837300
1.543000    4.000000    4.000000    60.975000   61.716000
1.545000    8.000000    4.000000    3.690000    3.681500
```

Figure 3-13. Example of data file format.

4. CABLE FIRE TESTS

4.1 Description

All of the 18 fire tests described here were conducted in a steel chamber measuring 3 m (10 ft) wide, 3 m (10 ft) deep, and 2.4 m (8 ft) high, shown in Figure 4-1. The chamber has an opening (door) ~76 cm (30 in.) wide by 2.1 m (7 ft) high in the center of one wall. The exposure fire was generated by flowing propane gas through a 30 cm (12 in.) × 30 cm (12 in.) diffusion burner (a "sand burner," see Figure 4-2). The fire intensity was controlled by the flow rate of the propane through the burner and ranged from 70 to 350 kW.

Figure 4-1. Fire test cell.

Figure 4-2. Diffusion burner—30 cm × 30 cm (12 in. × 12 in.).

Most of the tests used a ladder-back type cable tray 30-cm (12-in.) wide, modified to create a sharp 90-degree bend at the center of the tray's length (Figure 4-3). The tray was positioned in the test cell in a horizontal plane at either 1.5, 1.8, or 2.1 m (5, 6, or 7 ft) above the floor, depending on the type of exposure desired for the test (plume or hot gas layer), as shown in Figure 4-4. One side of the tray was parallel to the back wall of the test cell and the other leg of the tray was parallel to the adjacent wall. Figure 4-5 is an overhead sketch of the horizontal tray arrangement in the test cell. The burner was positioned either directly below the corner of the tray for plume exposure tests or placed in the center of the test cell for the hot gas layer tests. A straight length of cable tray was used for the vertical fire test with the burner positioned 0.6 m (2 ft) behind the center of the tray (Figure 4-6).

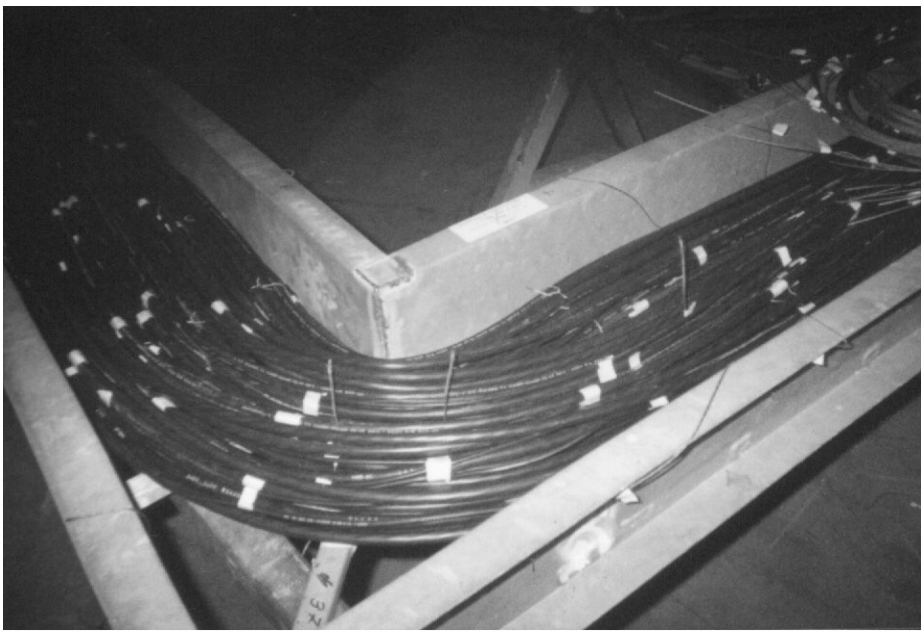

Figure 4-3. Cable arrangement near corner of tray.

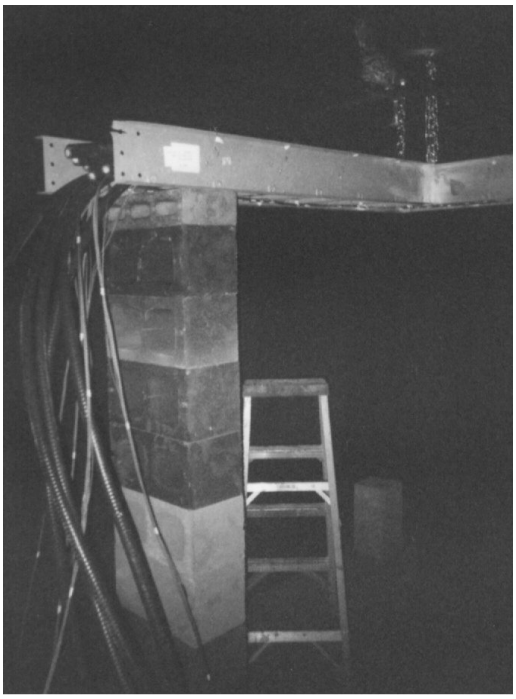

Figure 4-4. Tray, with cables, installed in fire test cell.

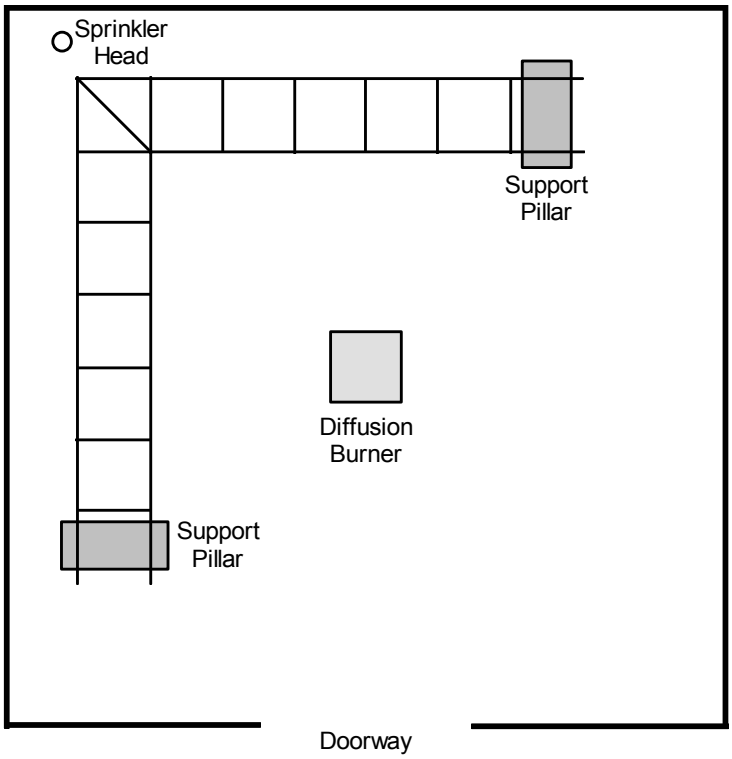

Figure 4-5. Overhead view of tray and burner arrangement inside test cell.

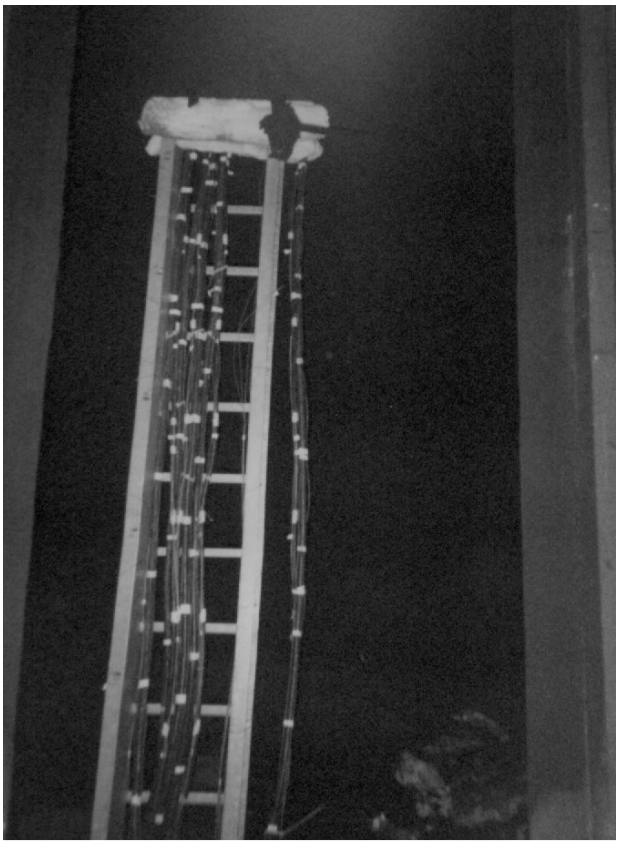

Figure 4-6. Vertical tray and cables installed in test cell.

A water sprinkler head (Figure 4-7) was located in the top of the test cell to provide water spray at the corner of the tray after the flame had been extinguished. The water spray was conducted for one minute at the end of most tests.

Figure 4-7. Water sprinkler head inside fire test cell.

4.2 Test Matrix

The parameters of the fire tests were selected to help explore certain factors that might influence cable failure modes during a fire. For that reason, three flame intensities, two exposure modes (plume and hot layer), a variety of cable tray loading conditions, and several available cable types were included in these tests.

The following provides a summary of the important parameters for each of the 18 tests conducted.

Test 1	**10:06 a.m. January 9, 2001**
Cable Tested	Armored 8/c control cable with the armor shields grounded. The IR system cable shield was not grounded but was monitored as a separate conductor. The conductors were insulated with cross-linked polyethylene (XLPE) and the outer jacket was polyvinyl chloride (PVC).
Tray Configuration	Horizontal, 1.8 m (6 ft) above floor, two rows of fill.
Test Conditions	350 kW heat release rate (HRR), plume exposure, 60-minute run followed by one minute of water spray.

Test 2	**6:07 p.m. January 9, 2001**
Cable Tested	A 7/c thermoset control cable with three 1/c thermoset cables attached. The conductors in the multiconductor cable were insulated with XLPE and contained within a Neoprene jacket. The single-conductor cables were insulated with ethylene propylene rubber (EPR) and each had a Hypalon jacket.
Tray Configuration	Horizontal, 1.5 m (5 ft) above floor, two rows of fill.
Test Conditions	70 kW HRR, plume exposure, 60-minute run followed by one minute of water spray.

Test 3	**11:36 a.m. January 10, 2001**
Cable Tested	A 7/c thermoset control cable with three 1/c thermoset cables attached. The cable materials used for this test were the same as those used in Test 2.
Tray Configuration	Horizontal, 1.8 m (6 ft) above floor, two rows of fill.
Test Conditions	145 kW HRR, plume exposure, 75-minute run followed by one minute of water spray. (The test was allowed to run an additional 15 minutes beyond the planned 60 minutes.)

Test 4	**10:50 a.m. January 11, 2001**
Cable Tested	A 7/c thermoplastic control cable with three 1/c thermoplastic cables attached. The multiconductor cable was insulated and jacketed with Tefzel; the single conductor cables were also insulated with Tefzel but did not have a jacket. Thermoset 5/c cable was used as tray fill.
Tray Configuration	Horizontal, 1.8 m (6 ft) above floor, two rows of fill.
Test Conditions	145 kW HRR, plume exposure; ~40-minute run with no water spray (The test was terminated early because all fuses were blown and the IR system showed total shorting to ground.)

Test 5	**3:43 p.m. January 11, 2001**
Cable Tested	A 7/c thermoset control cable with three 1/c thermoset cables attached. All the cables were insulated with EPR and had a Hypalon outer jacket.
Tray Configuration	Horizontal, 2.1 m (7 ft) above floor, two rows of fill.
Test Conditions	200 kW HRR, hot gas layer exposure; ~75-minute run followed by one minute of water spray. (The test was extended by 15 minutes because there were indications that device actuations/blown fuses were about to occur in the NEI MOV control circuits.)

Test 6	**11:53 a.m. January 12, 2001**
Cable Tested	A 7/c thermoplastic control cable with three 1/c thermoplastic cables attached. The cable materials used for this test were the same as those used in Test 4. Again, thermoset cable was used as tray fill.
Tray Configuration	Horizontal, 2.1 m (7 ft) above floor, two rows of fill.
Test Conditions	200 kW HRR, hot gas layer exposure; ~45-minute run followed by no water spray. (The test was terminated after all fuses had blown and the IR system showed total shorting to ground.)

Test 7	**2:18 p.m. January 23, 2001**
Cable Tested	A 7/c thermoset control cable with three 1/c thermoset cables attached. The types of cables tested were the same as those used in Test 5.
Tray Configuration	Horizontal, 2.1 m (7 ft) above floor, two rows of fill.
Test Conditions	350 kW HRR, plume exposure, ~66-minute run followed by one minute of water spray.

Test 8	**10:10 a.m. January 24, 2001**
Cable Tested	Two 5/c thermoset cables (identified as fire retardant ethylene propylene (EP)) without external conductors attached; one cable was routed in the tray and the other in the conduit.
Tray Configuration	Horizontal, 1.8 m (6 ft) above floor, three rows of fill; a conduit with one MOV control circuit cable and one of the 5/c IR cables was installed along the inside edges (toward the center of the test cell) of the tray. The conduit also had a 90-degree bend.
Test Conditions	145 kW HRR, plume exposure, ~93-minute run followed by one minute of water spray.

Test 9	**3:20 p.m. January 24, 2001**
Cable Tested	A 7/c thermoset control cable (same type as used in Test 5) with three 1/c thermoset cables attached.
Tray Configuration	Horizontal, 1.8 m (6 ft) above floor, one row of fill.
Test Conditions	145 kW HRR, plume exposure, ~60-minute run followed by one minute of water spray. The IR system was configured for ungrounded 100 VDC operation.

Test 10	**3:18 p.m. January 25, 2001**
Cable Tested	A 7/c thermoset control cable (same type as used in Test 5) with three 1/c thermoset cables attached. The IR bundle only had one 1/c external cable attached.
Tray Configuration	Vertical, one row of fill, one actuating device bundle was located next to the tray to simulate an air drop.
Test Conditions	200 kW HRR, hot gas/radiant exposure; ~90-minute run followed by two one-minute operations of the water spray. The IR system was configured for ungrounded 100 VDC operation.

Test 11	**9:50 a.m. January 25, 2001**
Cable Tested	Two instrument cables without external conductors attached, one was a 2/c and one was a 6/c.
Tray Configuration	Horizontal, 1.8 m (6 ft) above floor, four rows of fill.
Test Conditions	145 kW HRR, plume exposure, ~75-minute run followed by one minute of water spray. The IR system was configured for ungrounded 24 VDC operation.

Test 12	**3:07 p.m. April 2, 2001**
Cable Tested	A 7/c thermoset (EPR/Hypalon) control cable with three 1/c thermoset (same type as used in Test 2) cables attached.
Tray Configuration	Horizontal, 1.8 m (6 ft) above floor, one row of fill.
Test Conditions	145 kW HRR, plume exposure, ~60-minute run followed by no water spray. The IR system was configured for grounded 100 VDC operation.

Test 13	**10:38 a.m. April 3, 2001**
Cable Tested	*IR measurement:* An armored 8/c control cable (same as used in Test 1) without external cables attached. The armor shield was grounded. *Instrument Loop circuit:* A shielded 2/c thermoset (EPR/Hypalon) instrumentation cable.
Tray Configuration	Horizontal, 2.1 m (7 ft) above floor, two rows of fill.
Test Conditions	350 kW HRR, hot gas layer exposure, ~38-minute run. The IR system was configured for 120 VAC operation.

Test 14	**2:55 p.m. May 31, 2001**
Cable Tested	*IR measurement:* Three 3/c thermoset control cables grouped into a single bundle and routed in the conduit. *Instrument Loop circuit:* A thermoplastic (polyethylene (PE)/PVC) 2/c instrument cable routed in the cable tray.
Tray Configuration	Horizontal, 1.8 m (6 ft) above floor, two rows of fill in the tray, a conduit with the IR cable bundle was mounted along the inside edge (toward the center of the test cell) of the tray. The conduit also had a 90-degree bend and was grounded.
Test Conditions	145 kW HRR, plume exposure, ~2 ½-hour run followed by two minutes of water spray. The IR system was configured for 120 VAC operation.

Test 15	**4:35 p.m. April 3, 2001**
Cable Tested	*IR measurement:* A 7/c thermoset control cable with three 1/c thermoset cables attached. The same type of cables as used in Test 12. *Instrument Loop circuit:* A 2/c thermoset instrument cable with shield and drain wire.
Tray Configuration	Horizontal, 1.8 m (6 ft) above floor, one row of fill.
Test Conditions	Variable HRR (350/200/450 kW), hot gas layer exposure, ~50-minute run followed by one minute of water spray. The IR system was configured for 120 VAC operation.

Test 16	**2:47 p.m. April 4, 2001**
Cable Tested	*IR measurement:* A 9/c thermoplastic control cable with three 1/c thermoplastic cables attached. These cables had PE insulation and a PVC jacket. *Instrument Loop circuit:* A three-pair thermoplastic (PVC/PVC) instrument cable with shield and drain wire.
Tray Configuration	The IR cable bundle was located in the horizontal conduit at 1.8 m (6 ft) above the floor. The instrument cable was located in the horizontal tray at 1.8 m (6 ft) above the floor with two rows of fill.
Test Conditions	145 kW HRR, plume exposure, ~30-minute run. The IR system was configured for 120 VAC operation.

Test 17	**9:54 a.m. April 5, 2001**
Cable Tested	*IR measurement:* A 9/c thermoplastic control cable with three 1/c thermoplastic cables attached. These are the same types of cables as used in Test 16. *Instrument Loop circuit:* A 2/c thermoset (EPDM/Hypalon) instrument cable.
Tray Configuration	Vertical, one row of fill.
Test Conditions	200 kW HRR, hot gas/radiant exposure; ~60-minute run followed by one minute of water spray. The IR system was configured for ungrounded 120 VAC operation.

Test 18	**11:59 a.m. June 1, 2001**
Cable Tested	*IR measurement:* Three 3/c thermoset control cables grouped into a single bundle and routed in the conduit. These are the same types of cables as used in Test 14.
	Instrument Loop circuit: A thermoset (EPR/Hypalon) 2/c instrument cable routed in the cable tray.
Tray Configuration	Horizontal, 2.1 m (7 ft) above floor, two rows of fill in the tray, a conduit with the IR cable bundle was mounted along the inside edge (toward the center of the test cell) of the tray. The conduit also had a 90-degree bend and was grounded.
Test Conditions	250 kW HRR, hot gas layer exposure; ~2-hour run followed by two minutes of water spray. The IR system was configured for 120 VAC operation.

4.3 IR Measurement Interfaces

As mentioned previously, the only interface the SNL/NRC measurement system had in the tests was with the designated IR cable bundle(s) for each run and the instrument loop cables included in the last six tests. Figure 4-8 shows the relative location of the IR bundle(s) and the instrument loop cables in the raceways (cable tray or conduit) for each of the 18 tests. The view shown is looking at the end of the cable tray closest to the doorway of the test cell for the horizontal raceway configurations. For Tests 10 and 17, the vertical tray tests, the view shown is as if one had turned the tray up and was looking up from the bottom end of the cable tray. Also shown in the figure is the relative position of the closest thermocouple instrumented "dummy" cables (i.e., cables not monitored for function but for temperature). In most cases, thermocouple cable TC-4 was the nearest indication of cable temperature for the IR bundle. However, for Test 8, since the IR system was connected to two separate five-conductor cables, TC-1 was the principal cable temperature measurement inside the conduit. Also, for Test 11, TC-4 would be the most closely-related temperatures for IR cable 1 and TC-1 would be the closest temperature readings for IR cable 3.

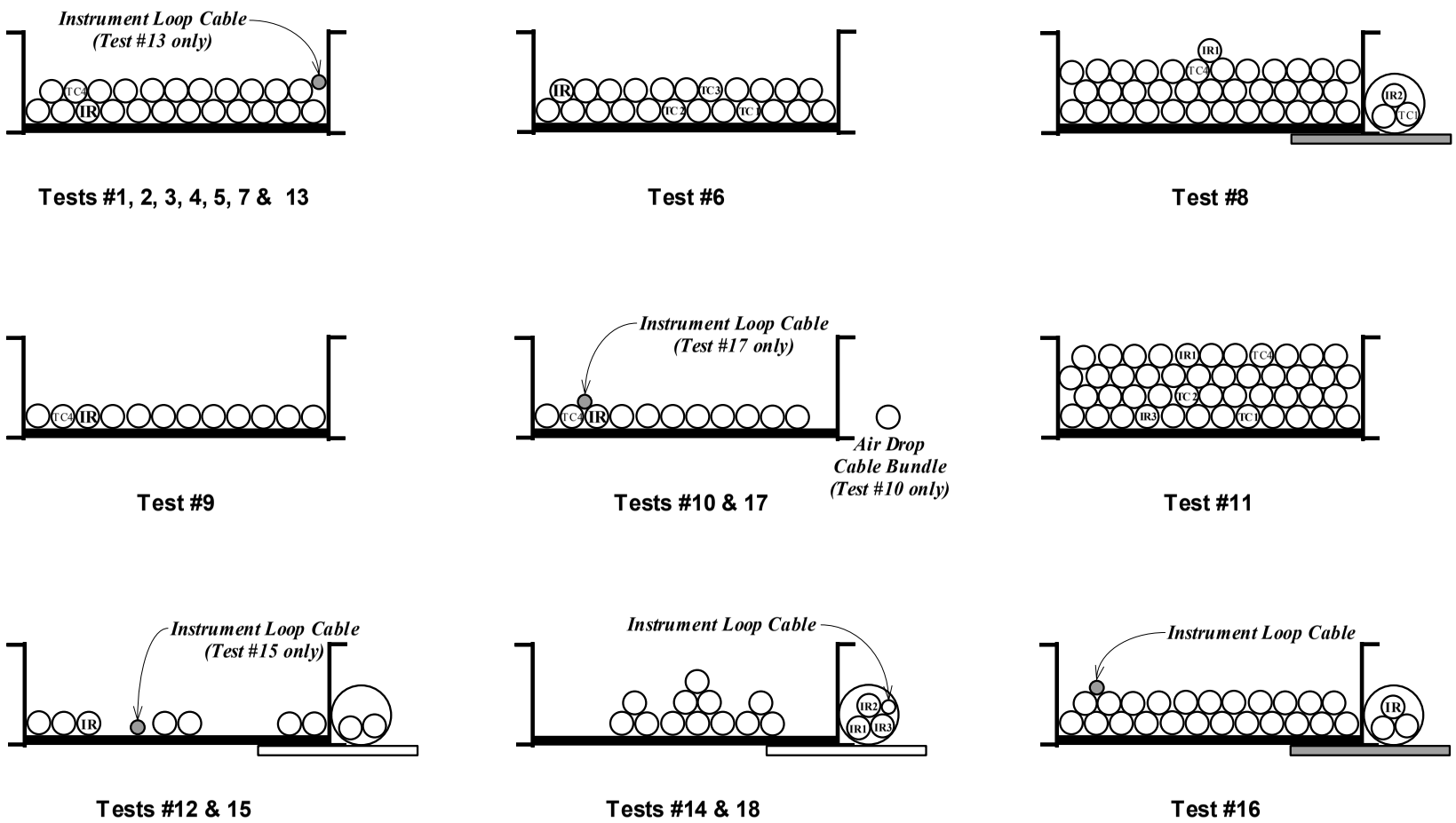

Figure 4-8. Cable arrangements in tray for the various tests[2].

[2] Based in part on information provided by the industry participants in the test program.

5. INSULATION RESISTANCE MEASUREMENT RESULTS

Eighteen tests were conducted as part of the cable fire test series. In each test, the SNL IR measurement system was used to monitor the change in conductor IR occurring in at least one cable or cable bundle. In a small number of tests, two separate cables that were not collocated were monitored. This section presents the results of the IR measurements. (Note that Section 6 provides a separate discussion of the instrument loop circuit results taken during the last six tests).

Of the tests conducted, seven (Tests 3, 4, 6 through 8, 12, and 18) involved clearly characterized cable failures including the mode of initial cable failure (e.g., conductor-to-conductor shorting versus shorts to ground) and failure mode transitions (i.e., transitions to a short to ground). Six tests saw no substantive cable failures (Tests 1, 2, 5, 10, 11, and 14). In Test 9, while failures were observed, the lack of a ground reference plane for the IR measurement system prevented determination of when shorts to ground occurred. For this test, only the conductor-to-conductor shorts are detected. Finally, during Tests 13 and 15 through 17, the IR measurement system was compromised by a wiring fault. As a result of this fault, only the total IR between each conductor and ground can be ascertained (conductor-to-conductor IR cannot be determined). Consequently, while the approximate time of failure can be determined based on shorts to ground, the initial failure mode could not be determined for these tests.

5.1 Tests 1 through 3

At the outset of the testing program, the building electric receptacle providing power to the SNL IR system instrument rack was miswired (reversed polarity of the hot and neutral leads). As a result, the polarity of the measurement circuit (as shown in Figure 3-7) was reversed. This problem was discovered and corrected immediately following Test 3. However, Tests 1 through 3 were run using the reversed polarity circuit.

As a result, the hot side of the power source was being fed to what was believed to be the grounded neutral side of the circuit. This effectively reversed the input and output sides of the circuit relative to the anticipated configuration. Fortunately, this reversing of the polarity did not seriously compromise the test data. Given knowledge of the wiring problem, full analysis of the data was still possible.

5.1.1 Test 1

Test 1 was a 350-kW heat release rate fire with armored cables laid in a horizontal cable tray and exposed to the fire plume. The IR sample was an eight-conductor armored cable. The armor of the cable was not grounded, but rather was treated in the IR system as a ninth conductor. This allowed for a determination of when the armor shorted to ground through the outer jacket. The IR system was operated in AC mode and, as previously discussed, the AC power source was reversed-polarity during this test.

No substantive degradation of the sample cable IR was observed in this test other than shorting of the cable armor to ground at approximately 800 seconds. Under in-plant conditions, the armor would likely be grounded as a part of the cable installation. Furthermore, the outer jacket of the cable is not intended to serve any electrical function, but rather provides only physical/mechanical protection. Hence, shorting of the armor to ground is not considered a functional failure of the cable. It is noted here only as a potential point of interest.

Figure 5-1 shows the time-temperature plots for two of the thermocouples monitored during the test. These two thermocouples were chosen because they showed the worst-case temperature exposure conditions (highest recorded temperatures) for the air near the IR bundle and for the instrumented cable closest to the IR bundle. TC #17 was mounted on the side of the tray about 1.2 m (4 ft) from the doorway, and TC #68 was located about mid-position on the instrumented cable TC-4. The peak tray temperature recorded was 438°C (820°F), and that for TC-4 was 357°C (675°F) near the end of the test run. Note that the rapid decrease in temperatures indicates the point when the flame was extinguished and the water spray was initiated.

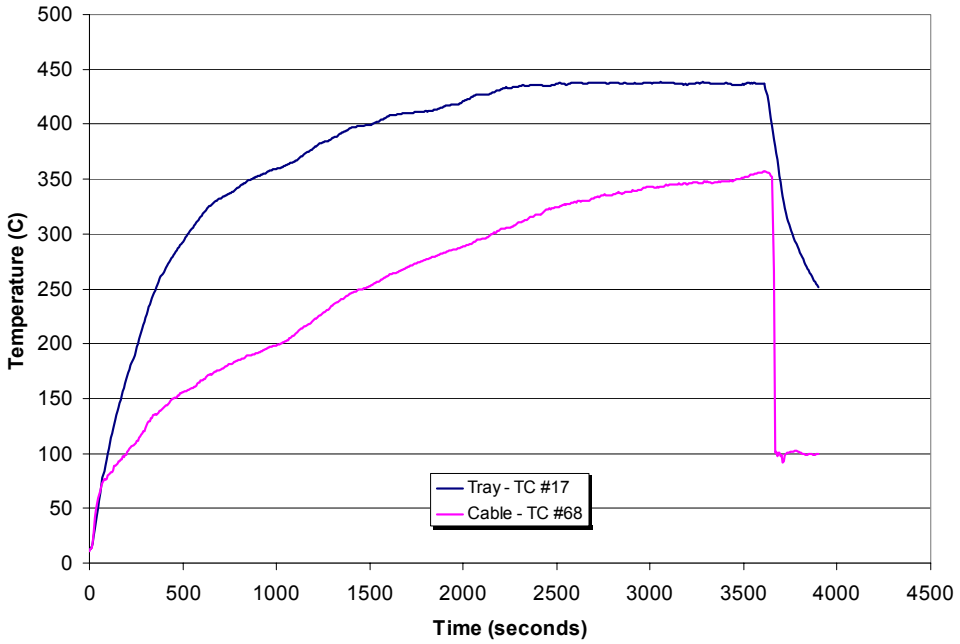

Figure 5-1. Representative tray and TC-4 cable temperatures recorded during Test 1.

Figure 5-2 shows the IR occurring between Conductor 1 and each of the other conductors in the IR cable. Conductor 1 was the center conductor in the cable and the other seven conductors surrounded Conductor 1 (see Figure 3-8 for an illustration of the cable configuration). Conductor 9 shown in the plot is the armor shield that surrounded all of the conductors (a spiral-wound metal band much like a flexible metal conduit).

The impact of the reverse polarity on the IR results associated with Conductor 9 is demonstrated in this figure. Note that once Conductor 9 shorts to ground (see Figure 5-3), there is a false indication of a very low IR existing between Conductor 9 and the other conductors. In reality, Conductor 9 is being continuously affected by electrical ground to the extent that it masks the true IR between Conductor 9 and Conductors 1 through 8. Hence, the appearance of a low IR between Conductor 9 and Conductor 1, for example (as shown in this plot), is not reflective of the actual conditions.

Note that the notation used in this figure is typical of that used in the remainder of the IR plots presented in this section. For example, "R12" signifies the measured IR between Conductors 1 and 2, "R13" would be the IR between conductors 1 and 3, and so on. In a similar manner, "R1G" indicates the IR between Conductor 1 and ground. A "0" is used to designate Conductor 10, so "R0G" is the IR between Conductor 10 and ground.

The IR change over time of the individual conductors to ground is shown in Figure 5-3. Recall that Conductor 9 is the armor. As shown in the plot, the armor shorts to ground early in the test (~820 seconds). Also note that the IR between all of the conductors and ground begins degrading noticeably near the end of the test (at ~3000 seconds).

The reduction in IR between conductor pairs and each to ground indicates an increase in the leakage currents. However, in this case, the leakage currents remained small. Figure 5-4 shows a plot of how the leakage currents for Conductors 1 and 2 changed in their relationship to one another and to ground as the test progressed. Based solely on the results of the IR measurements made during Test 1, it does not appear that the IR cable experienced damage to the point of allowing leakage currents high enough to cause device actuation or blown fuses.

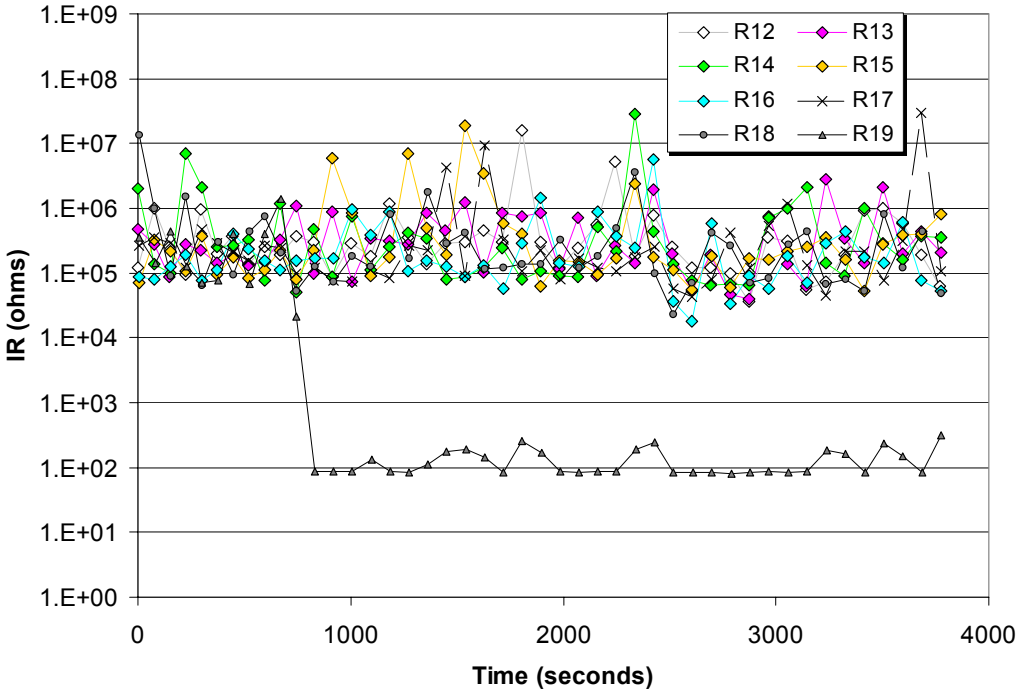

Figure 5-2. Representative conductor-to-conductor IRs obtained during Test 1. This plot shows the IRs between Conductor 1 and Conductors 2 through 9.

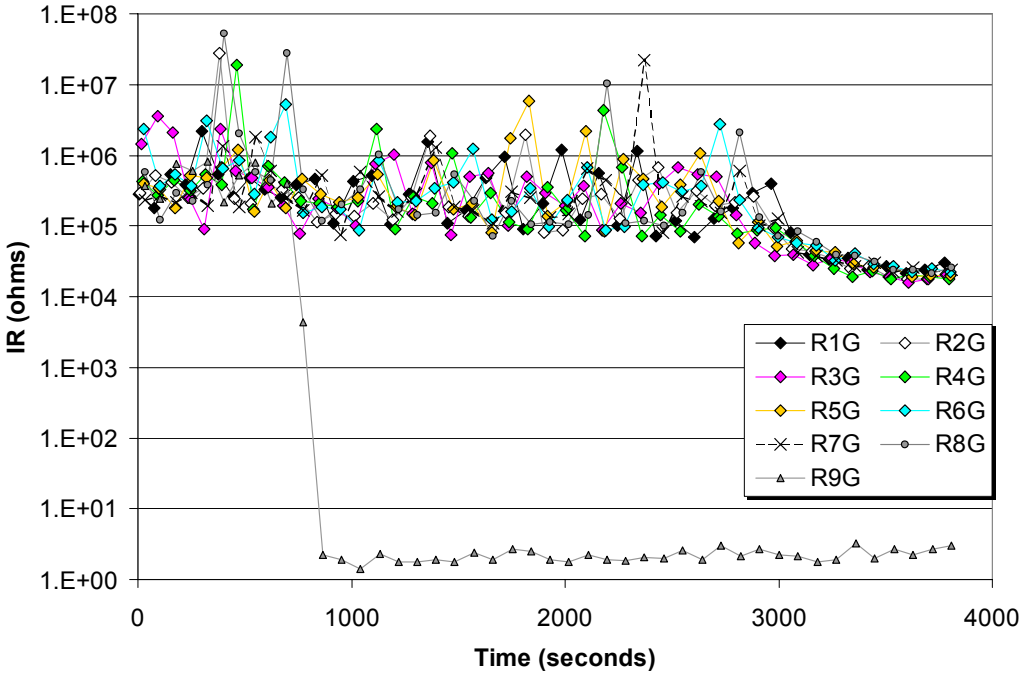

Figure 5-3. Conductor-to-ground IRs obtained during Test 1.

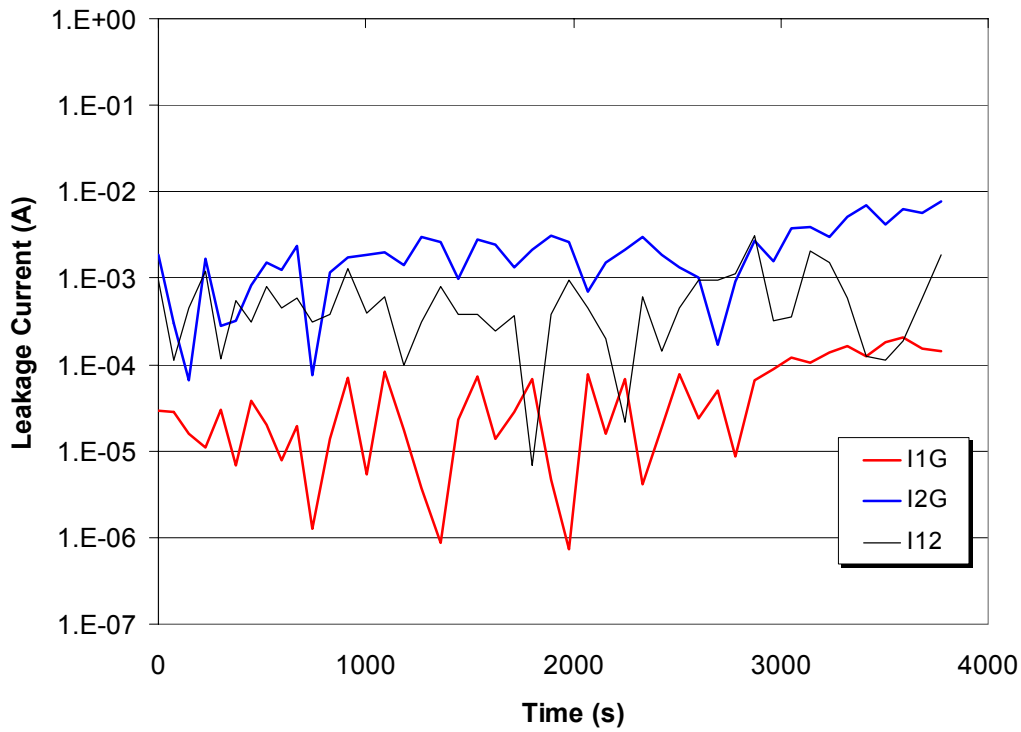

Figure 5-4. Leakage currents resulting from IR changes in Conductors 1 and 2 during Test 1.

5.1.2 Test 2

Test 2 was a 70-kW heat release rate fire with thermoset-insulated cables laid in a horizontal cable tray and exposed to the fire plume. The IR sample bundle was a seven-conductor cable bundled with three single-conductor cables. Conductor 1 represents the central conductor of the multiconductor cable; Conductors 2 through 7 represent the other conductors in the multiconductor cable connected in sequence going around the cable (i.e., Conductor 2 is next to Conductor 3, which is next to Conductor 4, etc.). Conductors 8 through 10 represent the three external conductors. The IR system was operated in AC mode and, as noted above, the AC power source was reversed-polarity during this test.

No substantive degradation of the sample cable IR was observed in this test. All of the conductor IR values remained at essentially the baseline values (nominally in the 10^5 to 10^6 Ω range).

Figure 5-5 shows the time-temperature plots for two of the thermocouples monitored during the test. These two thermocouples were chosen to illustrate the worst-case temperature exposure conditions (highest recorded temperatures) for the air near the IR bundle and for the instrumented cable closest to the IR bundle. TC#26 was mounted on the rung at the corner of the tray, and TC#74 was located about mid-position on the instrumented cable TC-4. The peak tray temperature recorded was 398°C (748°F) and the peak cable temperature was 298°C (568°F). Again, the rapid temperature drop-off at the end of the test run was due to the water spray.

Figure 5-6 shows the IR occurring between the center conductor in the seven-conductor cable (Conductor 1) and each of the other conductors in the IR cable. There was no noticeable impact of the reverse polarity problem on the IR results for this test.

There did not appear to be any substantial degradation of the cable IR values during this test. The IR relationships between Conductor 1 and each of the other conductors in the IR cable bundle, as shown in Figure 5-6, is typical of all of the conductors in the IR cable.

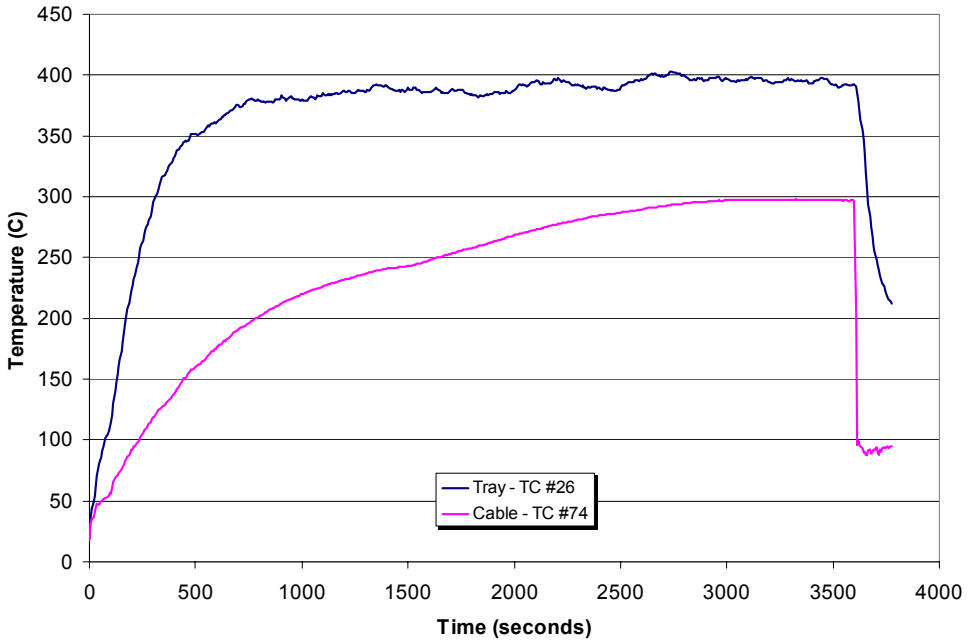

Figure 5-5. Representative tray and TC-4 cable temperatures recorded during Test 2.

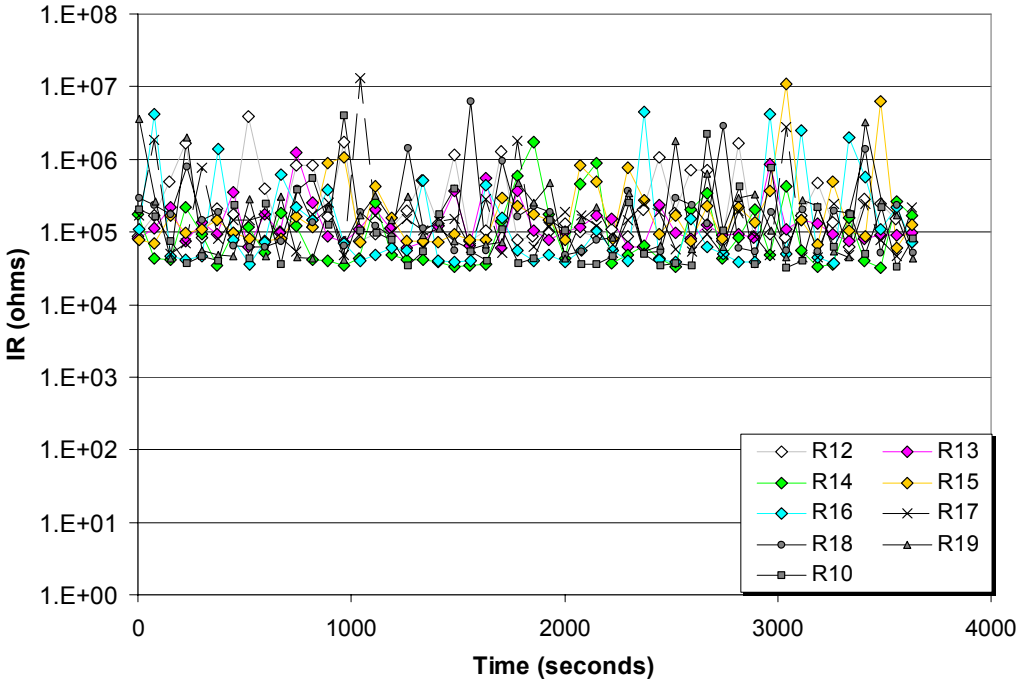

Figure 5-6. Representative conductor-to-conductor IRs obtained during Test 2.

The IR change over time of each individual conductor to ground is shown in Figure 5-7. Here again, it appears that the 70-kW fire did not cause sufficient damage to the cable to change the IR. Figure 5-8 shows a plot of how the leakage currents for Conductors 1 and 2 changed in their relationship to one another and to ground as the test progressed. Based solely on the results of the IR measurements made during Test 2, it appears that the IR cable experienced virtually no damage and would not have caused any device actuation or blown fuses.

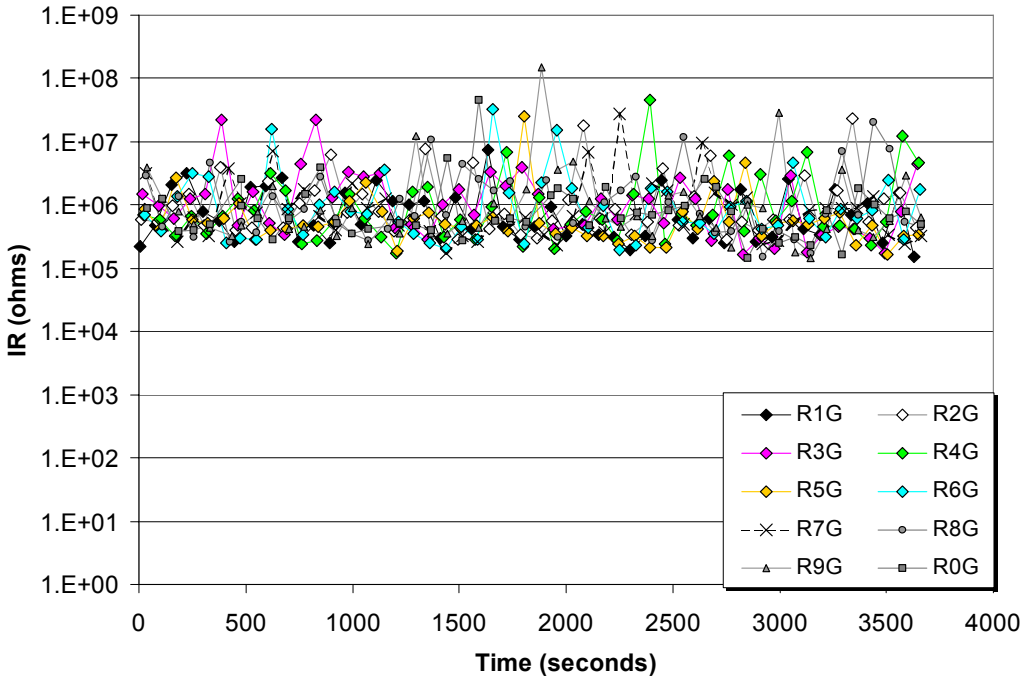

Figure 5-7. Conductor-to-ground IRs obtained during Test 2.

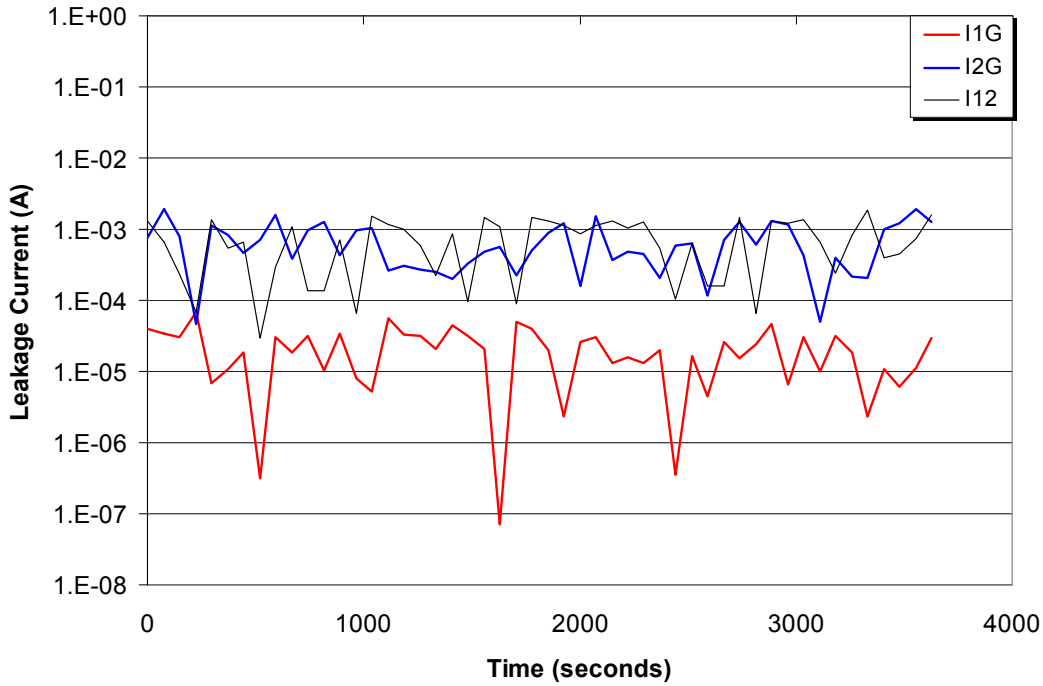

Figure 5-8. Leakage currents resulting from IR changes in Conductors 1 and 2 during Test 2.

5.1.3 Test 3

Test 3 was a 145-kW heat release rate fire with thermoset cables laid in a horizontal cable tray and exposed to the fire plume at the corner of the tray. The IR sample bundle was, again, a seven-conductor cable bundled with three single-conductor cables. Conductor 1 represents the central conductor of the multiconductor cable; Conductors 2 through 7 represent the other conductors in the multiconductor cable connected in sequence going around the cable (i.e., Conductor 7 is next to Conductor 2, which is next to Conductor 3, which is next to Conductor 4, etc.). Conductors 8 through 10 represent the three external conductors.

The IR system was operated in AC mode and, as noted above, the AC power source was reversed-polarity during this test. As discussed in Section 5.1, the primary impact of this is seen as various conductors short to ground. When such shorts occur, and the grounded conductors are switched in to the IR monitoring system, the voltage potential across the IR system drops to zero and no meaningful data is obtained. Given foreknowledge of the problem, this does not substantially compromise the test results, and failure modes can be clearly discerned in the data. Various conductor failures were observed in this test, as described below. These failures included both conductor-to-conductor and conductor-to-ground failures.

Figure 5-9 shows the time-temperature plots for two of the thermocouples monitored during the test. These two thermocouples were chosen because they showed the worst-case temperature exposure conditions (highest recorded temperatures) for the air near the IR bundle and for the instrumented cable closest to the IR bundle. TC #27 was mounted on a rung at the corner of the tray, and TC #74 was located about mid-position on the instrumented cable TC-4. The peak tray temperature recorded during this test was 503°C (937°F) at ~3100 seconds into the test. The tray temperature then decreased and stabilized at ~475°C (887°F) for the duration of the test run. The peak cable temperature was 404°C (759°F) recorded near the end of the test. Note that there was a problem with this thermocouple for the first 1365 seconds of the test, which was corrected during the run.

Figure 5-10 shows the changes in IR occurring between the center conductor of the multiconductor (Conductor 1) and each of the other conductors in the IR cable bundle during the test. The impact of the reverse polarity problem on the IR results for this test appears to be only slightly noticeable.

Two separate transitions from the initial IR values to lower IR values were observed during this test. The first of these transitions occurs between 1300 and 2200 seconds into the test. At this time, the conductor-to-conductor IR values decrease from ~100 kΩ down to ~10 kΩ. The second transition happens in the 2700 to 2900 second range where most of the IRs drop to ~10 Ω. The IR relationships between conductor 1 and each of the other conductors in the IR cable bundle, as shown Figure 5-10, are typical of all of the conductors in the IR cable bundle.

The IR change over time of the individual conductors to ground is shown in Figure 5-11. Here it appears that the effect of the 145 kW fire causes a very smooth transition to a lower IR to ground during the time between 1700 and 3000 seconds. It also appears that a very limited amount of IR recovery occurs at the very end of the test run, possibly due to the cooling effect of the water spray.

Figure 5-12 shows a plot of how the leakage currents for Conductors 1 and 2 changed in their relationship to one another and to ground as the test progressed. The multiple transition phases are evident here as well. Note that since the 125 Ω resistors in the IR measurement system limit the peak available leakage currents to ~1 A, the resulting leakage current plots presented in this report should be considered to represent the fraction of available leakage current that could be shunted through another conductor or to ground.

Table 5-1 summarizes the various IR failures observed. The times are based on the IR of a given conductor to ground or conductor pair dropping below 100 Ω. It would appear that the first conductor failures involved conductor-to-conductor shorting between Conductors 1, 6, and 7 within the multiconductor cable (time ~ 2751 seconds). This failure is seen clearly in Figure 5-10. The next conductor failures appeared to involve Conductors 3 and 4 shorting to each other and to ground at approximately the same time (time ~ 2767 seconds). The exact progression of the failures cannot be discerned because the transitions all occurred within a single full cycle of the IR

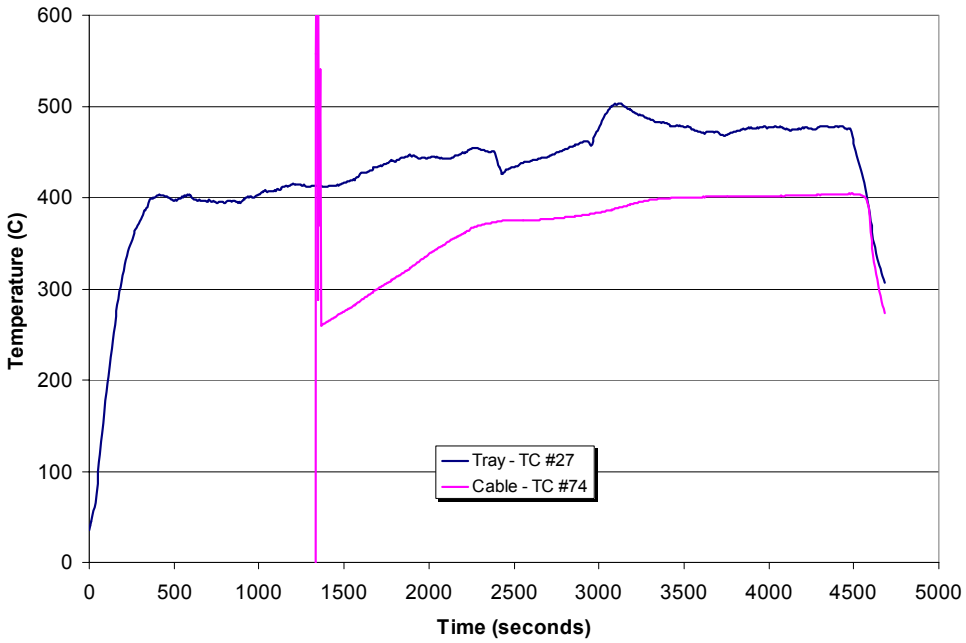

Figure 5-9. Representative tray and TC-4 cable temperatures recorded during Test 3.

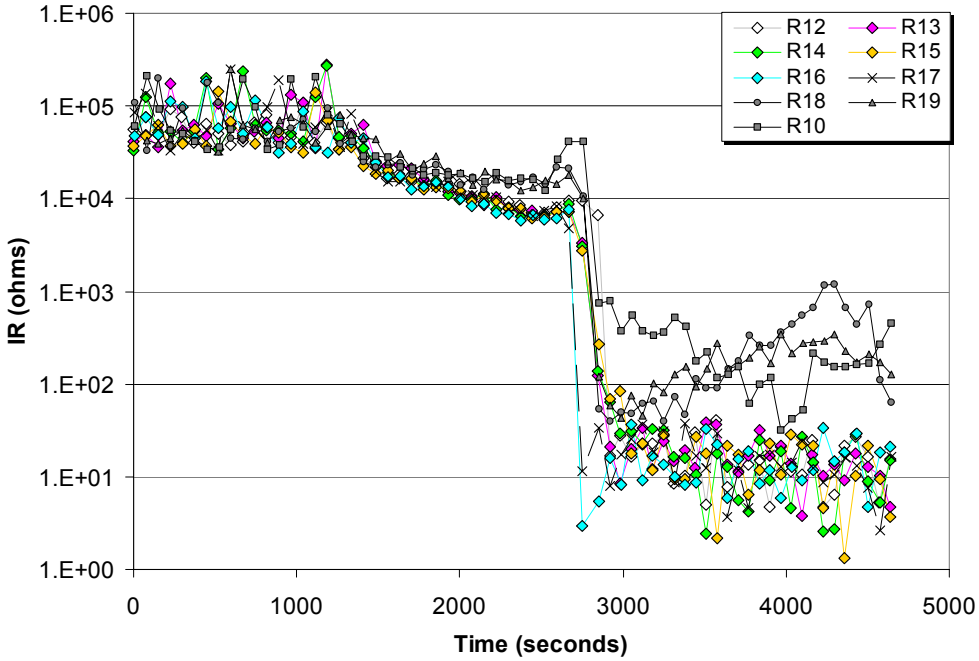

Figure 5-10. Representative conductor-to-conductor IRs obtained during Test 3.

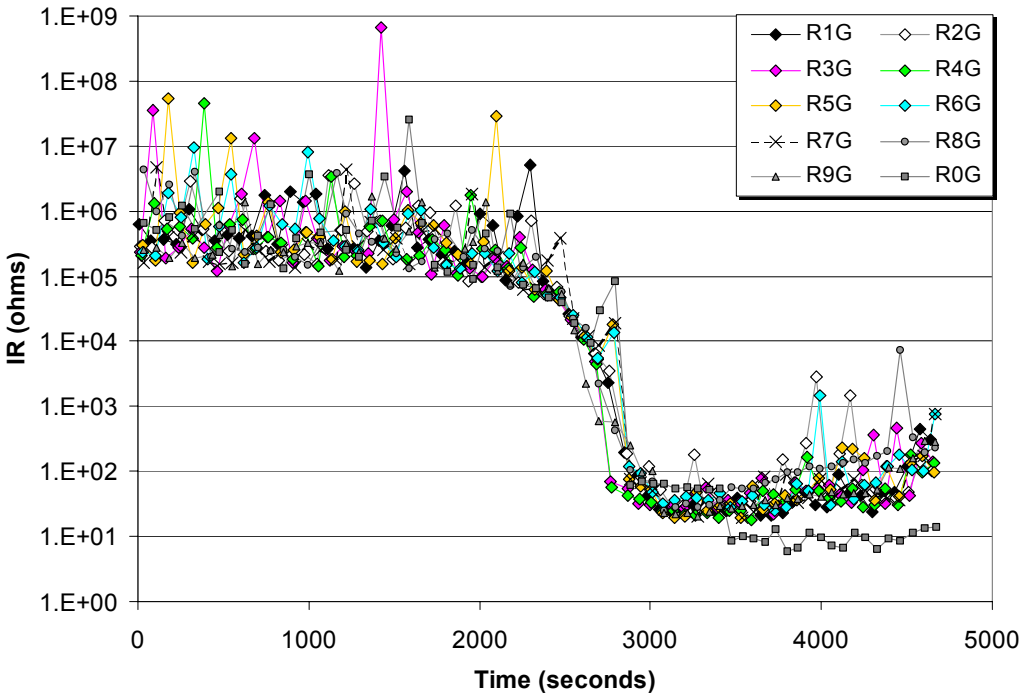

Figure 5-11. Conductor-to-ground IRs obtained during Test 3.

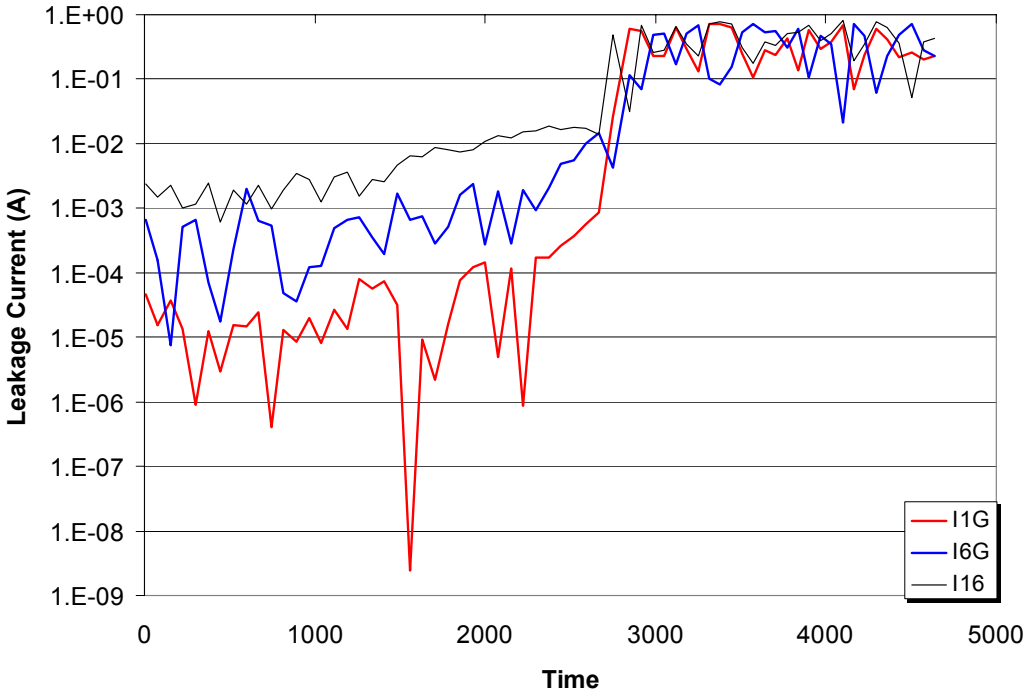

Figure 5-12. Leakage currents resulting from IR changes in Conductors 1 and 6 during Test 3.

Table 5-1. Approximate Conductor Failure Times and Modes in Test 3

Time (s)	Failure Mode
2751	Conductor 1 shorts to Conductors 6 and 7
2767–2773	Conductors 3 and 4 short to each other and to ground at approximately the same time (exact progression cannot be discerned due to measurement cycle time)
2852–2875	Conductor 8 shorts to several conductors (1, 2, 3, 4)
2873–3009	All conductors short to ground

measurement system (less than one minute). Between 2852 and 2875 seconds, Conductor 8, one of the three external conductors, apparently shorted to several conductors in the multiconductor cable; namely, Conductors 1, 2, 3, and 4. Finally, between 2873 and 3009 seconds, all remaining conductors shorted to ground.

Based on the results of the IR measurements made during Test 3, it appears that the IR cable bundle did experience substantial fire-induced damage. The degradation of IR was sufficient to allow leakage currents high enough to possibly cause either device actuation or blown fuses in a control circuit.

The specific mode of cable failure during Test 3 appears to have involved both conductor-to-conductor shorts and shorts-to-ground at roughly the same time during the test. The initial failure mode was intracable conductor-to-conductor shorting within the multiconductor cable. The time from this initial failure to all conductors shorting to ground was approximately four minutes. For the three external 1/C cable conductors, the first failure appeared to be an intercable conductor-to-conductor short, but this short appears to have transitioned almost immediately to a short-to-ground. As noted, the conductor-to-ground IR degradation was relatively smooth and consistent for all of the conductors. In contrast, the conductor-to-conductor IRs show somewhat more abrupt transitions to shorting with specific conductor combinations. Note, for example, the case of Conductor 1: there is an apparent abrupt short transition involving Conductors 6 and 7 at about 2750 seconds. The IR between Conductor 1 and the external Conductors 8 through 10 remains higher than that to the internal conductors for the duration of the test.

5.2 Tests 4 through 8

Tests 4 through 8 were conducted after the discovery and correction of the reverse polarity problem on the building receptacle feeding the IR measurement system. These tests were all conducted at 120 VAC on the power supply side to the test cable bundle. The types of cables tested included thermoplastic materials as well as thermoset cables.

Failures were noted in four of these five tests, Test 5 being the exception, with no observed failures.

5.2.1 Test 4

Test 4 was a 145-kW heat release rate fire with thermoplastic test cable bundles and thermoset cable used as supplemental tray fill. The IR sample bundle was, again, a seven-conductor cable bundled with three single-conductor cables. Conductor 1 represents the central conductor of the multiconductor cable, Conductors 2 through 7 represent the other conductors in the multiconductor cable connected in sequence going around the cable (i.e., Conductor 7 is next to Conductor 2, which is next to Conductor 3, which is next to Conductor 4, etc.). Conductors 8 through 10 represent the three external conductors. The IR system was operated in AC mode. Various conductor failures were observed in this test.

The cables were laid in a horizontal tray and exposed to the fire plume at the corner of the tray. Figure 5-13 shows the time-temperature plots for two of the thermocouples monitored during the test. Two thermocouples were chosen to illustrate the worst-case temperature exposure conditions (highest recorded temperatures) for the air near the IR bundle and for the instrumented cable closest to the IR bundle. TC #27 was mounted on a rung at the corner of the tray, and TC #73 was located about mid-position on the instrumented cable TC-4. The peak tray temperature was 417°C (783°F) and the peak cable temperature recorded during this test was 287°C (549°F).

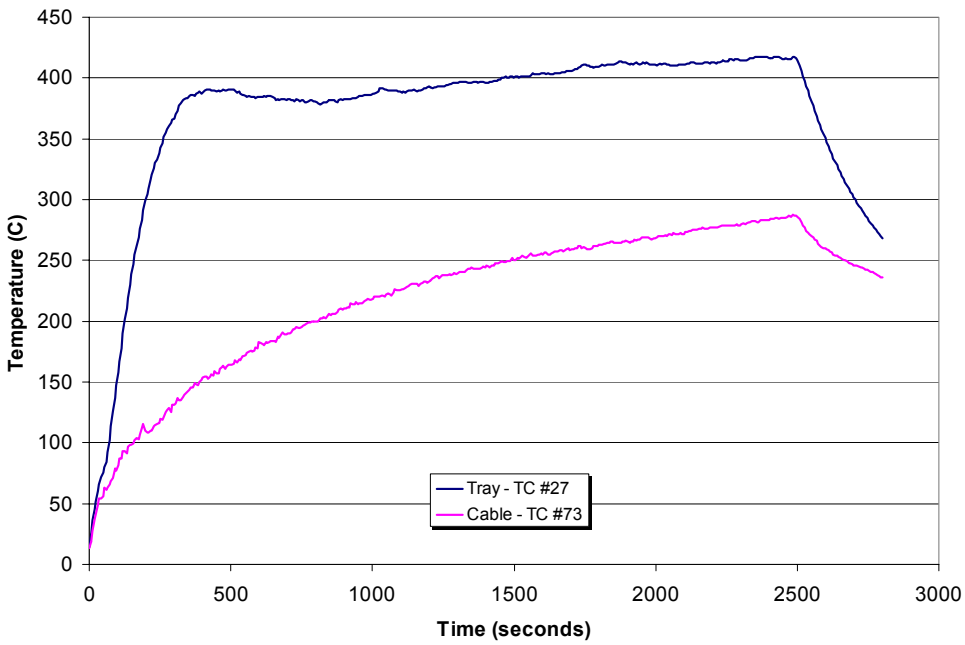

Figure 5-13. Representative tray and TC-4 cable temperatures recorded during Test 4.

Figure 5-14 shows the changes in IR occurring between Conductor 5 of the multiconductor cable and each of the other conductors in the IR bundle during the test. The apparent decrease in IR between Conductors 5 and 8, by about an order of magnitude, is the result of conductor 8 being shorted to ground rather than an actual indication of the conductor-to-conductor IR. Figure 5-14 clearly shows an intercable conductor-to-conductor short between Conductors 5 and 10 occurring at ~1032 seconds. Conductors 4 and 9 join this shorting group at ~1200 seconds, a second intercable and the first intracable conductor-to-conductor short. The abrupt reduction in the other IR values at ~1400 seconds reflects all the conductors shorting to ground in a relatively short period of time.

Figure 5-15 shows the conductor-to-ground IR for each conductor in the bundle. Figure 5-15 illustrates a gradual decrease from the initial IR (~10^6 Ω) to ground for the conductors until they individually short to ground during the test. At approximately 374 seconds into the test, Conductor 8, one of the three external conductors, shows a clear short to ground – the first actual failure observed. The remaining conductors short to ground over the period of ~1200 to 1500 seconds.

Table 5-2 summarizes that nature of the various cable failure modes observed for Test 4. In this table, failure is defined as an IR drop to below 100 Ω, either between conductor pairs or between a conductor and ground. In general, the conductors each saw a relatively abrupt drop in IR values from about 10^5 Ω down to 10 Ω or less over the period of one or, at most, two measurement cycles. This precipitous drop in IR was defined as a failure.

Note that the first failure observed was a short-to-ground on one of the external single-conductor cables (C8). This failure occurred rather early in the test (~374 seconds) compared to the subsequent failures. The next failures involved intracable conductor-to-conductor hot shorts. The first of these involved a second 1/C external conductor (C10) shorting to a conductor within the multiconductor cable (C5). A short time later, the third external conductor (C9) and a second adjacent conductor within the multiconductor cable (C4) joined this shorting group. At about the same time, one of the internal conductors (C6) shorted to ground. A second hot-short group then formed involving two conductors within the multiconductor cable (C1, and C7). All of the remaining conductors (i.e., except C8 and C6) short to ground over the period between 1280 to 1480 seconds.

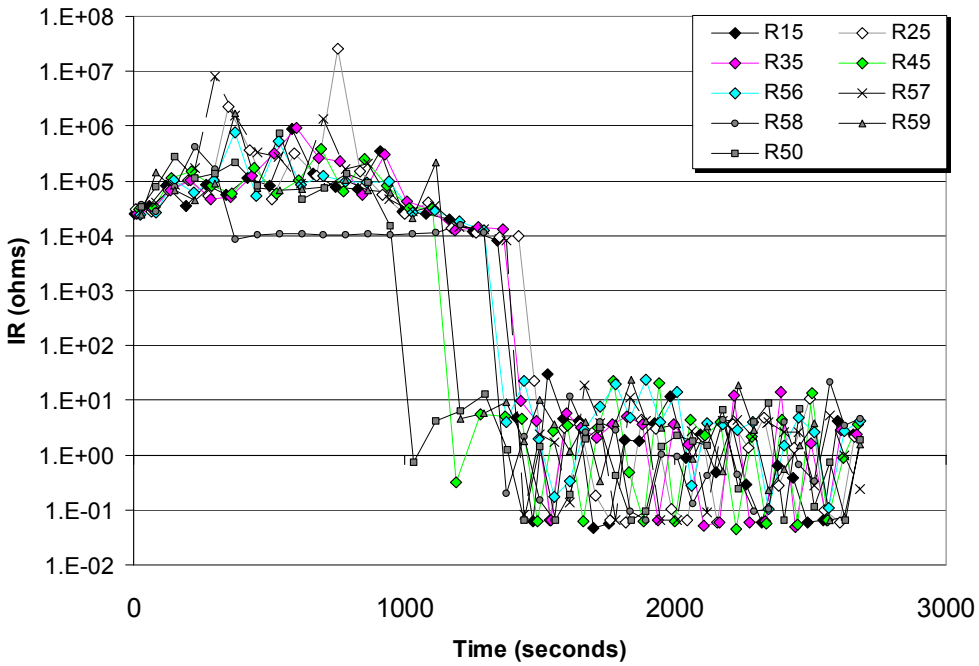

Figure 5-14. Representative conductor-to-conductor IRs obtained during Test 4. This plot shows the IRs between Conductor 5 and the other nine conductors in the IR cable bundle.

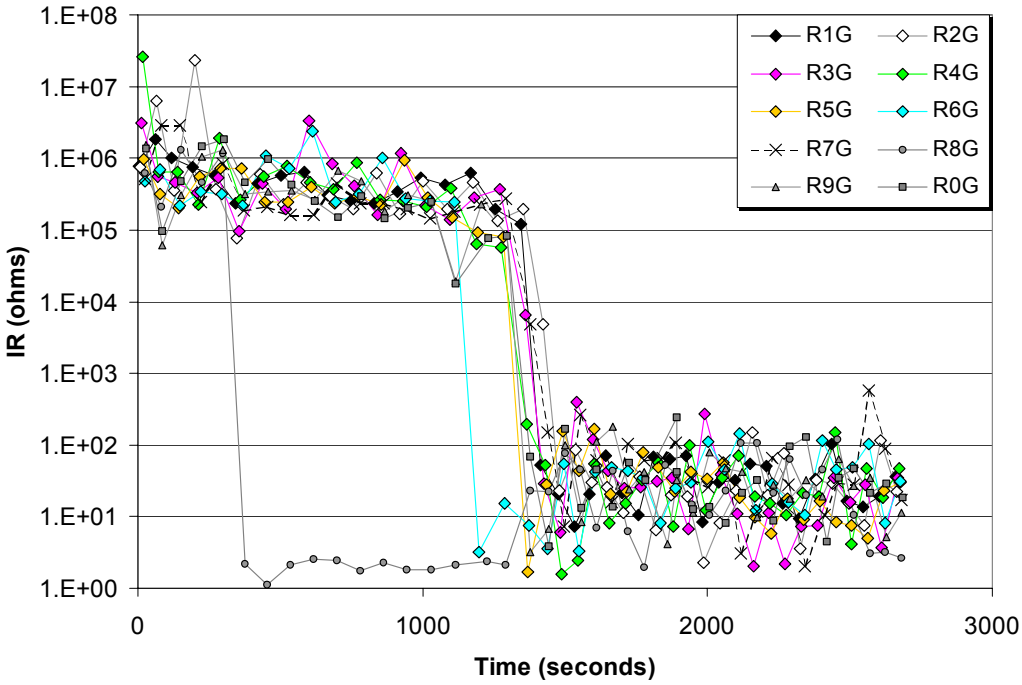

Figure 5-15. Conductor-to-ground IRs obtained during Test 4.

Table 5-2. Summary of Cable Failure Times and Modes during Test 4

Time (s)	Failure Mode Observed
~374	Conductor 8 shorts to ground – external 1/c to ground
~1032	Conductor 10 shorts to conductor 5 – external 1/c to internal conductor (intracable conductor-to-conductor short)
~1192	Conductors 4 and 9 join in the short circuit between Conductors 5 and 10 – two externals and two internals shorted
~1197	Conductor 6 shorts to ground
~1346	Conductors 1 and 7 short together – internal conductors shorted
~1365–1379	Conductors 4, 5, and 10 short to ground
~1415–1442	Conductors 1, 3, 7, and 9 short to ground
by 1480	All conductors have shorted to ground

Various artifacts appear in the data as a result of the early short-to-ground on Conductor 8. For example, Figure 5-15 shows an apparent reduction in IR between Conductor 5 and Conductor 8 at about the time Conductor 8 shorted to ground. This is attributed to the fact that Conductor 8 shorted to ground, rather than an actual short between Conductors 5 and 8. Other conductors also saw similar behavior in relationship to Conductor 8 following Conductor 8's short to ground. These data are thought to be an artifact of the early short-to-ground on Conductor 8 rather than reflective of actual behaviors.

Figure 5-16 shows a plot of how the leakage currents for Conductors 5 and 10 changed in their relationship to one another and to ground as the test progressed.

Based solely on the results of the IR measurements made during Test 4, it appears that the IR cable experienced fire-induced damage that allowed leakage currents high enough to cause device actuation or blown fuses. The faults included both shorts-to-ground and conductor-to-conductor hot shorts. Two of the three external single conductor cables shorted to conductors of the multiconductor cable before shorting to ground while the third single conductor shorted to ground early in the test.

5.2.2 Test 5

Test 5 was a 200-kW heat release rate fire with thermoset test cable bundles. The cables were laid in a horizontal tray, positioned 2.1 m (7 ft) above the floor, and exposed to the hot gas layer. The burner was offset from the corner of the tray by 0.6 m (2 ft). The IR sample bundle was, again, a seven-conductor cable bundled with three single-conductor cables and was wired in the same manner as described for Test 4. The IR system was operated in AC mode. No conductor failures were observed in this test.

Figure 5-17 shows the time-temperature plots for two of the thermocouples monitored during Test 5. These two thermocouples were chosen because they showed the worst-case temperature exposure conditions (highest recorded temperatures) for the air near the IR bundle and for the instrumented cable closest to the IR bundle. TC #40 was located at about the center of the tray's width, approximately 0.6 m (2 ft) from the doorway end of the tray and oriented so that it was monitoring the air temperature above the cables filling the tray. TC #69 was located at about 0.3 m (1 ft) from the doorway end of the tray on the instrumented cable TC-4. The peak air temperature recorded was 356°C (673°F) and the peak cable temperature was 330°C (626°F) during this test.

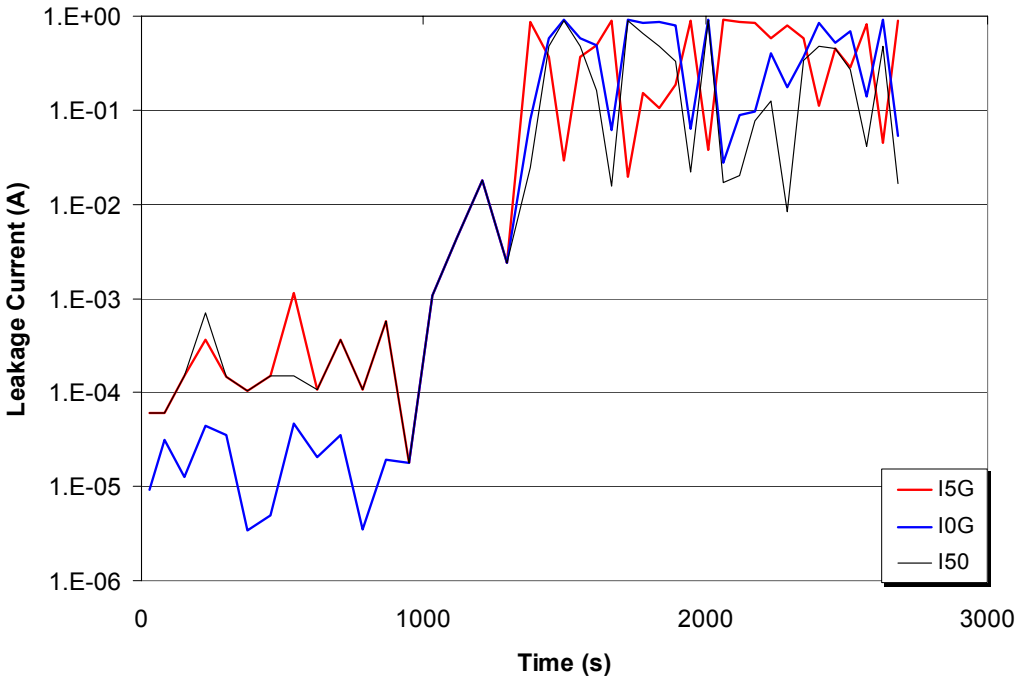

Figure 5-16. Leakage currents resulting from IR changes between Conductors 5 and 10 during Test 4.

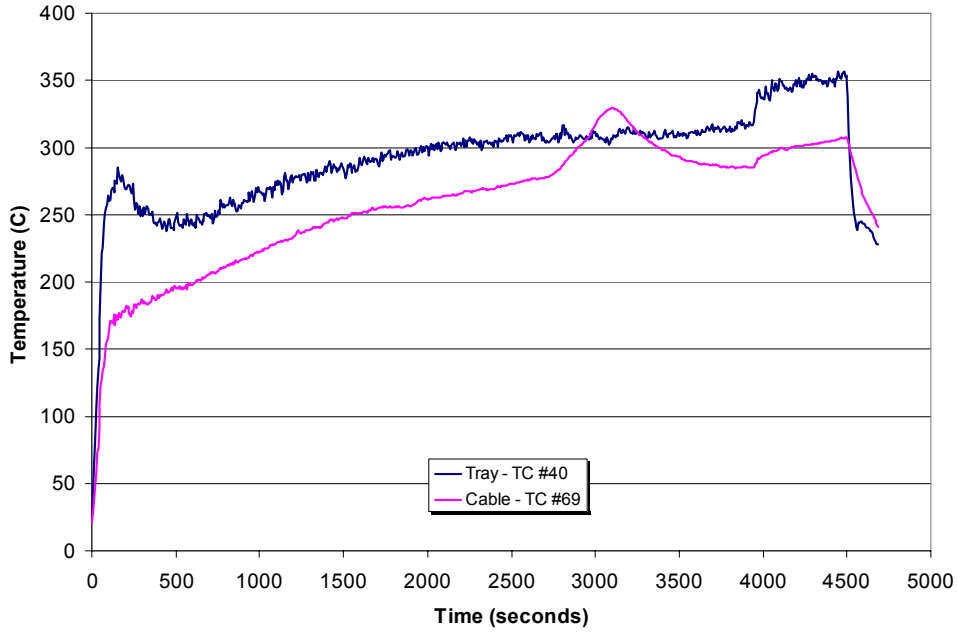

Figure 5-17. Representative tray and TC-4 cable temperatures recorded during Test 5.

As Figure 5-18 shows, no changes in IR occurred between Conductor 1 and any of the other conductors in the IR cable during the test. Conductor 1 was the center conductor in the seven-conductor cable and the other six conductors surround Conductor 1 and are immediately adjacent to it. Conductors 8, 9, and 10 are the three single conductor cables bundled with the seven-conductor cable to make up the IR bundle.

The IR to ground of the individual conductors remained nearly constant over time, as shown in Figure 5-19. Figure 5-20 shows a plot of how the leakage currents for Conductors 1 and 2 changed in their relationship to one another and to ground as the test progressed. Leakage currents remained at very low levels throughout the test.

Based solely on the results of the IR measurements made during Test 5, it appears that the IR cable experienced virtually no damage and would not have caused any device actuation or blown fuses.

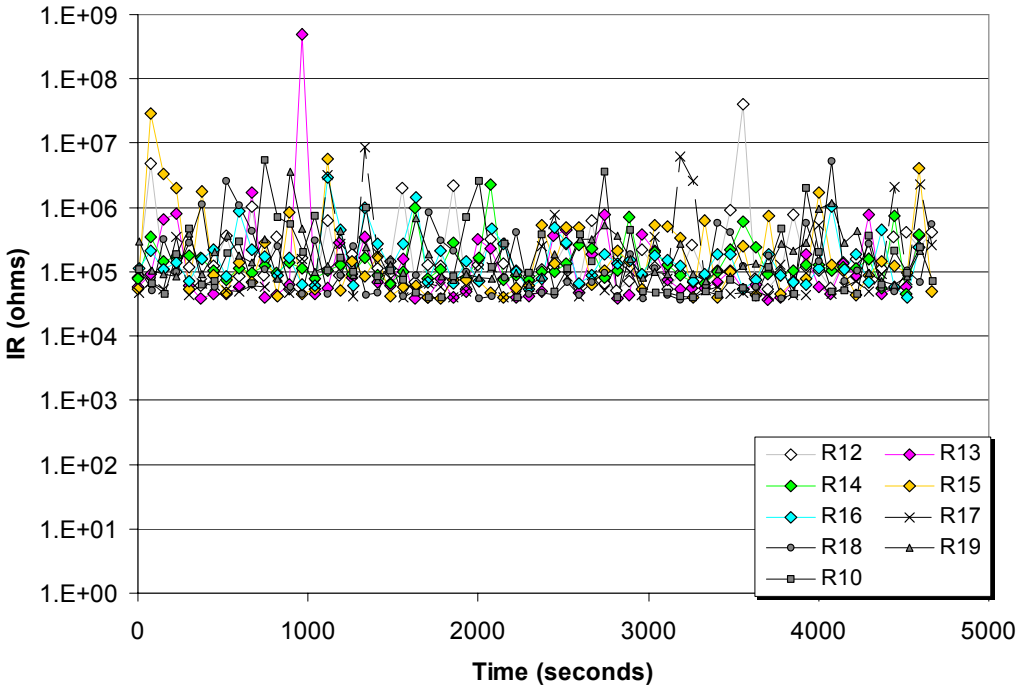

Figure 5-18. Representative conductor-to-conductor IRs obtained during Test 5.

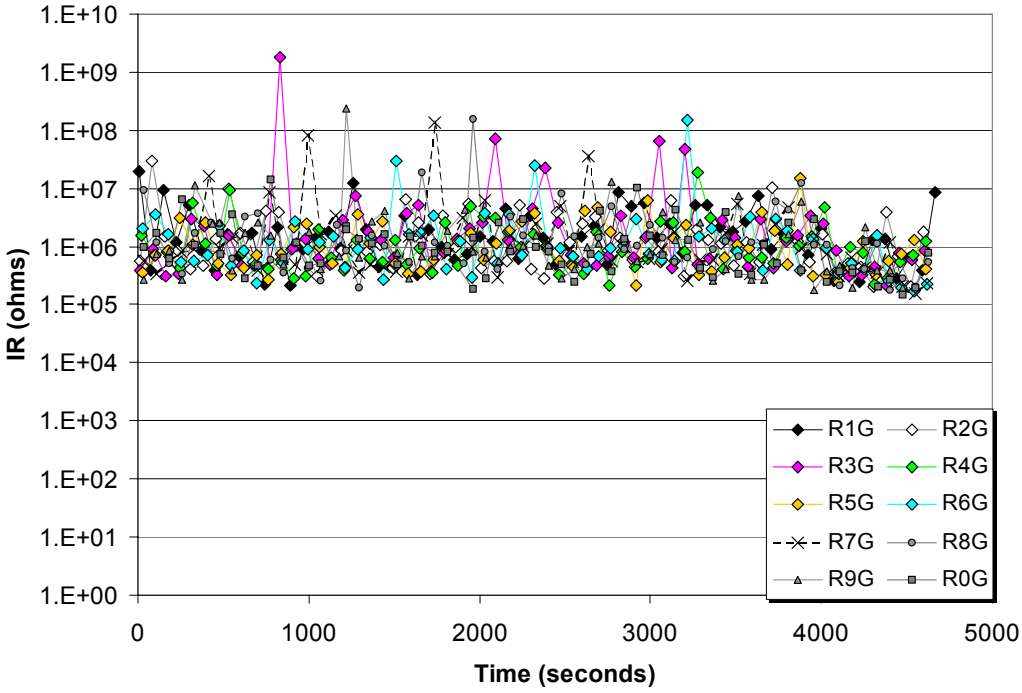

Figure 5-19. Conductor-to-ground IRs obtained during Test 5.

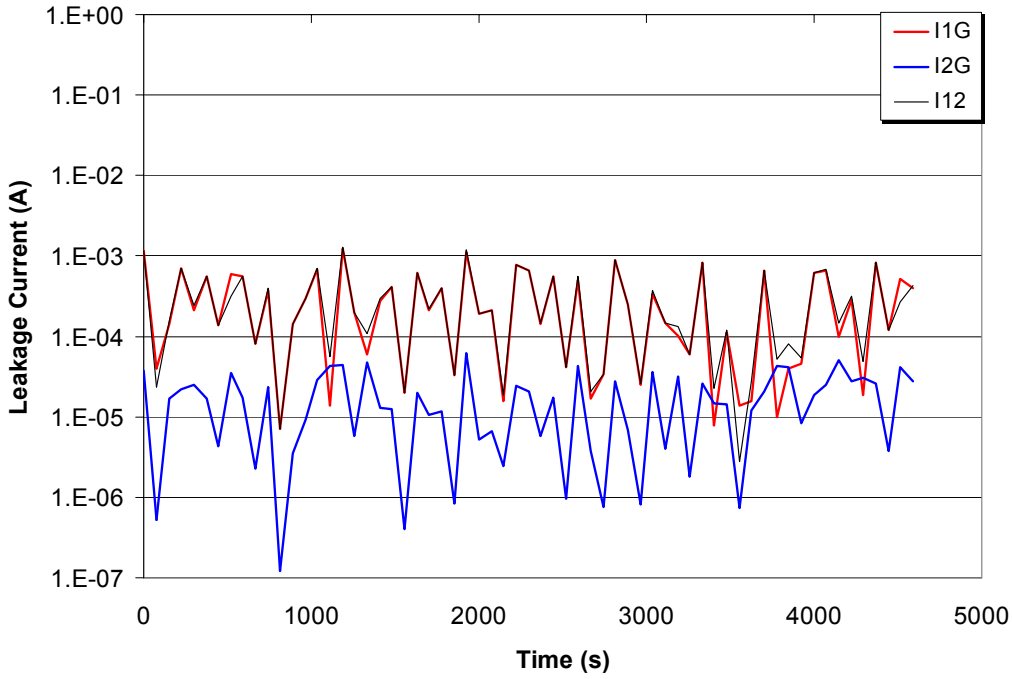

Figure 5-20. Leakage currents resulting from IR changes between Conductors 1 and 2 during Test 5.

5.2.3 Test 6

Test 6 was a 200-kW heat release rate fire with thermoplastic test cable bundles. The cables were laid in a horizontal tray, positioned 2.1 m (7 ft) above the floor, and exposed to the hot gas layer. Thermoset cables were used as fill in the tray. The burner was placed in the center of the fire test cell. The IR sample bundle was, again, a seven-conductor cable bundled with three single-conductor cables and wired in the same manner as described for Test 4. The IR system was operated in AC mode. Various conductor failures were observed in this test.

Figure 5-21 shows the time-temperature plots for two of the thermocouples monitored during the test. These two thermocouples were chosen because they showed the worst-case temperature exposure conditions (highest recorded temperatures) for the air near the IR bundle and for the instrumented cable closest to the IR bundle. TC #40 was located at the center of the tray's width approximately 0.6 m (2 ft) from the doorway end of the tray and oriented so that it was monitoring the air temperature above the cables filling the tray. TC #61 was located at the mid-position on the instrumented cable TC-3. A fourth (TC-4) instrumented cable was not included in this test. The peak temperatures recorded during this test were 356°C (673°F) in the air around the cable tray and 299°C (570°F) on the instrumented cable in the tray.

As Figure 5-22 shows, changes in IR occurred between Conductor 4 and the other conductors in the IR cable at about 1870 to 2100 seconds into the test. Conductor 1 was the center conductor in the seven-conductor cable and the other six conductors surrounded Conductor 1 and were immediately adjacent to it. Conductors 8, 9, and 10 are the three single conductor cables bundled with the seven-conductor cable to make up the IR bundle.

Table 5-3 summarizes the various failure times and modes for Test 6. The IR of Conductors 8 and 10 to ground dropped to ~3 Ω between 1730 and 1740 seconds. Conductor 9 appears to have shorted to Conductor 4 at about 1989 seconds, an intercable conductor-to-conductor hot short. These two conductors subsequently shorted to ground between 2123 and 2134 seconds. All of the remaining conductors shorted to ground over the time interval of 1990 to 2126 seconds, as shown in Figure 5-23. Figure 5-24 shows a plot of how the leakage currents for Conductors 4 and 9 changed in their relationship to one another and to ground as the test progressed. Peak leakage currents reached ~1 A.

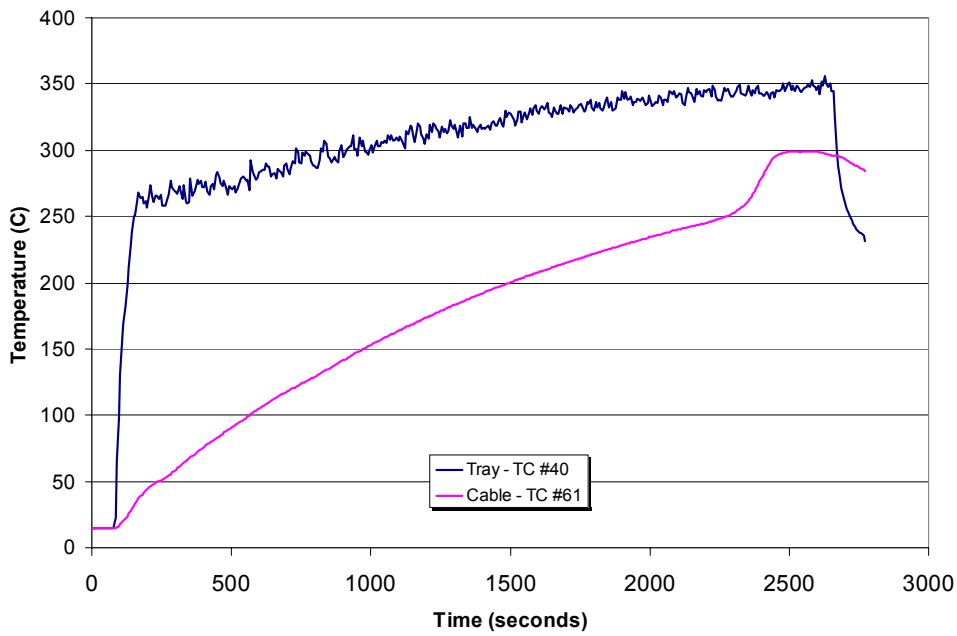

Figure 5-21. Representative tray and TC-3 cable temperatures recorded during Test 6.

Based solely on the results of the IR measurements made during Test 6, it appears that the IR cable experienced fire-induced damage that allowed leakage currents high enough to cause device actuation or blown fuses.

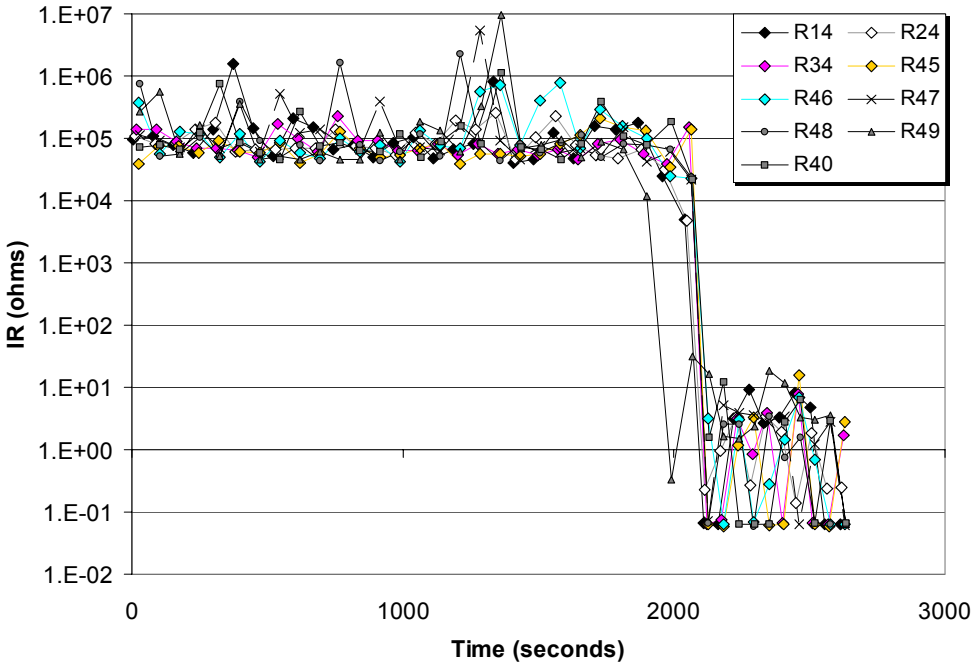

Figure 5-22. Representative conductor-to-conductor IRs obtained during Test 6. This plot shows the resistance between Conductor 4 and the other nine conductors in the IR cable bundle.

Table 5-3. Summary of Cable Failure Times and Modes during Test 6

Time (s)	Failure Mode Observed
~ 1700	Conductors 8 and 10 short to ground – external 1/C conductor to ground (failure induces IR artifacts on conductor 1)
~ 1989	Conductors 4 and 9 short – external 1/C to a conductor of the multiconductor (inter-cable conductor-to-conductor hot short)
~ 1993	Conductor 7 shorts to ground
~ 2039-2126	Conductors 1, 2, 3, 5, and 6 short to ground
~ 2123-2134	Conductors 4 and 9 short to ground

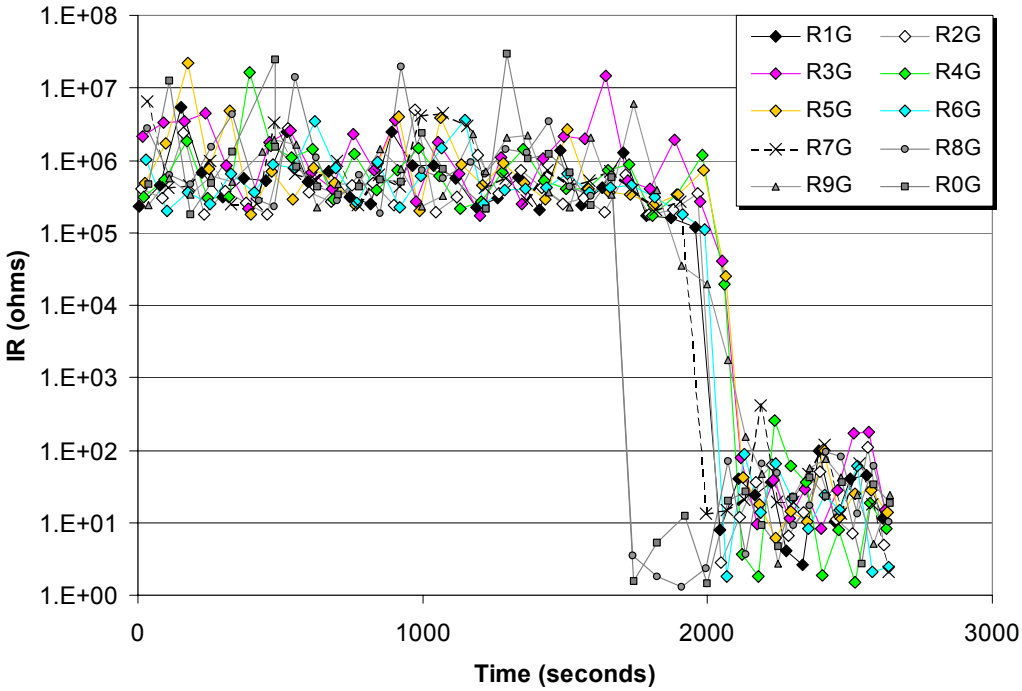

Figure 5-23. Conductor-to-ground IRs obtained during Test 6.

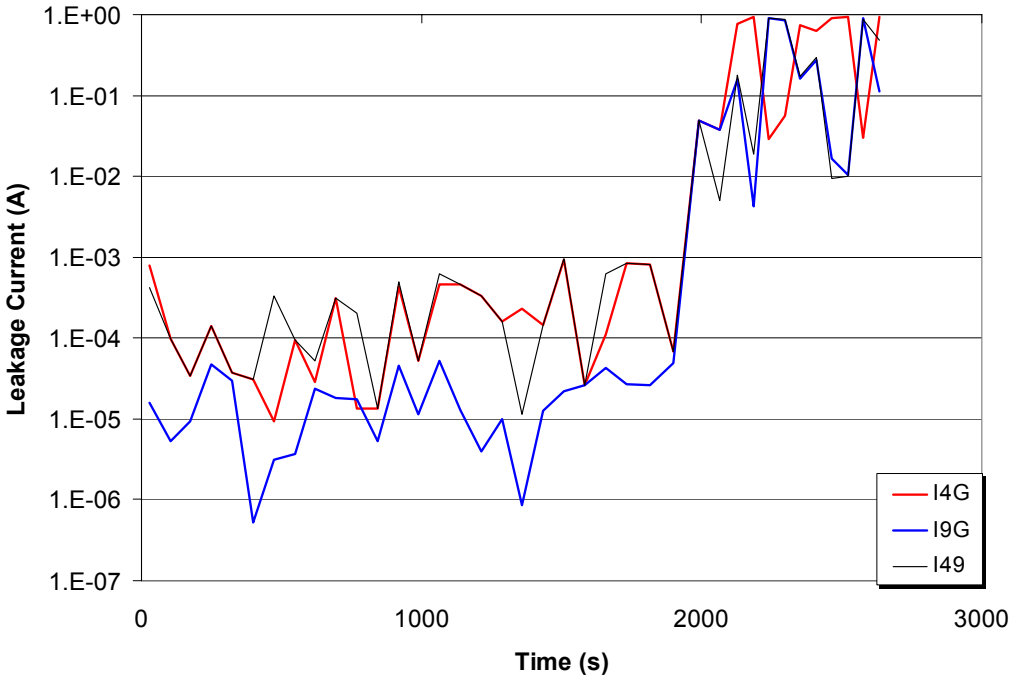

Figure 5-24. Leakage currents resulting from IR changes between Conductors 4 and 9 during Test 6.

5.2.4 Test 7

Test 7 was a 350-kW heat release rate fire with thermoset test cable bundles. The cables were laid in a horizontal tray, positioned 2.1 m (7 ft) above the floor, and exposed to the hot gas layer. The burner was placed in the center of the fire test cell. The IR sample bundle was, again, a seven-conductor cable bundled with three single-conductor cables and wired in the same manner as described for Test 4. The IR system was operated in AC mode. Various conductor failures were observed in this test

Figure 5-25 shows the time-temperature plots for two of the thermocouples monitored during the test. These two thermocouples were chosen because they showed the worst-case temperature exposure conditions (highest recorded temperatures) for the air near the IR bundle and for the instrumented cable closest to the IR bundle. TC #17 was mounted on the side of the tray about 1.2 m (4 ft) from the doorway, and TC #77 was located about 0.3 m (1 ft) from the end of the tray further from the doorway on the instrumented cable TC-4. The peak tray temperature was 526°C (979°F) and then dropped and stabilized at ~500°C (932°F). The peak cable temperature was 492°C (918ºF).

As Figure 5-26 shows, two transitions in IR occurred between Conductor 5 and the other conductors in the seven-conductor cable over the time interval of 1700 to 3100 seconds (10^5 Ω down to ~2,000 Ω) and again at 3100 to 3260 seconds (2000 Ω to ~1 Ω) during the test. Conductor 1 was the center conductor in the seven-conductor cable and Conductors 2 through 7 surrounded Conductor 1 and were immediately adjacent to it. Conductors 8, 9, and 10 are the three single-conductor cables bundled with the seven-conductor cable to make up the IR bundle.

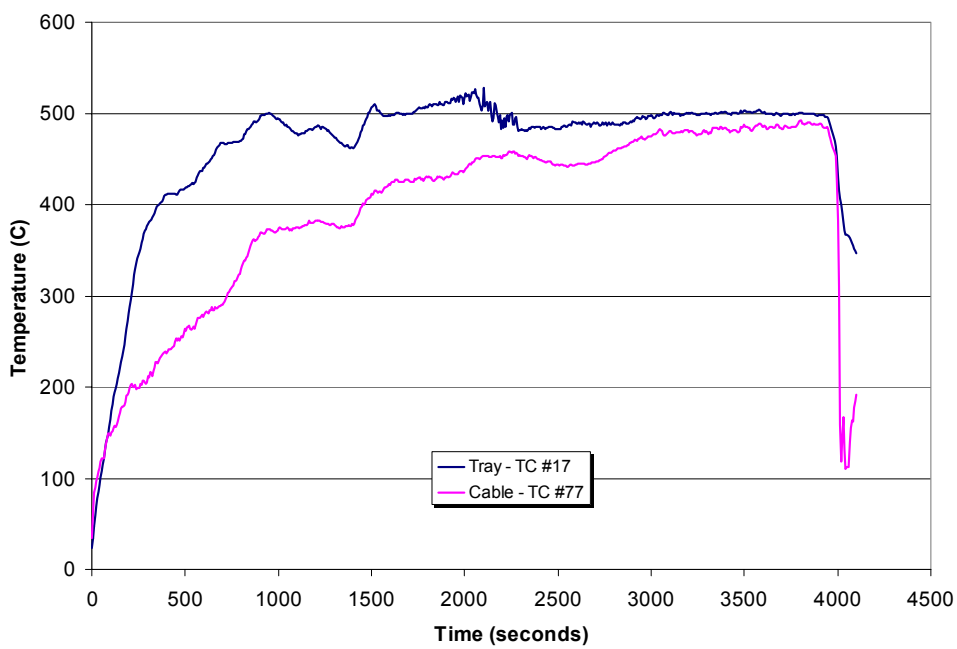

Figure 5-25. Representative tray and TC-4 cable temperatures recorded during Test 7.

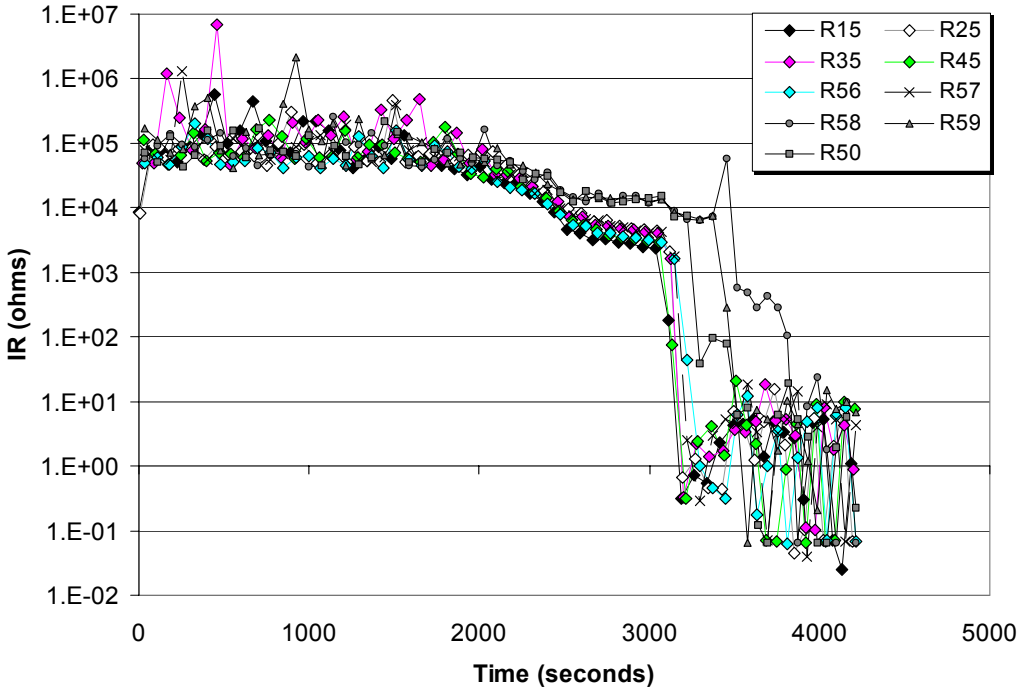

Figure 5-26. Representative conductor-to-conductor IRs obtained during Test 7. This plot shows the IR between Conductor 5 and the other nine conductors in the IR cable bundle.

The IR of the individual conductors to ground demonstrated three transitions in IR, as shown in Figure 5-27. The first occurred at 1660 to 2100 seconds, the next was at 2625 to 3220 seconds, and finally the IRs went as low as 10 Ω at 3220 to 3600 seconds.

Table 5-4 summarizes the conductor failure modes and times for Test 7. The first failures observed involved a rather complex sequence of intracable failures within the multiconductor cable. Initially, at about 3134 seconds, Conductors 4 and 5 shorted together. This shorting group was joined by Conductors 1 and 3 about 54 seconds later, and by Conductor 2 an additional 7 seconds later. A second independent internal short between Conductors 6 and 7 is observed at about 3228 seconds. By 3264 seconds, it appears that all of the seven conductors within the multiconductor cable have shorted together. The next failures involve various shorts to ground beginning with Conductor 10, which shorts to ground at about 3298 seconds. The remaining conductors, with the exception of Conductor 8, short to ground between 3431 and 3514 seconds. Conductor 8 is the last conductor to fail, and shorts to ground at 3872 seconds.

Figure 5-28 plots how the leakage currents for Conductors 4 and 5 changed in their relationship to one another and to ground as the test progressed.

Based solely on the results of the IR measurements made during Test 7, it appears that the IR cable experienced fire-induced damage that allowed leakage currents high enough to cause device actuation or blown fuses.

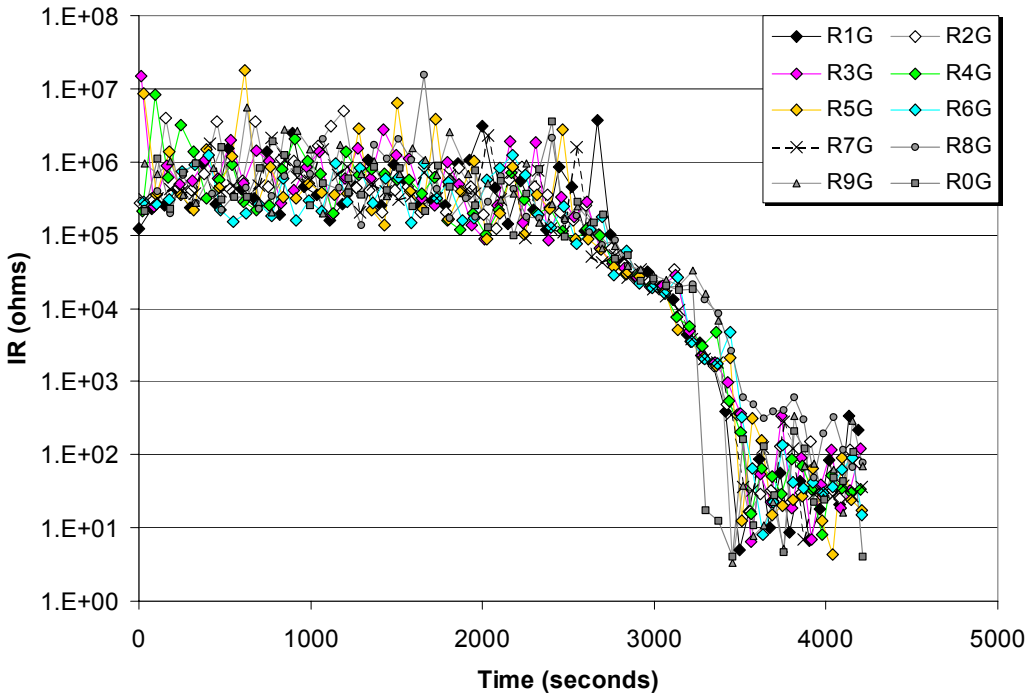

Figure 5-27. Conductor-to-ground IRs obtained during Test 7.

Table 5-4. Summary of Cable Failure Times and Modes during Test 7

Time (s)	Failure Mode Observed
~ 3134	Conductors 4 and 5 short – intracable conductor-to-conductor hot short within the multiconductor cable
~ 3188	Conductors 1 and 3 join short involving 4 and 5
~ 3195	Conductor 2 joins short involving 1, 3, 4, and 5
~ 3228	Conductors 6 and 7 form a separate short
~ 3264	All conductors of the multiconductor cable (C1-C7) have shorted together
~ 3298	Conductor 10 shorts to ground
~3431-3514	Conductors 1 through 7 and 9 short to ground
~ 3872	Conductor 8 shorts to ground

5.2.5 Test 8

Test 8 was a 145-kW heat release rate fire with thermoset test cable bundles. The cables were laid in a horizontal tray, positioned 1.8 m (6 ft) above the floor, and exposed to the plume. In addition, one of the industry test cables, one IR cable, and one cable instrumented with thermocouples were place inside a steel conduit, which was mounted along the inner edge of the cable tray (see Figure 5-29). The burner was placed under the corner of the tray. There were actually two IR sample cables in this test. Both were five-conductor cables, one located in the tray and one located in the conduit. Conductors 1 through 5 represent the cable in the tray while Conductors 6 through 10 represent the cable in the conduit. The conductors in each cable were wired in sequential order following the conductors

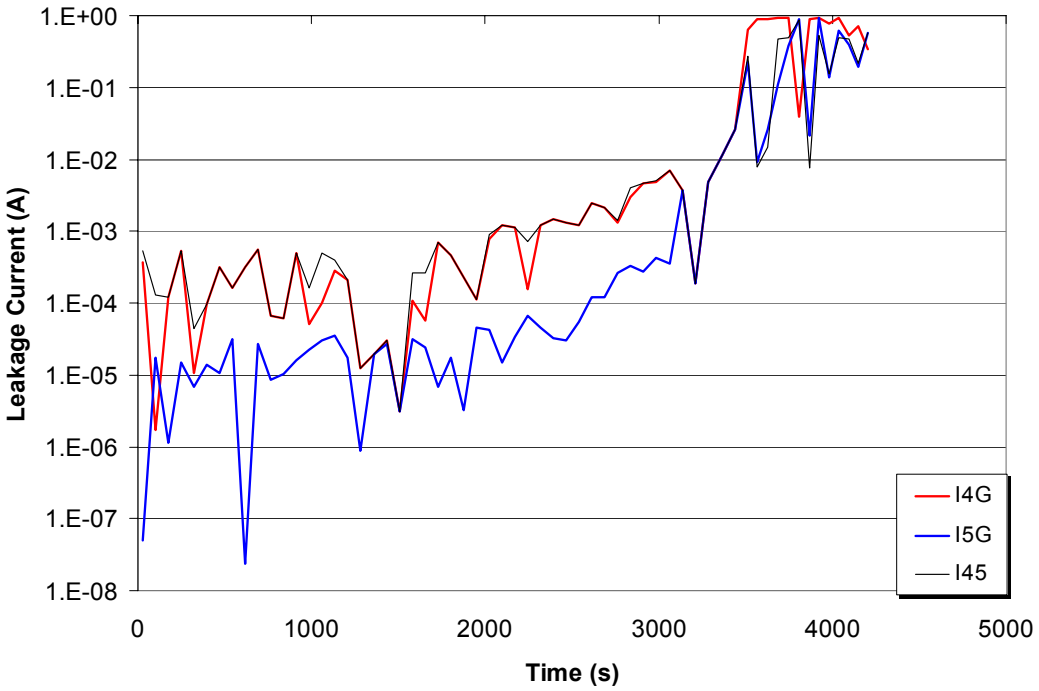

Figure 5-28. Leakage currents resulting from IR changes between Conductors 4 and 5 during Test 7.

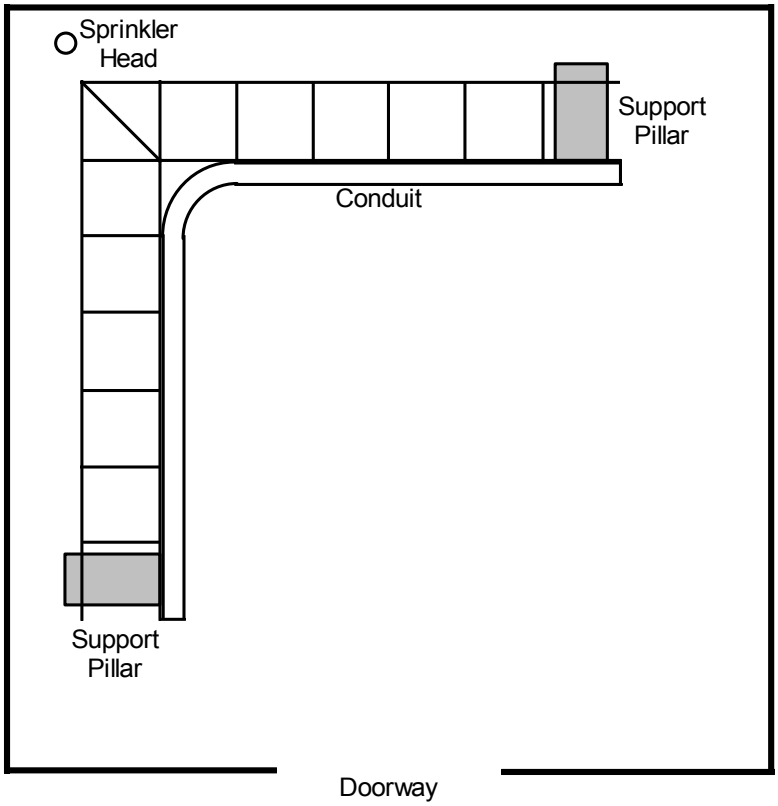

Figure 5-29. Overhead sketch of the tray and conduit locations in the fire test cell during Test 8.

around the cable (the five conductors in each cable were in the configuration of a single ring of conductors with no central conductor). No single conductor cables were bundled with either of the two five-conductor cables that made up the IR test cables. The IR system was operated in AC mode.

The cable located in the tray saw no significant failures. However, various conductor failures were observed for the cable in the conduit.

Figure 5-30 shows the time-temperature plots for four of the thermocouples monitored during the test. These thermocouples were chosen because they showed the worst-case temperature exposure conditions (highest recorded temperatures) for the air near the IR bundle and for the instrumented cable closest to the IR bundle. TC #25 was mounted on a rung located near the corner of the tray; TC #14 was located on the side of the tray near the corner and next to the conduit; TC #73 was located about mid-position on the instrumented cable TC-4 in the cable tray; and TC #45 was located near mid-position on the instrumented cable TC-1 inside the conduit. As indicated in the figure, the peak tray temperature was 536°C (997°F) but then decreased and stabilized at 485°C (905°F) for the duration of the test. The peak temperature of the IR cable laid in the tray was 316°C (601°F). The peak conduit temperature was 417°C (783°F), whereas the peak temperature of the cable located inside the conduit was 422°C (792ºF).

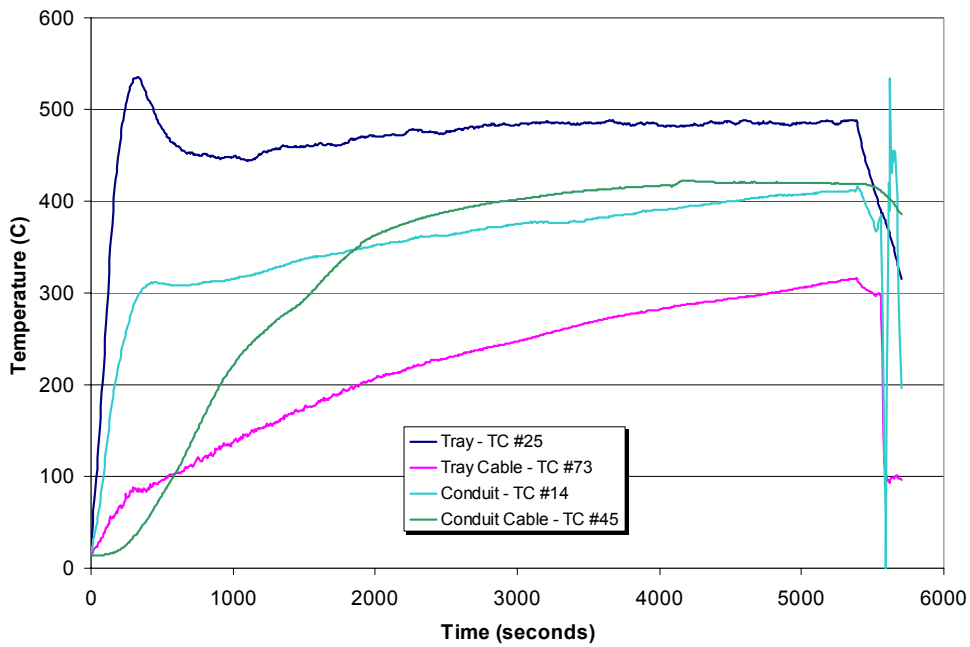

Figure 5-30. Representative temperatures for tray, conduit, TC-1, and TC-4 cables recorded during Test 8.

As Figure 5-31 shows, none of the conductors for the IR cable located in the tray appear to suffer significant degradation. The IR between Conductor 1 and the other conductors in the cable (2–5) remained at about 10^5 Ω throughout the test.

Figure 5-32 shows two transitions in IR occurring between Conductor 7 and the other conductors in the IR cables located in the conduit. The first transition is a relatively smooth degradation of IR between about 2000 seconds and 4200 seconds when the IRs between Conductor 7 and the other conductors in the cable in the conduit decreased from 10^5 down to 10^3 Ω. This is followed by relatively abrupt drops in IR to about 10 Ω at ~4200 seconds.

The IR of the individual conductors to ground demonstrated four transitions in IR, as shown in Figure 5-33. The first occurs between 2770 and 4100 seconds and involves a steady and relatively consistent degradation in all IR values.

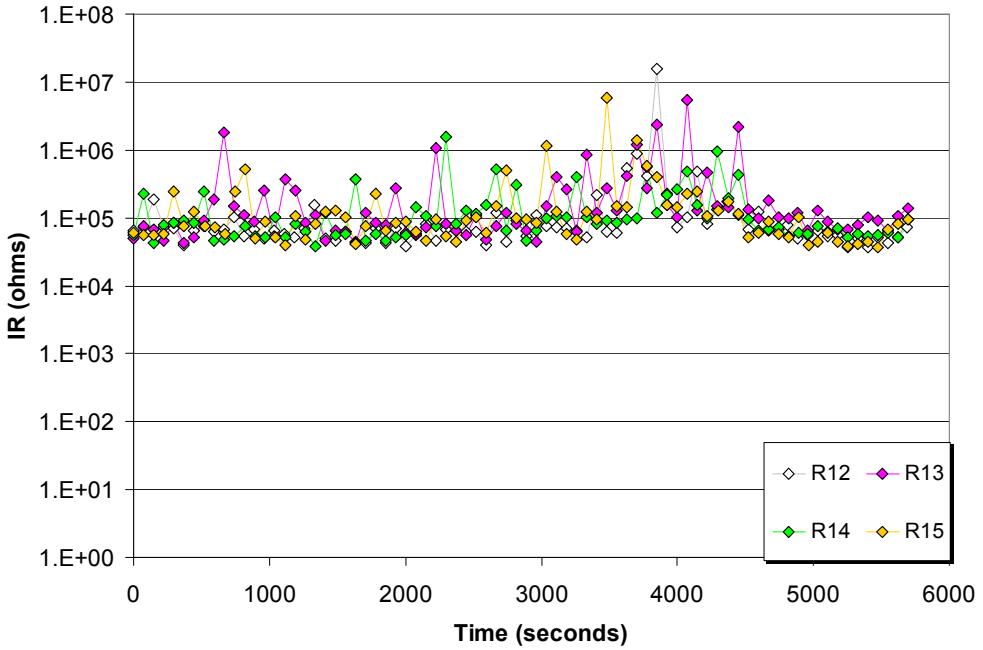

Figure 5-31. Representative conductor-to-conductor IRs for cable IR1 in the cable tray during Test 8. This plot shows the IR between Conductor 1 to the other four conductors in the cable located in the tray during the test.

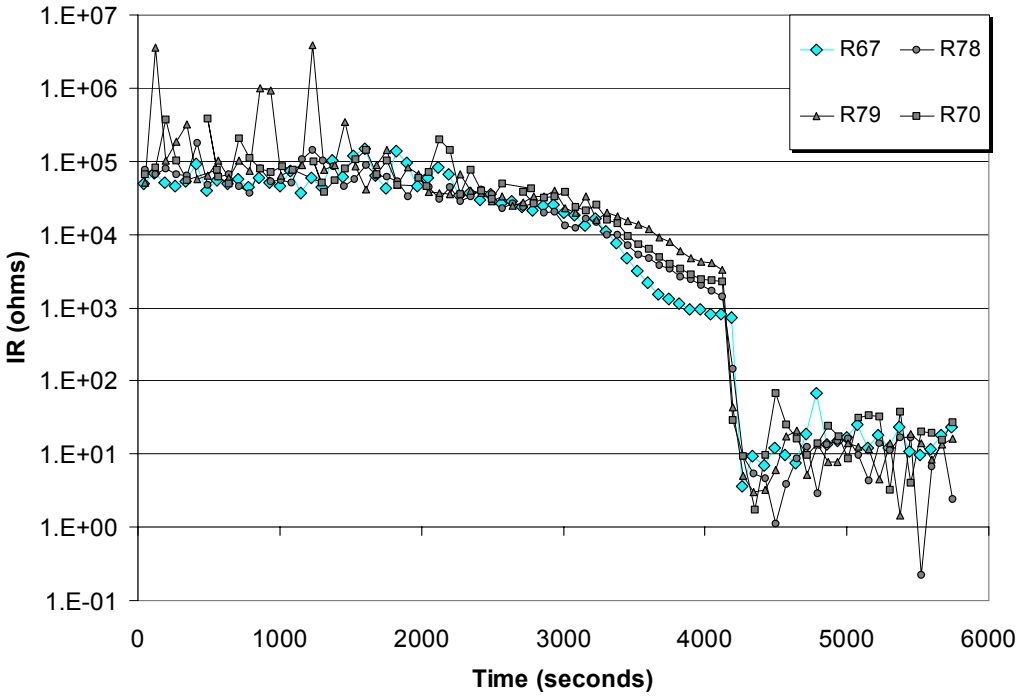

Figure 5-32. Representative conductor-to-conductor IRs for cable IR2 in the conduit during Test 8. This plot shows the IR between Conductor 7 and the other four conductors (6, 8, 9 and 10) in the cable located inside the conduit during the test.

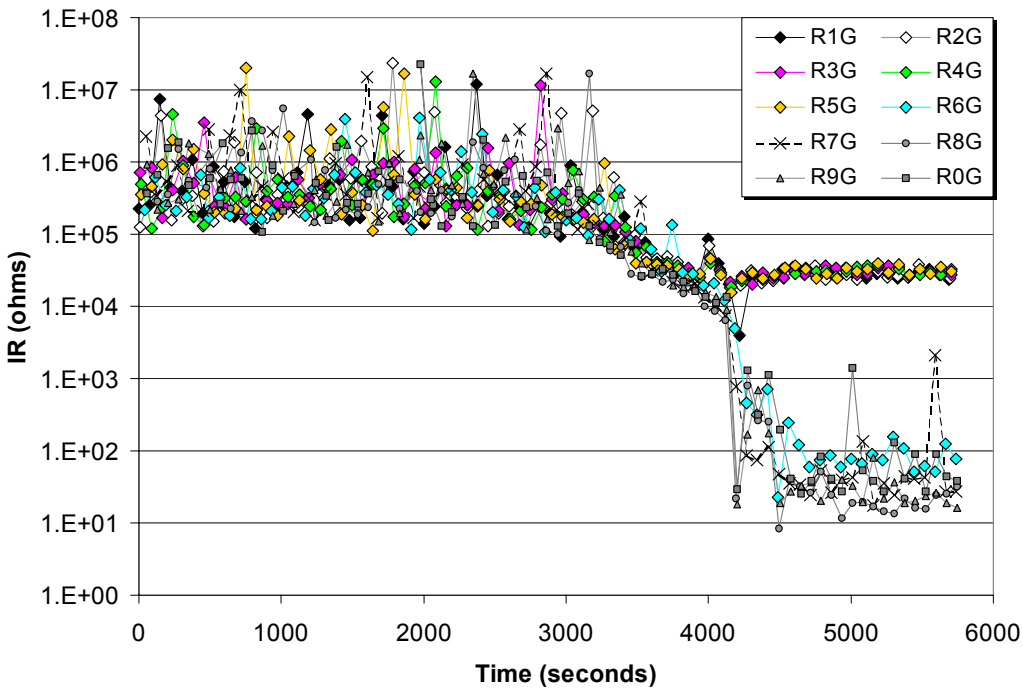

Figure 5-33. Conductor-to-ground IRs obtained during Test 8.

The next two transitions occur between 4100 and 4250 seconds affecting the tray cable conductors and at 4100 to 4480 seconds affecting the conduit cable conductors. Finally, the IRs of the conductors in the tray appear to stabilize at ~30,000 Ω sometime between 4100 to 4300 seconds. However, these IR values are likely an artifact of the multiple shorts to ground on the cable in the conduit rather than an actual reflection of the cable tray cable's IR. In all likelihood, the IR of the cable in the tray remained at or above 10^5 Ω for the test duration.

For the cable in the conduit, the first failures were observed to occur at ~4200 seconds. At this time, Conductors 8, 9, and 10 all shorted to ground, apparently sporadically. This behavior is not fully reflected in Figure 5-33 because the data plotted represents an average across all complimentary conductor pairs involving each conductor. When the root data is examined, it appears that these two conductors did show distinct shorts to ground that persisted for some tens of seconds. These short circuits would break and the conductors recovered significant IR (hundreds to thousands of ohms) for short periods of time before the ground short would again appear. Overall, it appears that the first failures were shorts to ground on these three conductors.

Subsequent to these sporadic failures, the data show various internal shorts, but all involve shorts to Conductors 8, 9, and/or 10 that had already shorted to ground. Hence, the initial ground shorts on Conductors 9 and 10 in this case dominated the failures. Conductors 7 and 6 eventually shorted to ground at ~4300 and ~4500 seconds, respectively.

Figures 5-34 and 5-35 show plots of how the leakage currents for Conductors 1 and 2, and 7 and 8 changed in their relationship to one another and to ground as the test progressed. Leakage currents for the cable in the tray peaked to ~25 mA and then stabilized at the ~3 mA level. Leakage currents for the cable in the conduit reached very high levels (~1 A).

Failures were observed for the cables in the conduit, and all of the failures appeared to involve shorts to ground as the initial failure mode. Based solely on the results of the IR measurements made during Test 8, it appears that the IR cable in the conduit experienced fire-induced damage that allowed leakage currents high enough to cause device actuation or blown fuses; however, the IR cable in the tray probably would not have caused device actuation or blown fuses.

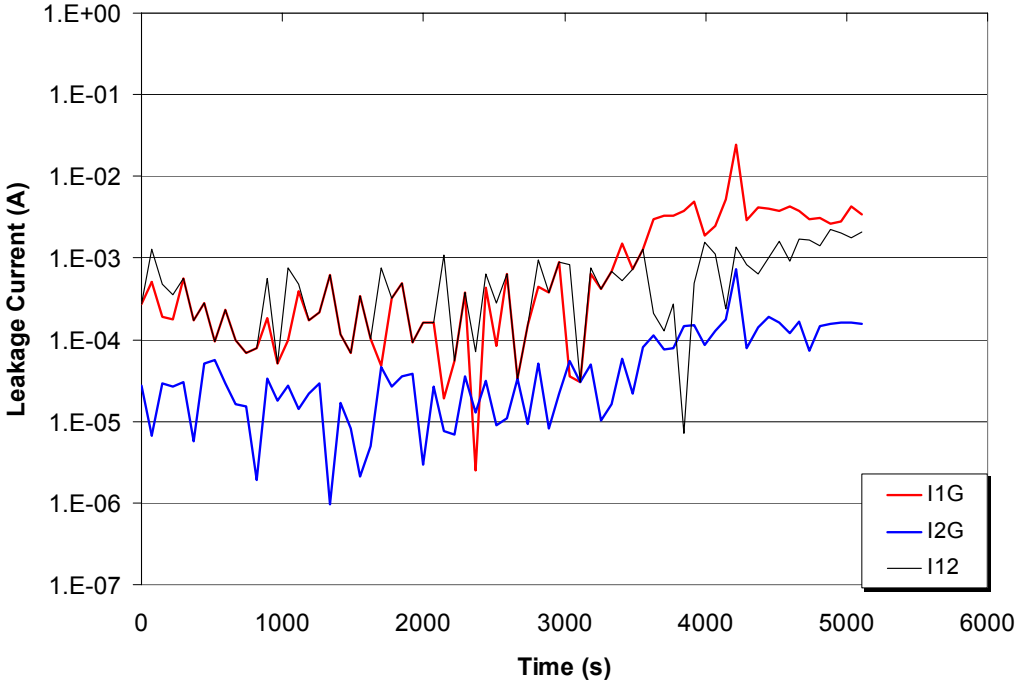

Figure 5-34. Leakage currents resulting from IR changes between Conductors 1 and 2 in the cable tray cable during Test 8.

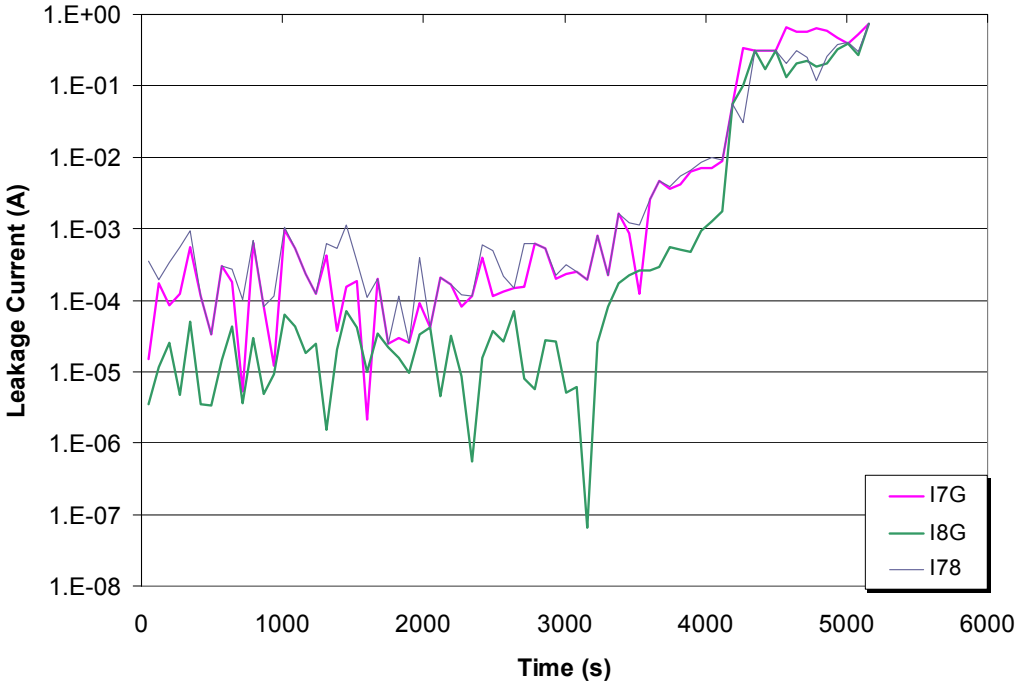

Figure 5-35. Leakage currents resulting from IR changes between Conductors 7 and 8 in the conduit cable during Test 8.

5.3 Tests 9 through 12

Tests 9 through 12 were conducted using the direct current power supply capability of the SNL IR measurement system. The intention was to simulate a typical ungrounded DC control power circuit and low voltage DC instrument circuit to determine if the response of a DC circuit materially differs from a similar AC circuit. However, running an ungrounded input prevented the determination of shorts to ground during Tests 9 through 11. Also, at the time the tests were conducted, the IR measurement system was limited to monitoring only eight conductors when operated in the DC mode. Test 12 was run using the IR measurement system operating in the DC mode with the negative side of the power supply attached to ground, allowing for determination of failure modes. All of the IR cables were of thermoset materials for these test runs.

5.3.1 Test 9

Test 9 was a 145-kW heat release rate fire with thermoset test cable bundles. The tray fill was limited to a single row of cables. The cables were laid in a horizontal tray and exposed to the fire plume at the corner of the tray. The IR sample bundle was, again, a seven-conductor cable bundled with three single-conductor cables and was wired in the same manner as described for Test 4 with the exception that the three external single conductor cables were ganged together as a single conductor on the IR system (C8). The IR system was operated in an ungrounded DC mode. Various conductor failures were observed in this test.

Figure 5-36 shows the time-temperature plots for two of the thermocouples monitored during the test. TC #27 was mounted on a tray rung at the corner of the tray, and TC #74 was located at the mid-position on the instrumented cable TC-4. These two thermocouples were chosen because they showed the worst-case temperature exposure conditions (highest recorded temperatures) for the air near the IR bundle and for the instrumented cable closest to the IR bundle. The peak tray temperature recorded during this test was 560°C (1040°F) and the peak cable temperature was 558°C (1036°F).

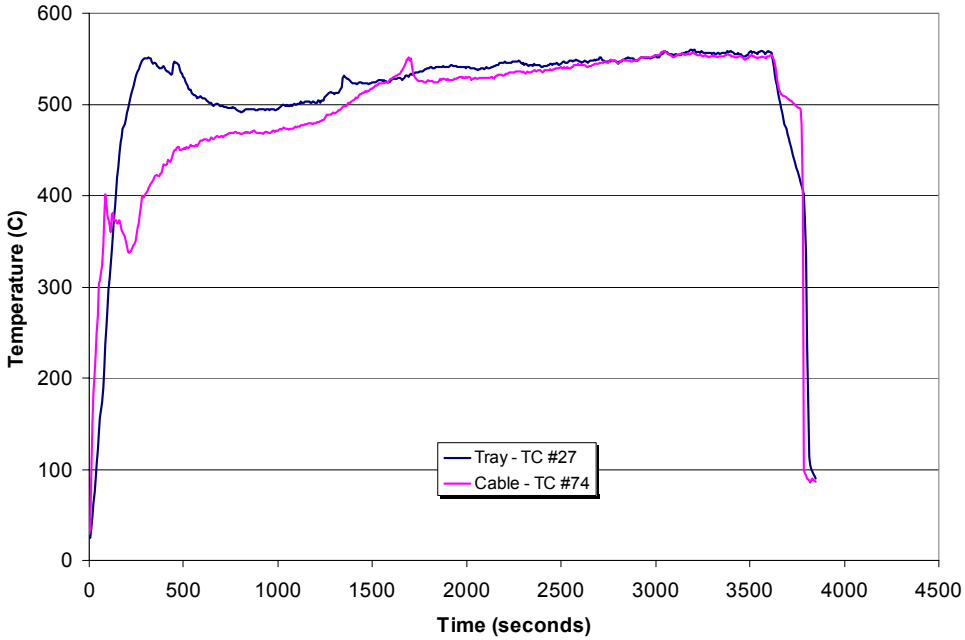

Figure 5-36. Representative tray and TC-4 cable temperatures recorded during Test 9.

The DC supply was set at 100 V for this test (the upper limit of the programmable power supply being used). In addition, since the IR measurement system is limited to monitoring only eight conductors in the DC operating mode, the three external single-conductor cables were ganged together as Conductor 8.

Figure 5-37 shows the IR changes occurring between Conductor 1 and each of the other conductors in the IR cable during the test. Conductor 1 was the center conductor in the seven-conductor cable and six of the other conductors surrounded Conductor 1 and were immediately adjacent to it. Conductor 8 is comprised of the three single conductor cables bundled with the seven-conductor cable to make up the IR bundle.

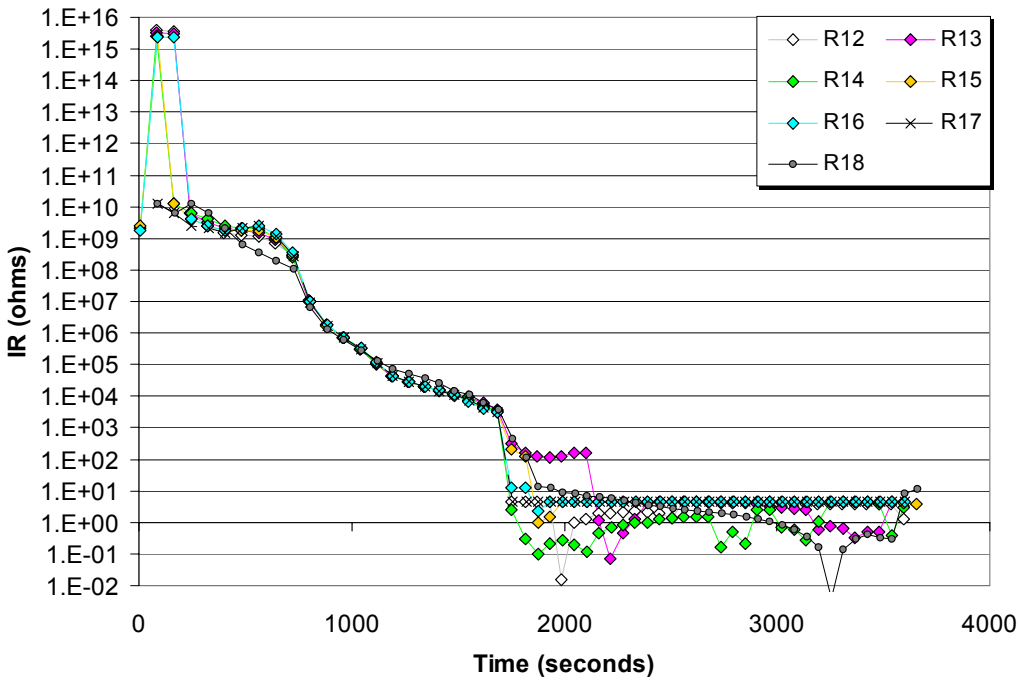

Figure 5-37. Representative conductor-to-conductor IRs obtained during Test 9. This plot shows the IR between Conductor 1 and the other seven conductors in the IR cable bundle.

As shown in the figure, the IR between the individual conductors gradually decreases from 10^{10} Ω at the beginning of the run to ~3,000 Ω at ~1700 seconds. The IRs between Conductor 1 and Conductors 2, 4, 6, and 7 all decrease to 2 to 5 Ω over the next minute. Table 5-5 summarizes the failures times and modes observed during Test 9. It would appear that the initial failures (IR less than 100 Ω) involved a short circuit between Conductors 1, 2, 4, 6, and 7 at about 1750 seconds. At about 1875 seconds (roughly two minutes later), Conductors 5 and 8 appear to join in the short circuit. The last conductor to fail is Conductor 3, which joined the short circuit at about 2120 seconds. Recall that the time of shorts to ground cannot be determined.

Table 5-5. Summary of Cable Failure Times and Modes during Test 9

Time (s)	Failure Mode Observed
~ 1753	Conductors 1, 2, 4, 6, and 7 form a short circuit
~ 1875	Conductors 5 and 8 join in the previous short circuit
~ 2120	Conductor 3 joins in the mutual short circuit – all conductors have shorted together

Figure 5-38 shows a plot of how the leakage currents between Conductors 1 and 2 changed as the test progressed. The peak leakage current appeared to be ~0.5 A between the conductors.

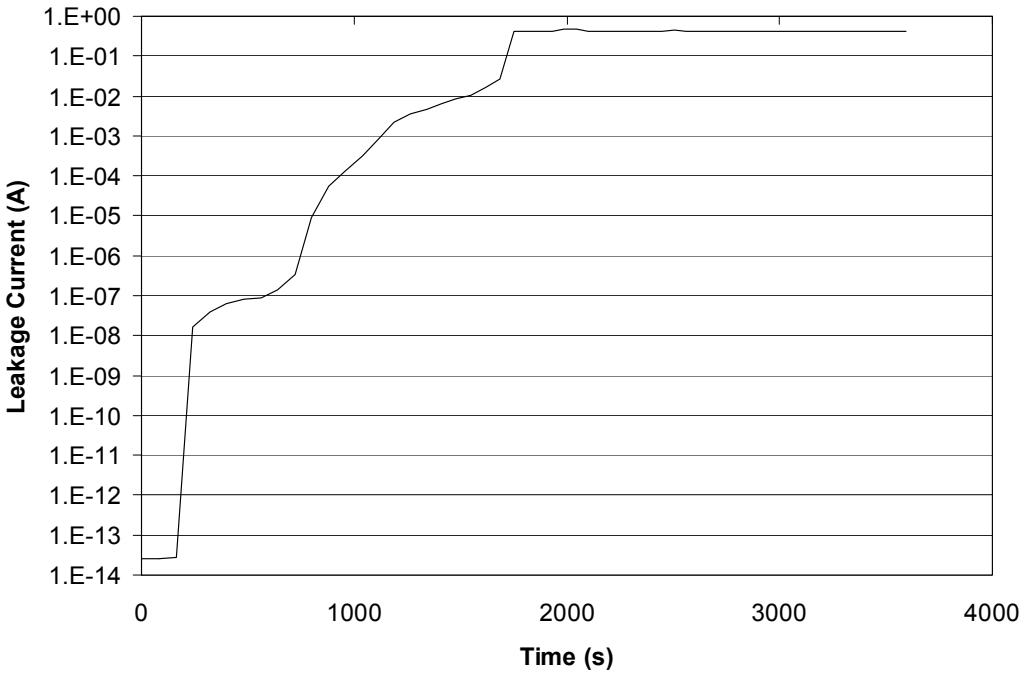

Figure 5-38. Leakage current resulting from IR changes between Conductors 1 and 2 during Test 9.

Based solely on the results of the IR measurements made during Test 9, it appears that the IR cable experienced fire-induced damage that allowed leakage currents high enough to cause device actuation in a DC control circuit. The modes of failure cannot, however, be determined with confidence.

5.3.2 Test 10

Test 10 was a 200-kW heat release rate fire with thermoset test cable bundles. The tray fill was limited to a single row of cables. The cables were installed in a vertical tray and exposed to the fire with the burner set 0.6 m (2 ft) behind the center of the tray. The IR sample bundle was, again, a seven-conductor cable but in this test, the multi-conductor was bundled with just one single-conductor cable. The cables were wired in the same manner as described for Test 4, except that there was only one external single-conductor cable (C8). The IR system was operated in an ungrounded DC mode. While substantial degradation in conductor IR was observed through the course of the test, all IR values remained in excess of 1000 Ω. Hence, using the same failure criteria applied to other tests (an IR of less than 100 Ω), no gross conductor failures were observed.

Figure 5-39 shows the time-temperature plots for two of the thermocouples monitored during the test. TC #23 was mounted on a tray rung at the top of the tray, and TC #49 was located at 15 cm (6 in.) from the bottom of the instrumented cable TC-4. These two thermocouples were chosen because they showed the worst-case temperature exposure conditions (highest recorded temperatures) for the air near the IR bundle and for the instrumented cable closest to the IR bundle. The peak tray temperature recorded was 508°C (946°F), whereas the peak cable temperature indication reached as high as 641°C (1186°F) at one point during the test.

The DC supply was set at 100 V for this test (the upper limit of the programmable power supply being used). In addition, since the IR measurement system is limited to monitoring only eight conductors in the DC operating mode, only one external single-conductor cable was bundled with the IR seven-conductor cable. This single external conductor was monitored as Conductor 8 of the IR measurement system.

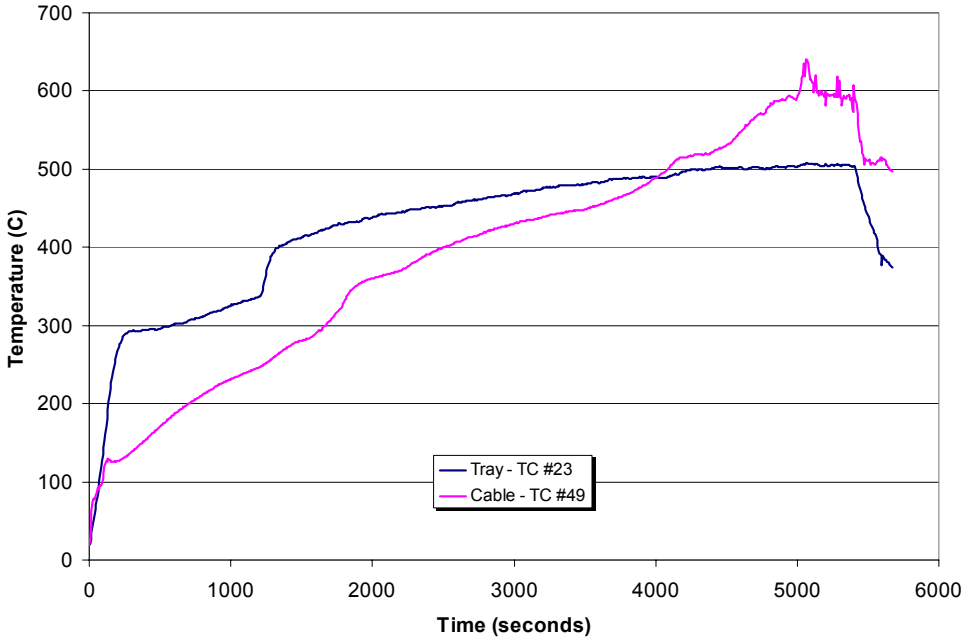

Figure 5-39. Representative tray and TC-4 cable temperatures recorded during Test 10.

Figure 5-40 shows the IR changes occurring between Conductor 1 and each of the other conductors during the test. Conductor 1 was the center conductor in the seven-conductor cable and the other six conductors surrounded Conductor 1 and were immediately adjacent to it. Conductor 8 is a single conductor cable bundled with the seven-conductor cable to make up the IR bundle for this test.

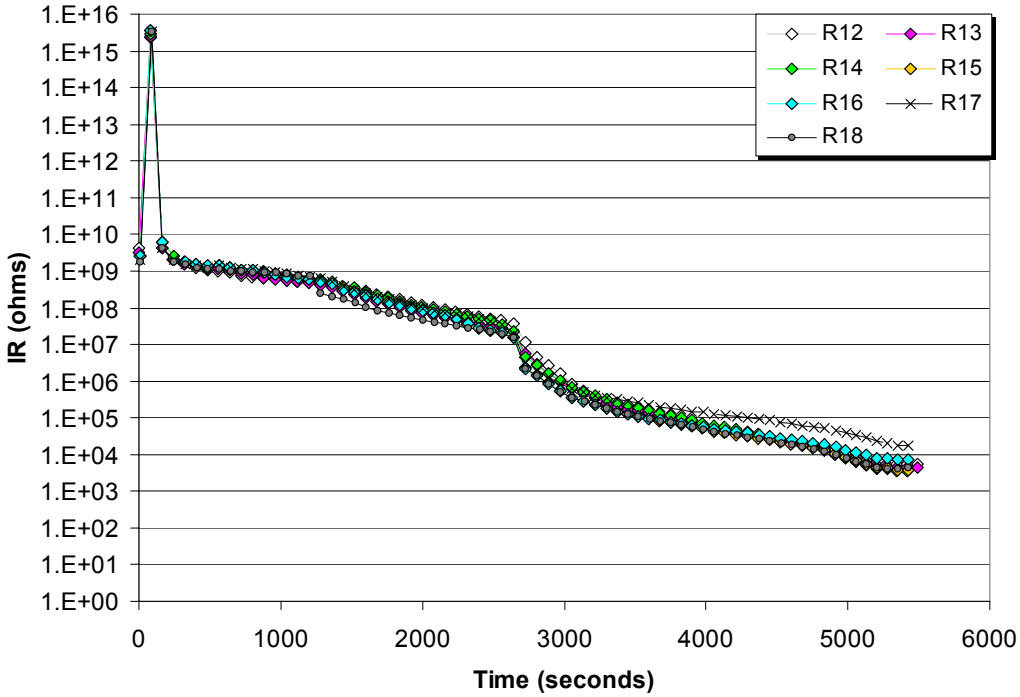

Figure 5-40. Representative conductor-to-conductor IRs obtained during Test 10. This plot shows the IR between Conductor 1 and the other seven conductors in the IR cable bundle.

As shown in the figure, there was a very gradual decrease in IRs between the conductors from start to end of the test run (3×10^9 down to 1×10^4 Ω).

Figure 5-41 plots how the leakage current between Conductors 1 and 2 changed as the test progressed. The peak leakage current appears to be ~20 mA between the conductors.

Based solely on the results of the IR measurements made during Test 10, while the cable did show substantial IR degradation, the test appears to have stopped short of actual failure. That is, it does not appear that the IR cable experienced fire-induced damage that would allow leakage current high enough to cause device actuation in a DC control circuit.

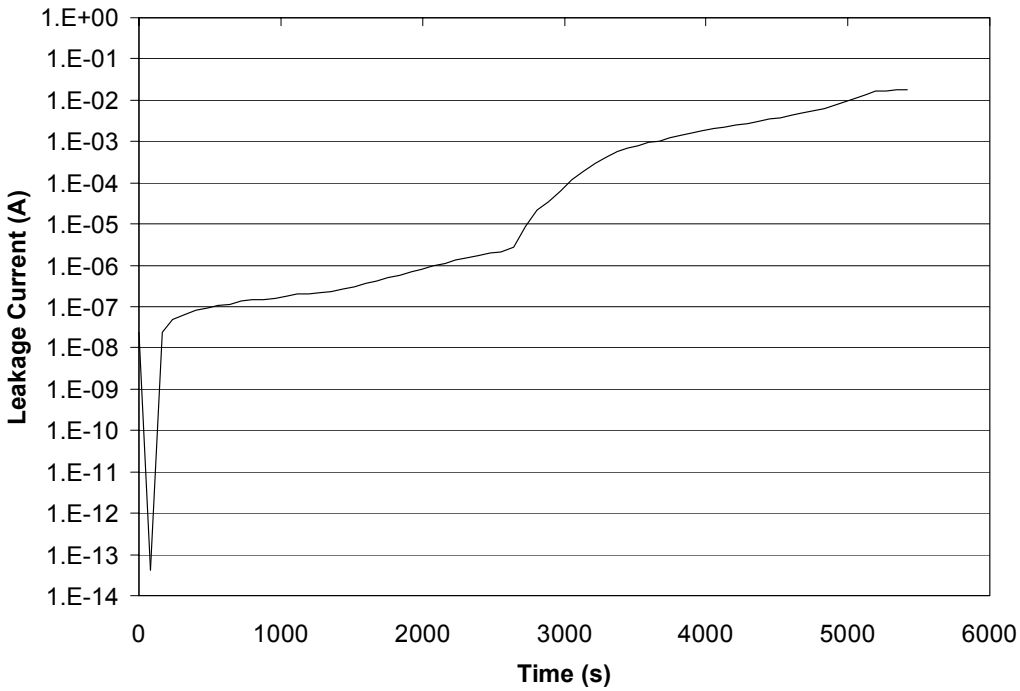

Figure 5-41. Leakage current resulting from IR changes between Conductors 1 and 2 during Test 10.

5.3.3 Test 11

Test 11 was a 145-kW heat release rate fire with thermoset test cable bundles. The tray was loaded with four full rows of cables. The cables were laid in a horizontal tray and exposed to the fire plume at the corner of the tray. The DC supply was set at 24 V for this test to simulate typical instrument signal conditions. In addition, the IR measurement system was connected to two separate instrumentation cables. One (IR1) was a shielded two-conductor cable; the other (IR3) was made up of three shielded pairs (six-conductor cable). Cable IR1 was laid in the top row of cables in the tray; IR3 was located in the bottom row of cables.

Based on the criteria applied to other tests (a conductor IR of less than 100 Ω), no gross failures were observed during this test – all IRs remained above 1000 Ω. However, substantial degradation was noted, particularly for the IR3 bundle. Given that these were instrument cables, alternate failure criteria may be appropriate. This report has not attempted to propose specific criteria for assessing the pass/fail behavior of an instrument cable.

Figure 5-42 shows the time-temperature plots for three of the thermocouples monitored during the test. TC #26 was mounted on a tray rung at the corner of the tray, TC #73 was located about the mid-position on the instrumented cable TC-4, and TC #46 was located about the mid-position on the instrumented cable TC-1. These

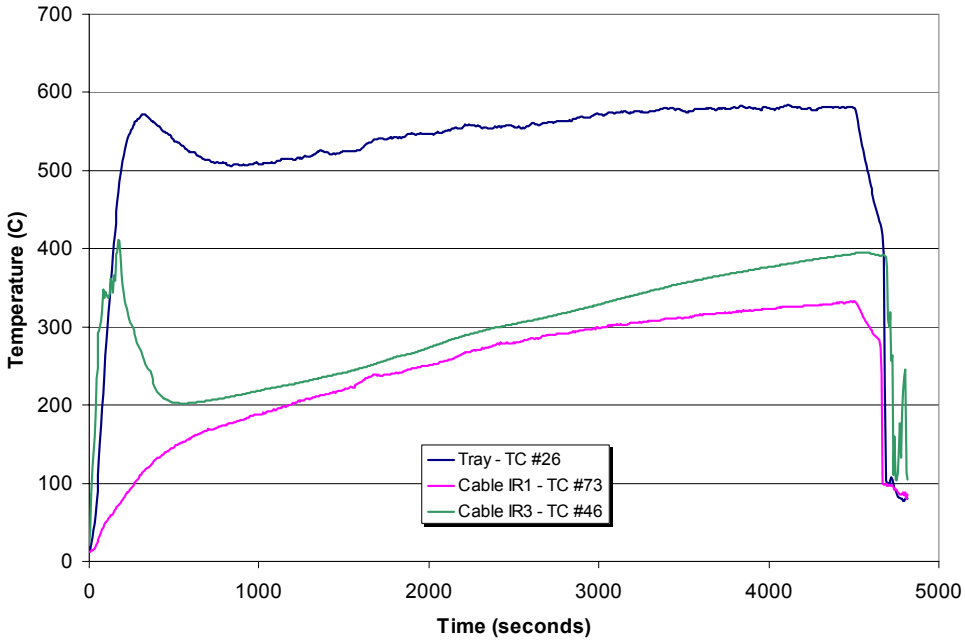

Figure 5-42. Representative tray and cable (TC-1 and TC-4) temperatures recorded during Test 11.

thermocouples were chosen because they showed the worst-case temperature exposure conditions (highest recorded temperatures) for the air near the IR bundle and for the instrumented cable closest to the IR bundle. Peak tray temperature was 584°C (1083°F), peak TC-1 cable temperature was 412°C (774°F), and the peak TC-4 cable temperature was 333°C (631°F).

Figure 5-43 shows the changes in IR occurring between Conductors 1 and 2 in the IR1 cable during the test. (Conductors 1 and 2 were the conductor pair within the IR1 cable.)

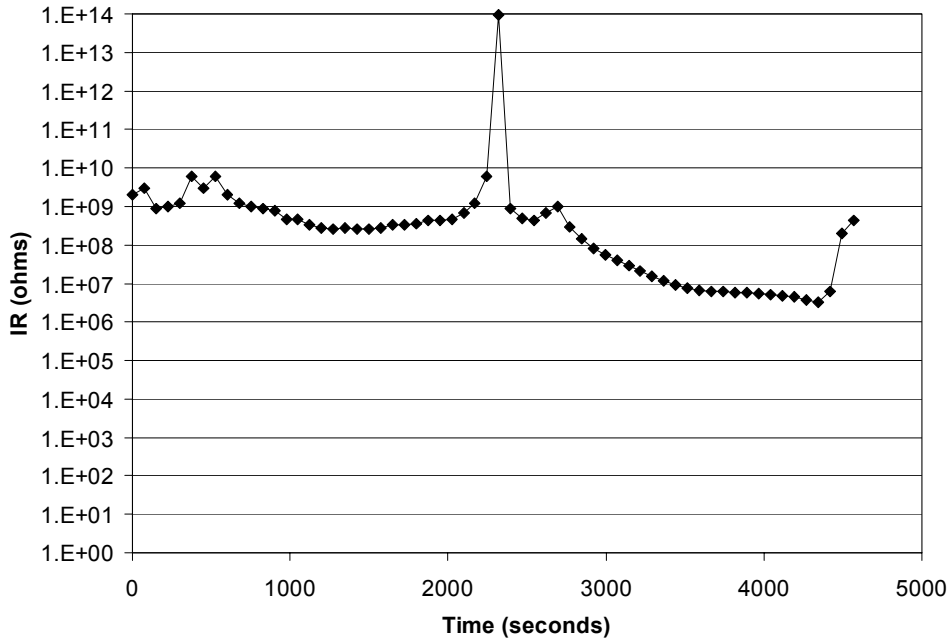

Figure 5-43. IR between Conductor 1 and 2 obtained during Test 11.

As shown in the figure, the IR between Conductors 1 and 2 remains fairly constant with very small variations until ~2700 seconds into the test run. Then the conductor IR gradually decreases from ~10^9 to ~3×10^6 Ω at ~4400 seconds; it then seems to be recovering over the remaining time of the test.

Figure 5-44 shows the IR change between Conductor 3 and the other conductors in IR3 cable during the test. In general, the behavior is the same as shown above for Conductors 1 and 2; however, a definite change in the conductor-to-conductor IRs occurs at ~3600 seconds, when the cable IR3 conductor IRs decrease smoothly from 3×10^6 down to 3×10^3 Ω near the end of the test run.

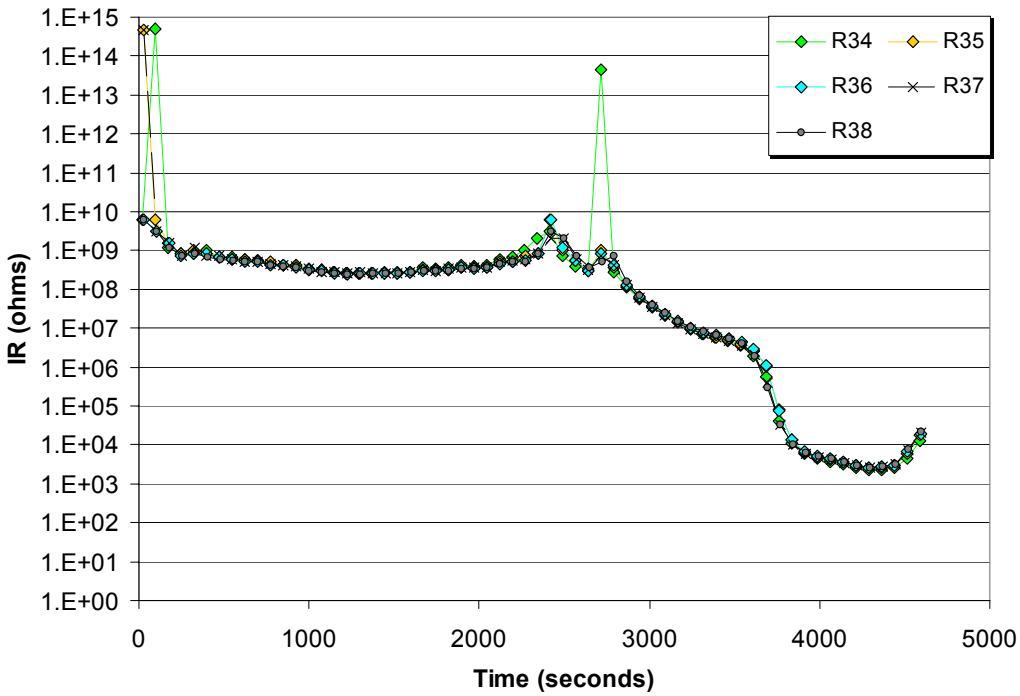

Figure 5-44. IRs between Conductor 3 and Conductors 4 through 8 obtained during Test 11.

Figure 5-45 plots how the leakage currents between Conductors 1 and 2, and 3 and 4 (a shielded pair within IR3), changed as the test progressed. The peak leakage current appears to be ~7 μA between Conductors 1 and 2, which is not enough to pose a serious problem, even to a typical instrument circuit. However, the peak leakage current between Conductors 3 and 4 is ~10 mA, which could cause a substantial instrument reading error in, for example, a 4-20 mA instrument circuit.

Based on the results of the IR measurements made during Test 11, it appears that the IR3 cable experienced substantial fire-induced degradation. While the IR did remain above 1000 Ω for the test duration, depending on the specific instrument circuit considered, this degradation might have been sufficient to cause incorrect instrument readings. The IR1 cable did not experience any substantial IR degradation.

5.3.4 Test 12

Test 12 was a 145-kW heat release rate fire with thermoset test cable bundles. The cables were laid in a horizontal tray positioned 1.8 m (6 ft) above the floor and exposed to the fire plume. The burner was positioned under the corner of the tray. The IR sample bundle was, again, a seven-conductor cable bundled with three single-conductor cables and wired in the same manner as described for Test 9 (i.e., the three external conductors were electrically ganged together and designated as Conductor 8). The IR system was operated in the DC mode at 100 V and the DC power supply was tied to ground on the negative terminal. Hence, both conductor-to-conductor and conductor-to-ground IR values can be determined. Various conductor failures were observed in this test.

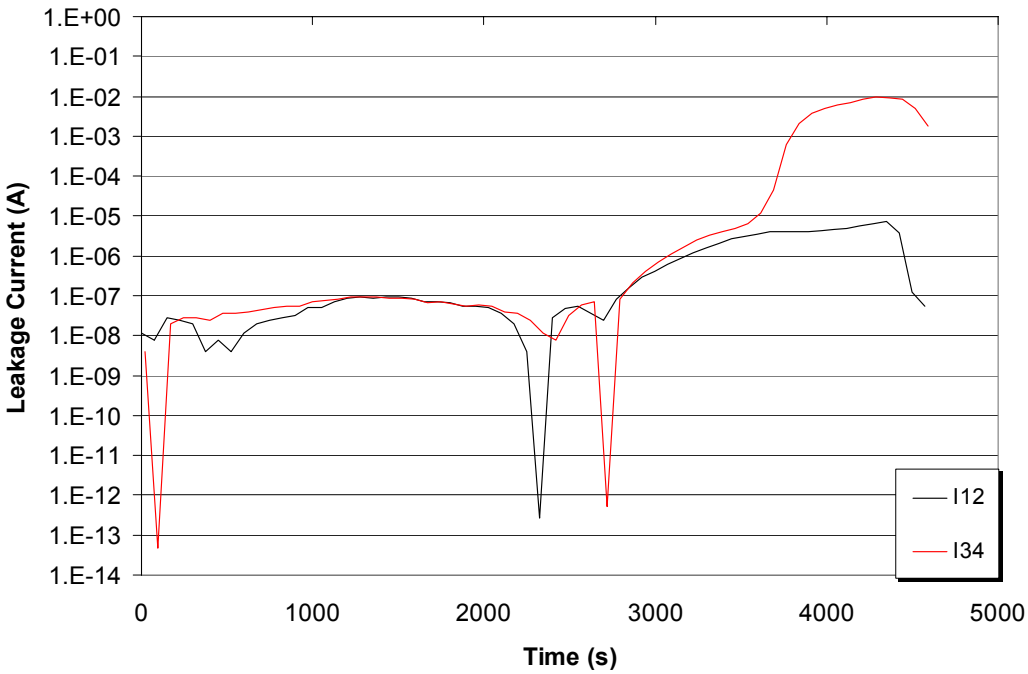

Figure 5-45. Leakage currents resulting from IR changes between Conductors 1 and 2 and between Conductors 3 and 4 during Test 11.

Figure 5-46 shows the time-temperature plots for two of the thermocouples monitored during the test. These two thermocouples were chosen because they showed the worst-case temperature exposure conditions (highest recorded temperatures) for the air near the IR bundle and for the instrumented cable closest to the IR bundle. TC #25 was mounted on a rung of the tray near the corner, and TC #64 was located about mid-way along the instrumented cable TC-3. The peak tray temperature was 611°C (1132°F) and then dropped and stabilized at 573°C (1063°F). The peak cable temperature was 465°C (869°F).

As Figure 5-47 shows, the change in IR occurring between Conductor 1 and the other conductors in the cable bundle was a fairly smooth transition from ~3×10^8 down to ~30 Ω beginning at ~1700 seconds and continuing throughout the rest of the test run. Conductor 1 was the center conductor in the seven-conductor cable and Conductors 2 through 7 surrounded Conductor 1 and were immediately adjacent to it. Conductor 8 was comprised of the ganged-together set of three single conductor cables bundled with the seven-conductor cable to make up the IR bundle.

The IR of the individual conductors to ground demonstrated three transitions in IR, as shown in Figure 5-48. The first occurred at 1140 to 1500 seconds; the next was between 1500 seconds and 1700 seconds; and finally the IRs shorted to ground in fairly smooth transitions.

Table **5-6** summarizes the conductor failure modes and times for Test 12. All of the initial failures observed involved the conductors shorting to ground. Initially, at about 1000 seconds, Conductor 8 (the three external conductors as a gang) shorts to ground. This short-to-ground failure is also manifested by the apparent reduction in IR between Conductor 8 and the other conductors in the cable bundle. A second ground short involving Conductor 3 is observed at about 1900 seconds. Over the period of 2200 to 3500 seconds, the rest of the conductors short to ground.

Figure 5-49 plots how the leakage currents for Conductors 1 and 2 changed in their relationship to one another and to ground as the test progressed.

Based solely on the results of the IR measurements made during Test 12, it appears that the IR cable experienced fire-induced damage that allowed leakage currents high enough to cause device actuation or blown fuses.

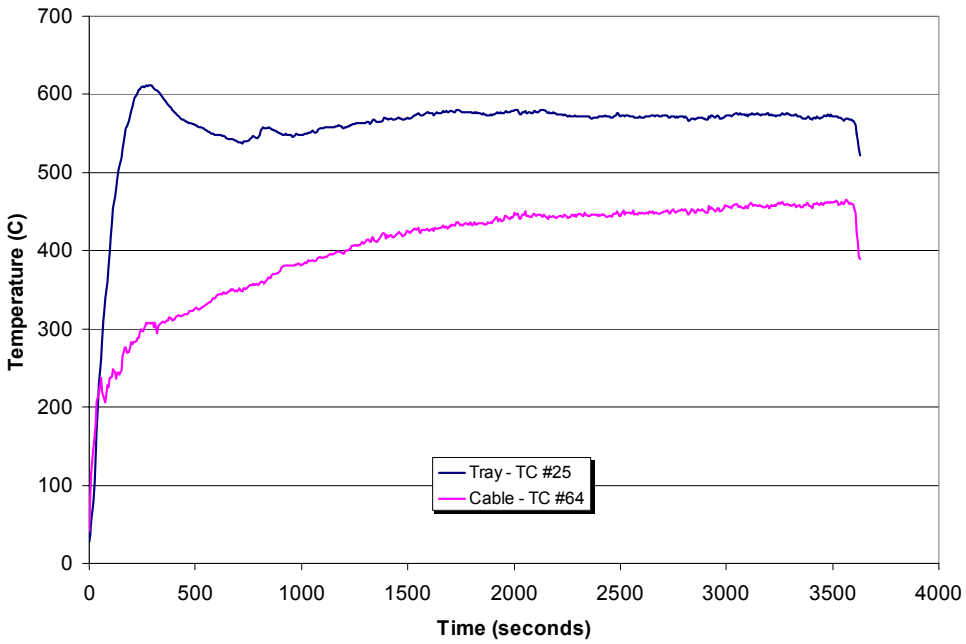

Figure 5-46. Representative tray and TC-3 cable temperatures recorded during Test 12

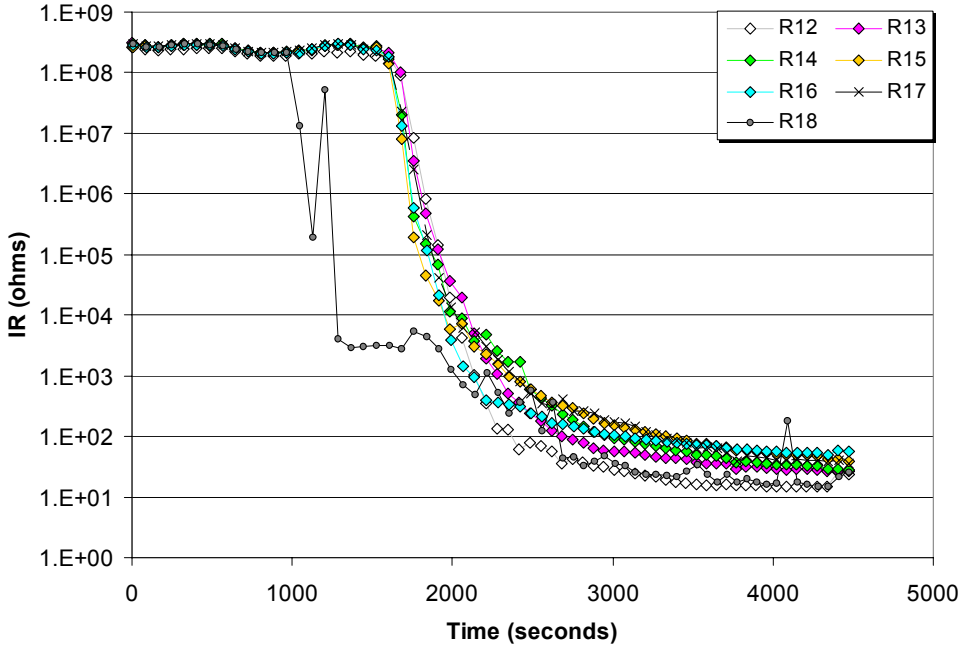

Figure 5-47. Representative conductor-to-conductor IRs obtained during Test 12. This plot shows the IR between Conductor 1 and the other seven conductors in the IR cable bundle.

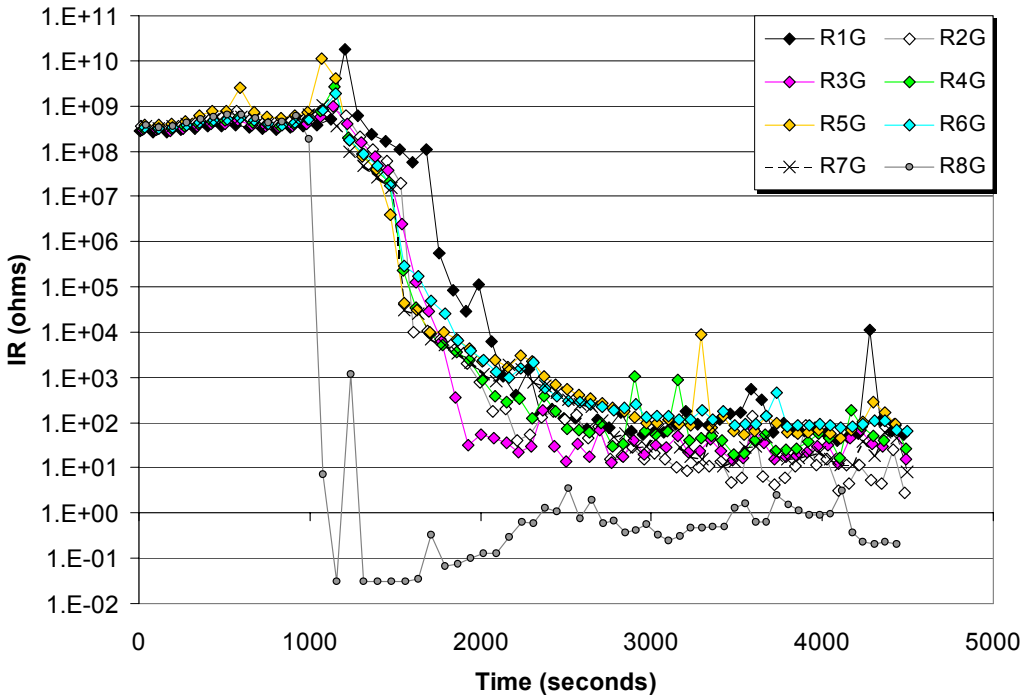

Figure 5-48. Conductor-to-ground IRs obtained during Test 12.

Table 5-6. Summary of Cable Failure Times and Modes during Test 12

Time (s)	Failure Mode Observed
~ 1000	Conductor 8 shorts to ground
~ 1900	Conductor 3 shorts to ground
~ 2200–2800	Conductors 1, 2, 4, and 7 short to ground
~ 3000	Conductor 5 shorts to ground
~ 3500	Conductor 6 shorts to ground – all conductors are grounded

5.4 Tests 13 through 18

Tests 13 through 18 were conducted using the SNL IR measurement system configured for AC operation. Unfortunately, the IR measurement system was miswired so that only the voltage supply side relays were operable during Tests 13 and 15 through 17. The measurement side relays were not properly connected to the relay control system. Also note that Tests 13 through 18 were not conducted in consecutive order; Tests 13 and 15 through 17 were conducted in April and Tests 14 and 18 were conducted in May. The problem with the IR measurement system was corrected before Tests 14 and 18 were run.

As a result of the wiring fault, for Tests 13 and 15 through 17, only the total change in IR for each conductor to ground can be determined. The specific initial failure mode cannot be ascertained.

5.4.1 Test 13

Test 13 was a repeat of Test 1, but employing a cable tray with a much less severe bend radius than before. The armored cables were tested in a 350-kW heat release rate fire and exposed to the hot gas layer. The burner was placed in the center of the test cell. The cables were laid in a horizontal tray and the tray was filled with two rows of cables, five of which were being monitored along with a monitored instrument cable that was also included in the tray fill (see Section 6). The IR cable was an eight-conductor armored cable, not bundled with any external cables. In contrast to Test 1, the armor shield for the IR cable was connected to ground and was not monitored as a separate conductor.

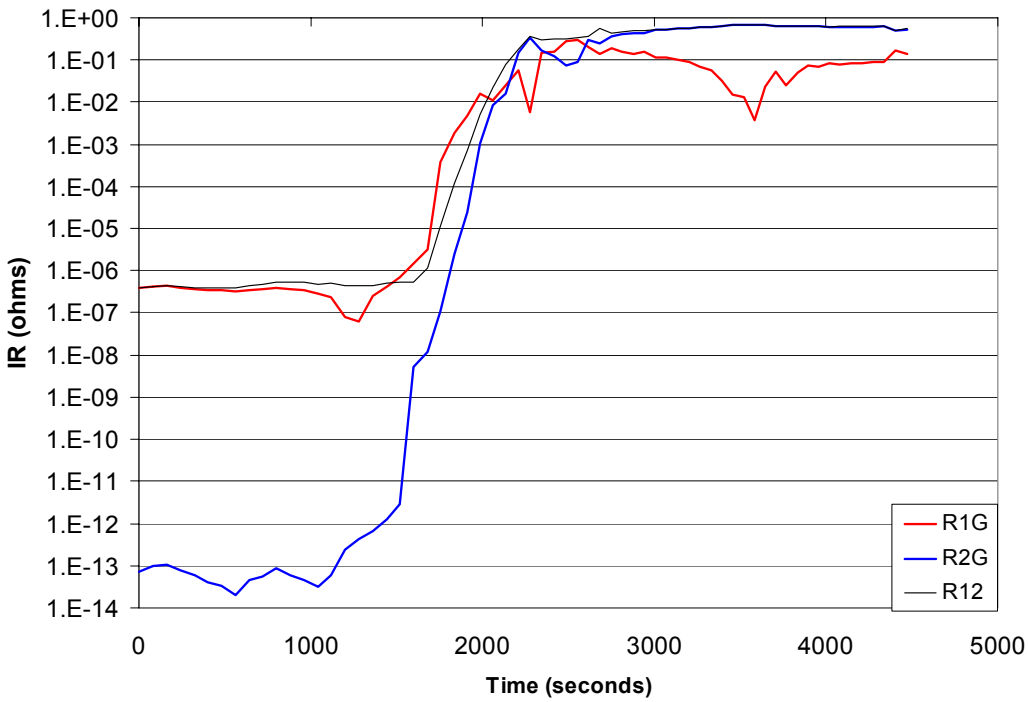

Figure 5-49. Leakage currents resulting from IR changes between Conductors 1 and 2 during Test 12.

shows the time-temperature plots for two of the thermocouples monitored during the test. TC #13 was mounted on the tray's side rail about 0.6 m (2 ft) from the corner of the tray, and TC #69 was located at the test cell doorway end of the instrumented cable TC-4. These two thermocouples were chosen because they showed the worst-case temperature exposure conditions (highest recorded temperatures) for the air near the IR cable and for the instrumented cable closest to the IR bundle. The peak tray temperature recorded during this test was 756°C (1393°F) and the cable temperature peaked at 772°C (1422°F) near the end of the run.

As noted previously, the IR measurement system was only capable of determining total IR to ground due to a wiring problem during Test 13. Figure 5-51 shows the time-dependent change in the total IR for each of the eight conductors in the IR cable measured during this test. The fact that the IR values fall to very low levels (<100 Ω) beginning at about 1900 seconds indicates that conductor failures have occurred. Figure 5-52 shows the associated leakage currents.

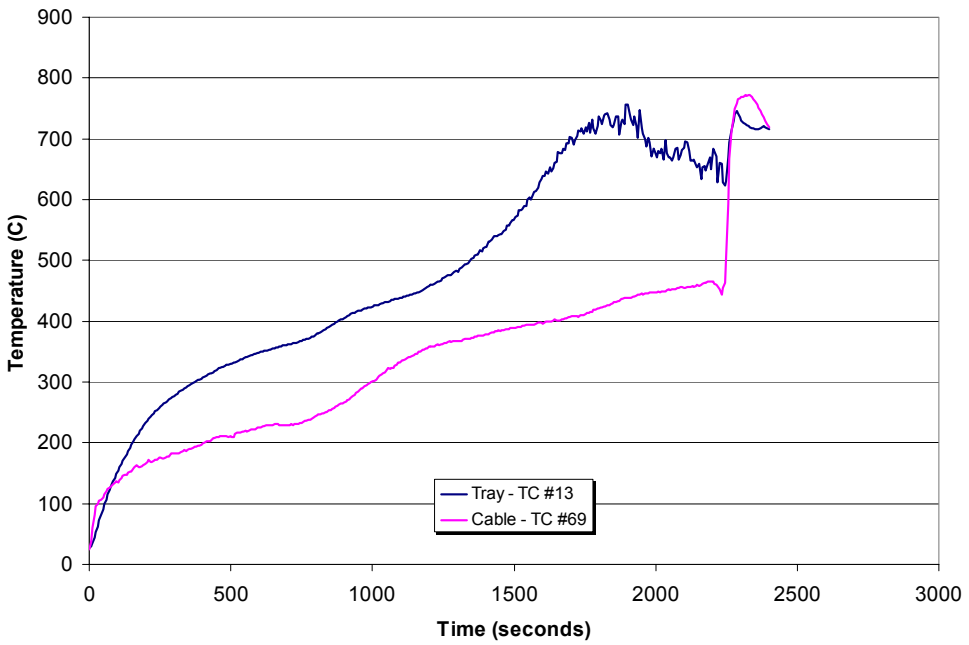

Figure 5-50. Representative tray and TC-4 cable temperatures recorded during Test 13.

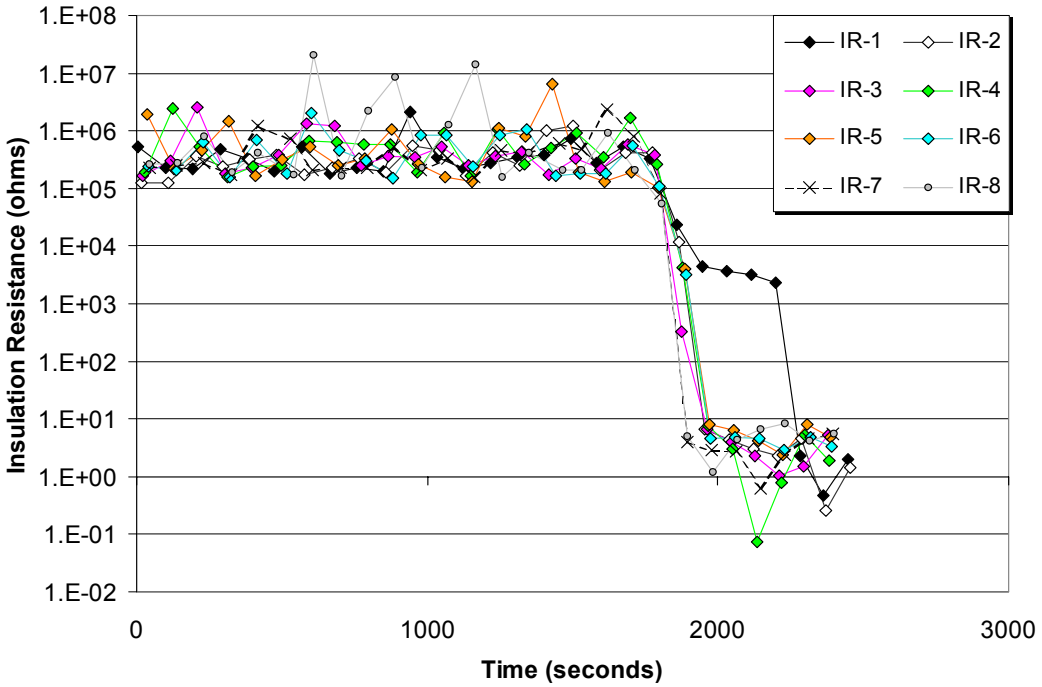

Figure 5-51. Total IR of each conductor recorded during Test 13.

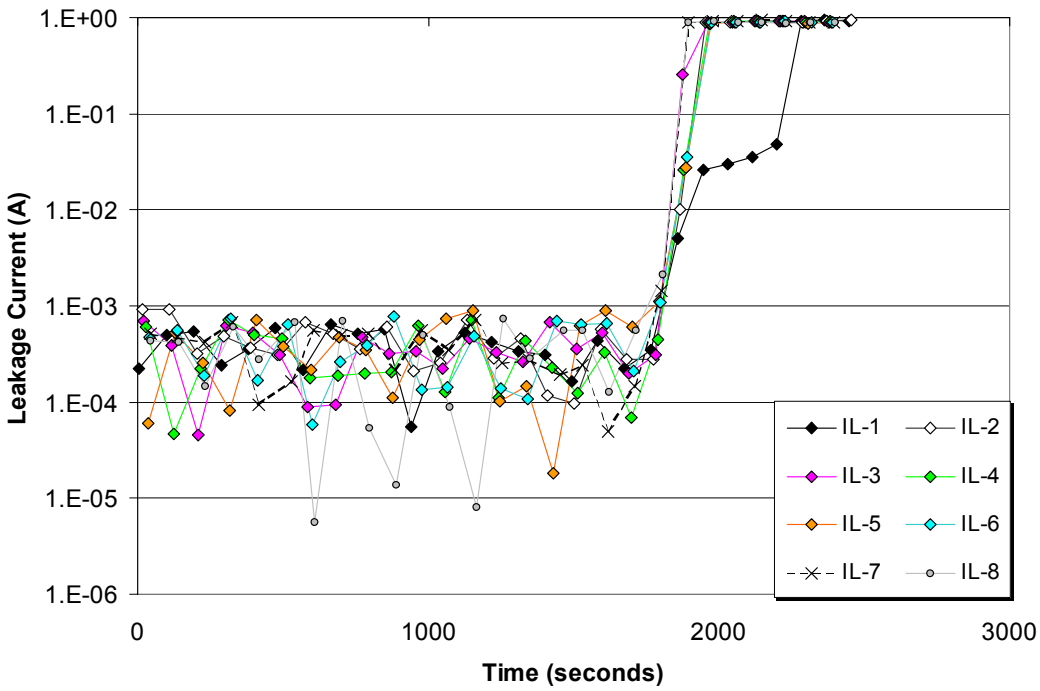

Figure 5-52. Total leakage currents resulting from IR changes for each conductor during Test 13.

5.4.2 Test 14

Test 14 was a 145-kW heat release rate fire with the cables exposed to the fire plume. The burner was placed under the corner of the cable tray and conduit. The IR cable bundle consisted of three thermoset three-conductor cables secured together and routed in the horizontal conduit. A thermoplastic instrument cable for the current loop circuit was also placed in the conduit (see Section 6). The wiring problem with the IR measurement system that had plagued Tests 13, 15, 16, and 17 had been diagnosed and corrected in time to allow its proper operation during this test.

No thermocouple-instrumented cable was routed in the conduit during this test; hence, there is no cable temperature data available. In addition, no direct measure of conduit temperature was made either. However, no failures of the IR cable bundle were identified based on the results of this test. Figure 5-53 shows a plot of the IRs between Conductor 1 and the other conductors in the IR bundle. Conductors 1 through 3 were enclosed in one of the three-conductor cables of the IR bundle, Conductors 4 through 6 were in a second cable, and Conductors 7 through 9 formed the third cable. As shown in the figure, the IRs declined very little over the course of the test run.

Figure 5-54 shows the values of IR between each of the IR cable conductors to ground recorded during Test 14. This figure also shows that the IRs to ground decreased very slightly during the test. Figure 5-55 presents the change in leakage current for Conductors 1 and 2 occurring during Test 14.

Based solely on the results of the IR measurements made during Test 14, it appears that the IR cable experienced virtually no damage and would not have caused any device actuation or blown fuses.

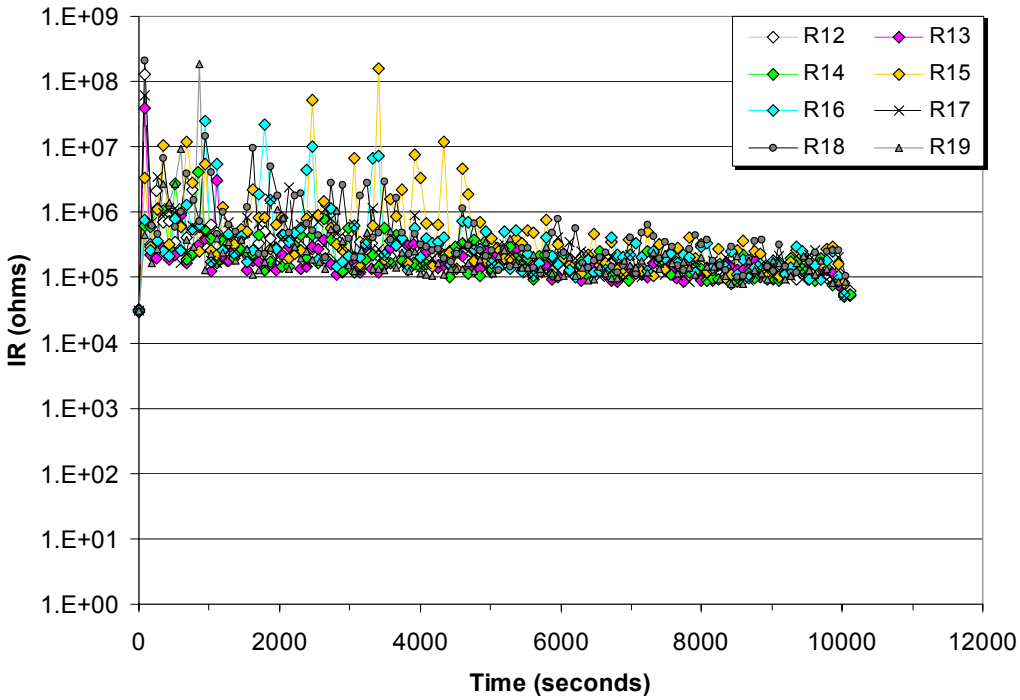

Figure 5-53. Representative conductor-to-conductor IRs obtained during Test 14.

5.4.3 Test 15

Test 15 was actually conducted prior to Test 14, and, like Test 13, was impacted by the problem with the IR measuring system. The IR cable bundle consisted of a seven-conductor thermoset control cable surrounded by three single-conductor thermoset cables. The test conditions for exposure consisted of a variable heat release rate fire where the flame intensity was adjusted from 350 kW to 200 kW and finally to 450 kW over the course of the test run. The cables were laid in a single row in a horizontal cable tray located 1.8 m (6 ft) above the floor and exposed to the hot gas layer generated by the fire. The burner was placed in the center of the test cell. A monitored instrument cable was also included in the tray for the current loop circuit (see Section 6).

Figure 5-56 shows the time-temperature plots for two of the thermocouples monitored during the test. TC #18 was mounted on the tray's side rail about 0.6 m (2 ft) from the end of the tray closest to the doorway, and TC #67 was located 0.6 m (2 ft) from the end of the of the instrumented cable TC-3 that ran parallel to the back wall of the test cell. These two thermocouples were chosen because they showed the worst-case temperature exposure conditions (highest recorded temperatures) for the air near the IR cable and for the instrumented cable closest to the IR bundle. The peak tray temperature recorded during this test was 573°C (1063°F) and the cable temperature was 540°C (1004°F).

As noted previously, the IR measurement system was only capable of determining total IR due to a wiring problem during Test 15. Figure 5-57 shows the time-dependent change in the total IR for each of the 10 conductors in the IR cable measured during this test. Table 5-7 summarizes the behavior of the cable in the test. Only five of the 10 conductors appear to have total IRs <100 Ω at the end of the test. The other conductors, while experiencing decreasing total IRs, did not reached the point of failure.

Figure 5-58 shows the resulting leakage currents allowed by the change in IR for each conductor. Although there is no direct evidence, the two external Conductors 8 and 10 may have been shorted together without ground interaction during the period of time their IRs decreased to and held at ~1000 Ω. This supposition is largely based on previous experience with conductors shorting together and the resulting voltage responses recorded on the IR system.

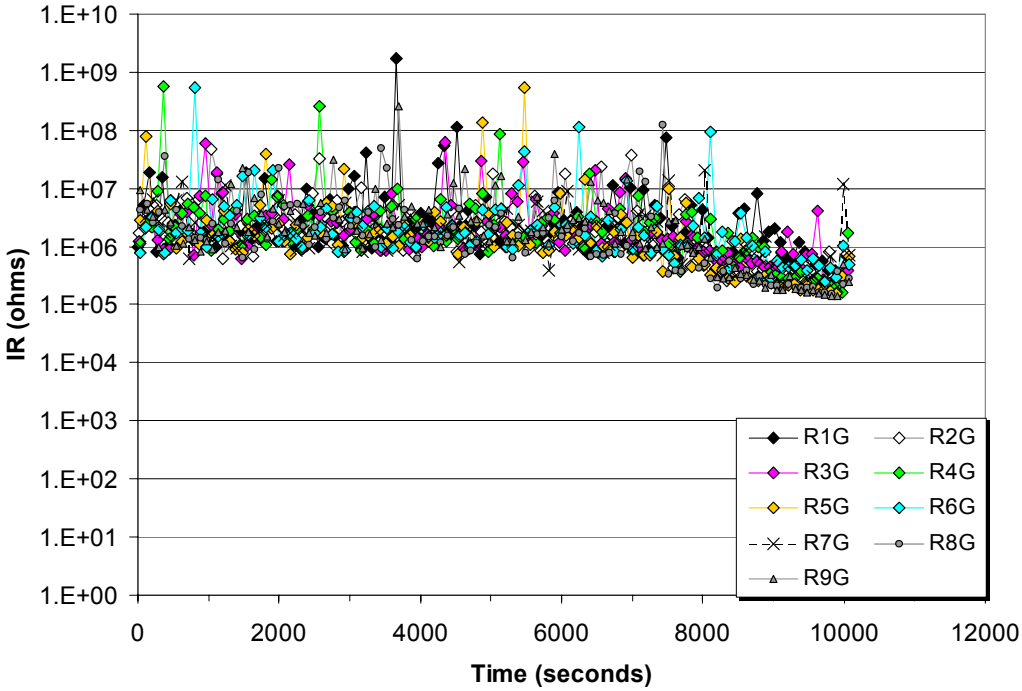

Figure 5-54. Conductor-to-ground IRs obtained during Test 14.

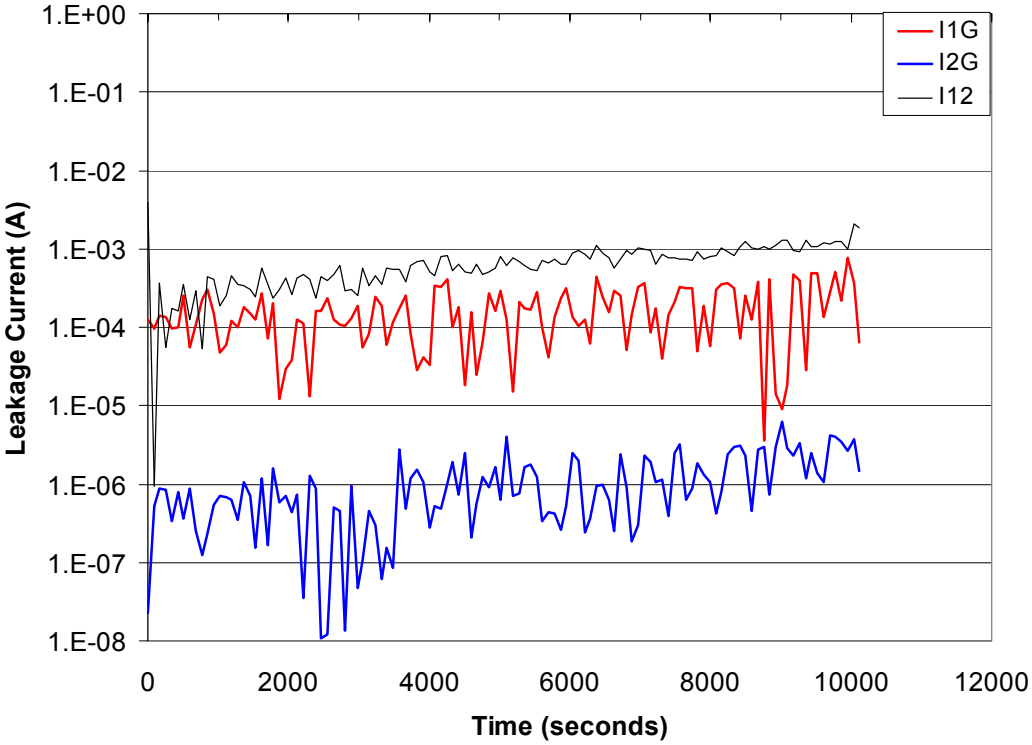

Figure 5-55. Leakage currents resulting from IR changes in Conductors 1 and 2 during Test 14.

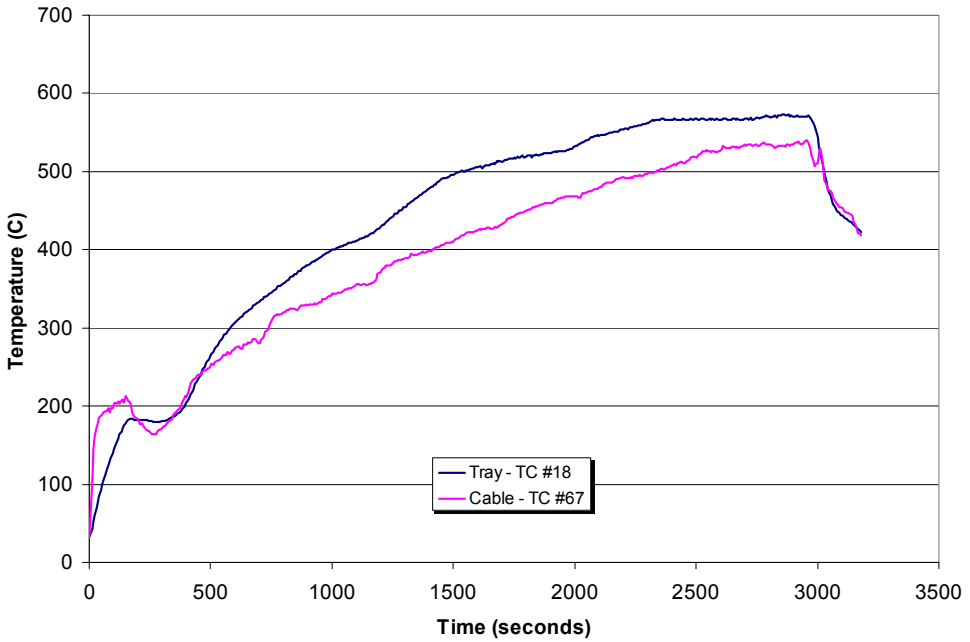

Figure 5-56. Representative tray and TC-3 cable temperatures recorded during Test 15.

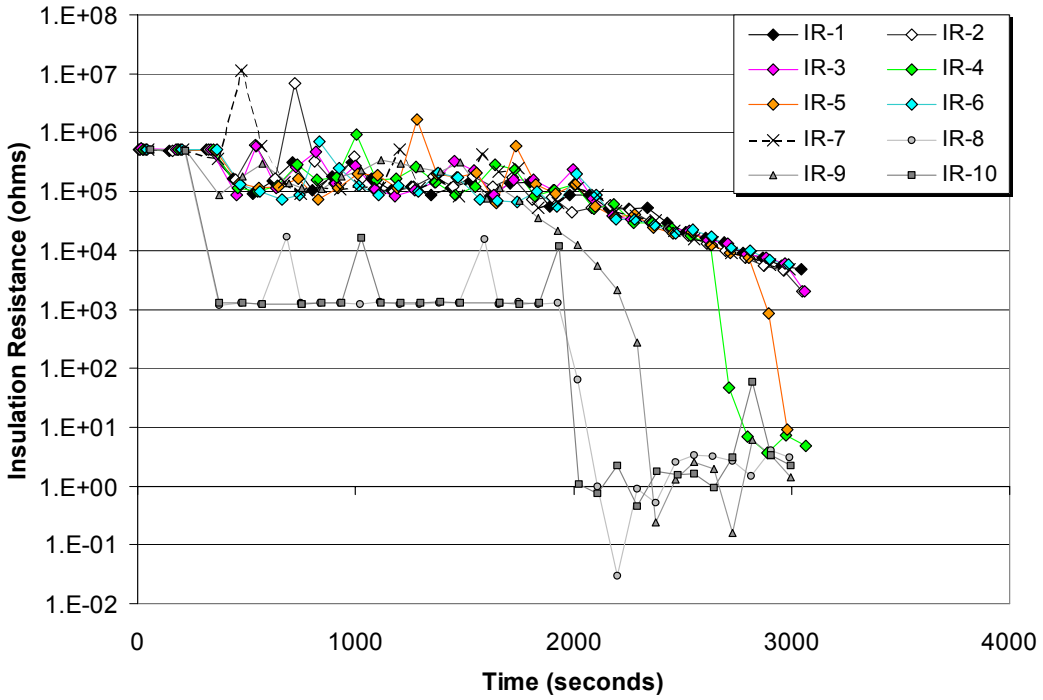

Figure 5-57. Total IR of each conductor recorded during Test 15.

Table 5-7. Summary of Cable Behavior during Test 15

Time (s)	Observations
~ 1250	Conductors 8 and 10 IRs decrease to ~1000 Ω
~ 2020	Conductors 8 and 10 IRs decrease to ~1 Ω, perhaps indicating shorts to ground
~ 2400	Conductor 9 IR decreases to < 1 Ω, perhaps indicating a short to ground
~ 2700	Conductor 4 IR decreases to < 100 Ω, perhaps indicating a short to ground
~ 3000	Conductor 5 IR decreases to < 100 Ω, perhaps indicating a short to ground

5.4.4 Test 16

Test 16 was also impacted by the wiring problem with the IR measuring system and was conducted prior to Test 14. The IR cable bundle consisted of a nine-conductor thermoplastic control cable surrounded by three single-conductor thermoplastic cables. The three external cables were electrically ganged together and monitored on channel 10. The test conditions for exposure consisted of a 145-kW heat release rate fire with the test cables exposed to the fire plume. The IR cable bundle was routed inside a conduit located alongside the cable tray toward the center of the test cell. The cable tray and conduit were set 1.8 m (6 ft) above the floor. The burner was set directly under the corner of the cable tray. A monitored instrument cable was also included in the tray for the current loop circuit (see Section 6).

Figure 5-59 shows the time-temperature plots for two of the thermocouples monitored during the test. TC #27 was mounted on a tray rung at the corner of the tray, and TC #73 was located at the mid-point of the instrumented cable TC-4. These two thermocouples were chosen because they showed the worst-case temperature exposure conditions (highest recorded temperatures) for the air near the IR cable and for the instrumented cable closest to the IR bundle. The peak tray temperature recorded during this test was 550°C (1022°F) and the cable temperature was 276°C (529°F).

As previously mentioned, the IR measurement system was only capable of determining total IR due to a wiring problem during Test 16. Figure 5-60 shows the time-dependent change in the total IR for each of the 10 conductors in the IR cable measured during this test. Table 5-8 summarizes the behavior of the cable in the test. While some of the conductor IRs increase again (~1000 Ω) near the end of the test, it is believed that all experienced failure and the apparent recovery was due more to noise than to real healing. Figure 5-61 shows the resulting leakage currents allowed by the change in IR for each conductor.

Table 5-8. Summary of Cable Behavior during Test 16

Time (s)	Observations
~ 850	Conductors 5, 6, 7, 8, and 9 IRs decrease to ~10 Ω
~ 900	Conductors 1, 3, and 4 IRs decrease to ~10 Ω
~ 990	Conductor 2 IR decreases to ~10 Ω
~ 1450	Conductor 10 IR decreases to <1 Ω

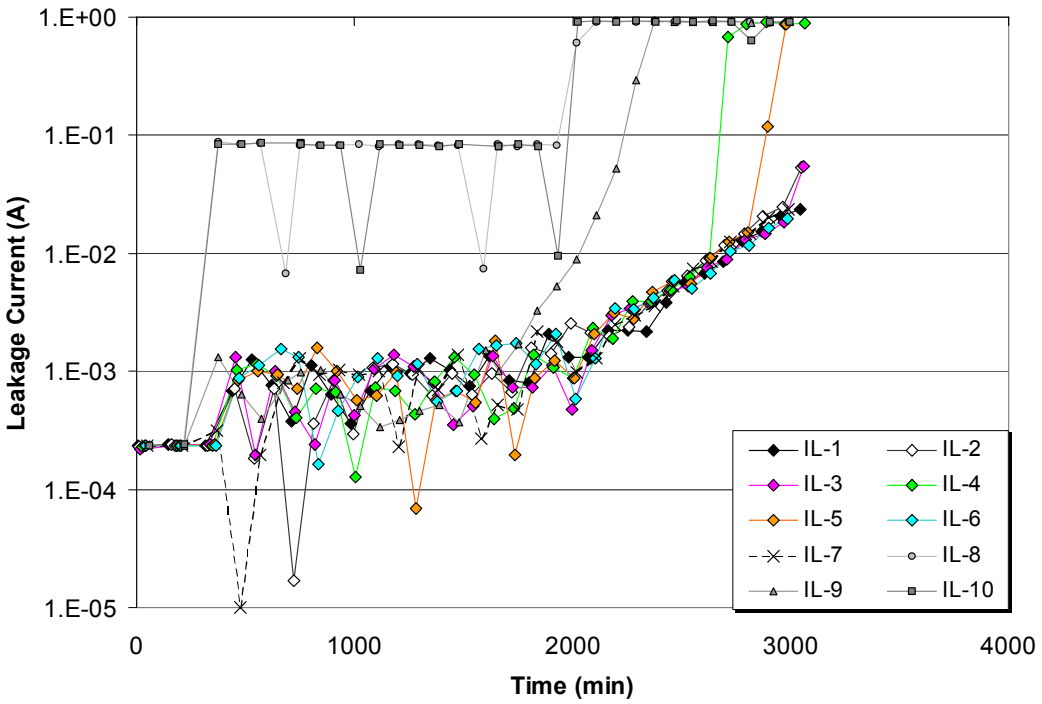

Figure 5-58. Total leakage currents resulting from IR changes for each Conductor during Test 15.

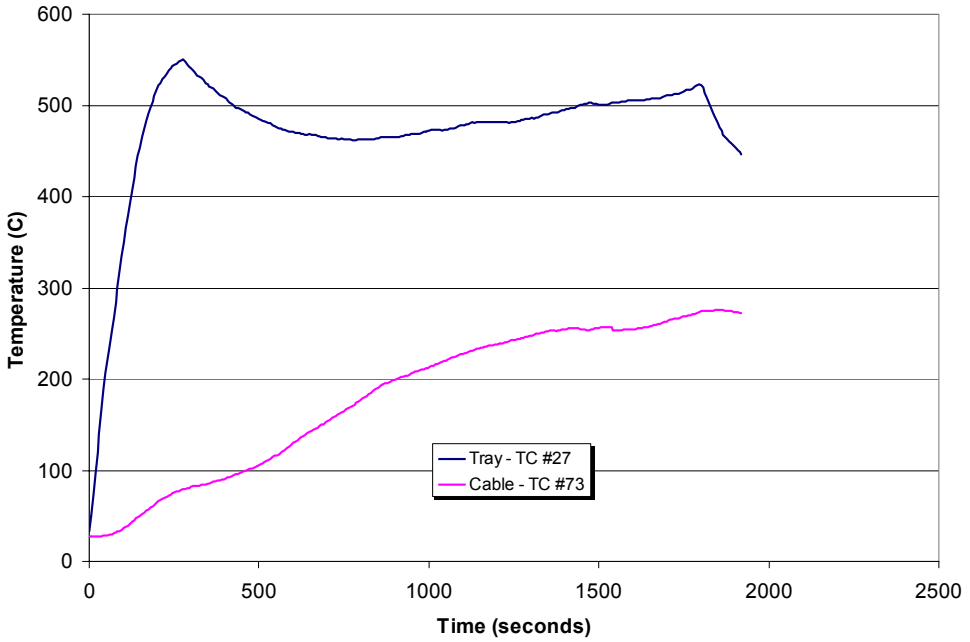

Figure 5-59. Representative tray and TC-4 cable temperatures recorded during Test 16.

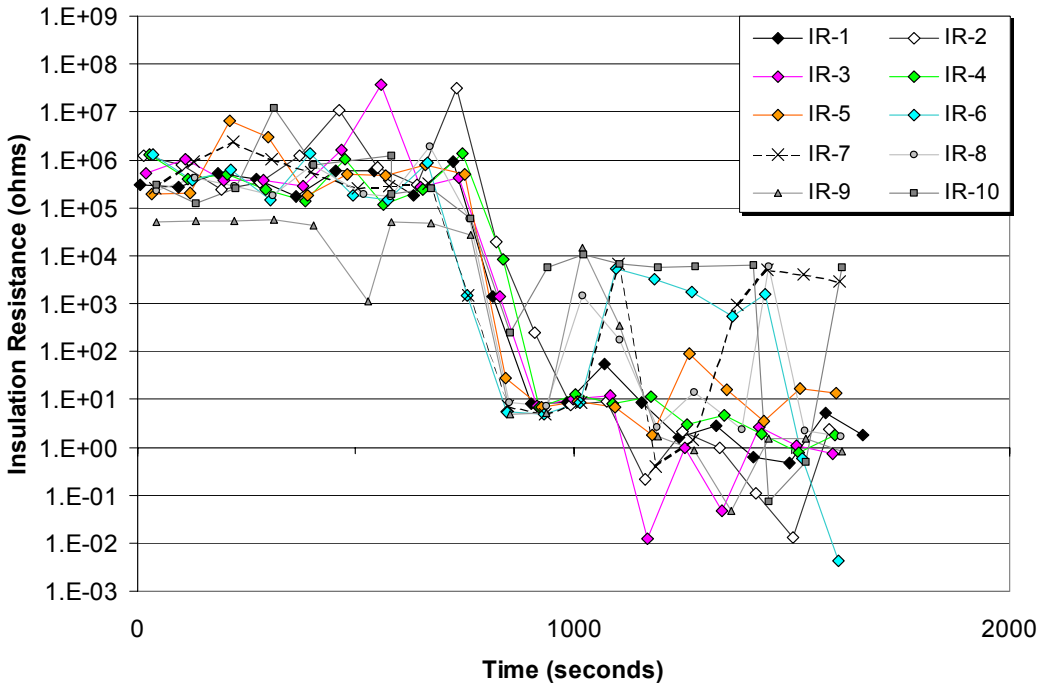

Figure 5-60. Total IR of each conductor recorded during Test 16.

5.4.5 Test 17

Test 17 was the last of the tests affected by the wiring problem with the IR measuring system and it was also conducted prior to Test 14. The IR cable bundle consisted of a nine-conductor thermoplastic control cable surrounded by three single-conductor thermoplastic cables. The three external cables were electrically ganged together and monitored on channel 10. The test conditions for exposure consisted of a 200-kW heat release rate fire with the test cables set in a vertical tray and exposed to a combined hot gas layer and radiant heat environment. The burner was set 0.6 m (2 ft) behind the center of the cable tray. A monitored instrument cable was also included in the tray for the current loop circuit (see Section 6).

Figure 5-62 shows the time-temperature plots for two of the thermocouples monitored during the test. TC #23 was mounted on a tray rung at the top of the vertical tray, and TC #56 was located at the top of the instrumented cable TC-4. These two thermocouples were chosen because they showed the worst-case temperature exposure conditions (highest recorded temperatures) for the air near the IR cable and for the instrumented cable closest to the IR bundle. The peak tray temperature recorded during this test was 482°C (900°F) and the peak cable temperature was 449°C (840°F).

Again, the IR measurement system was only capable of determining total IR due to a wiring problem during Test 17. Figure 5-63 shows the time-dependent change in the total IR for each of the 10 conductors in the IR cable measured during this test. Table 5-9 summarizes the behavior of the cable in the test. Figure 5-64 shows the resulting leakage currents allowed by the change in IR for each conductor.

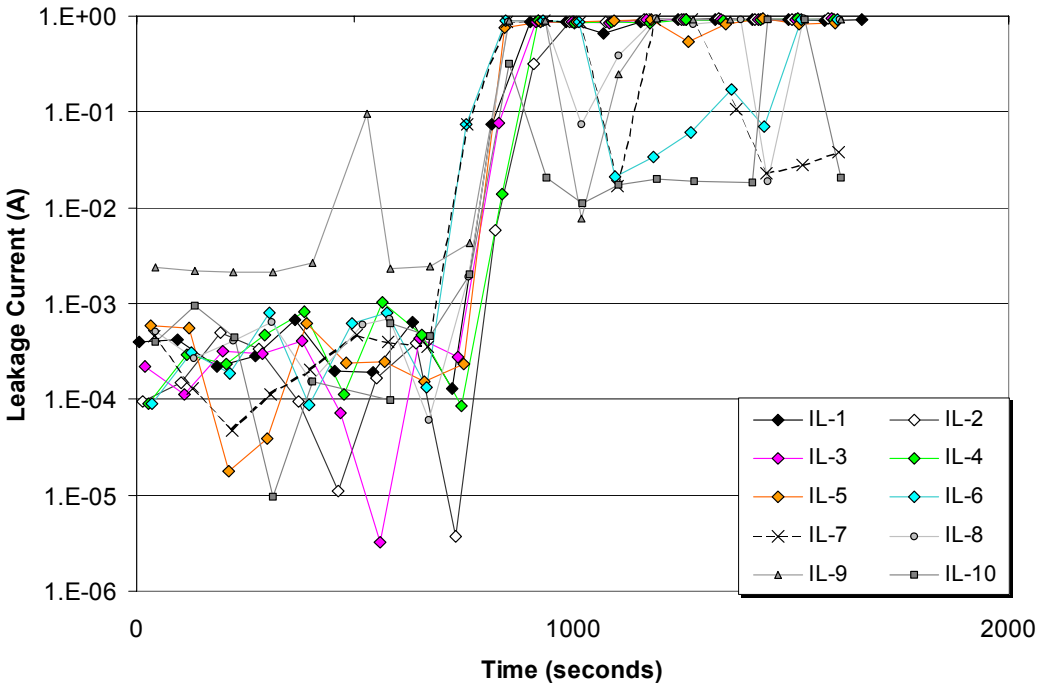

Figure 5-61. Total leakage currents resulting from IR changes for each conductor during Test 16.

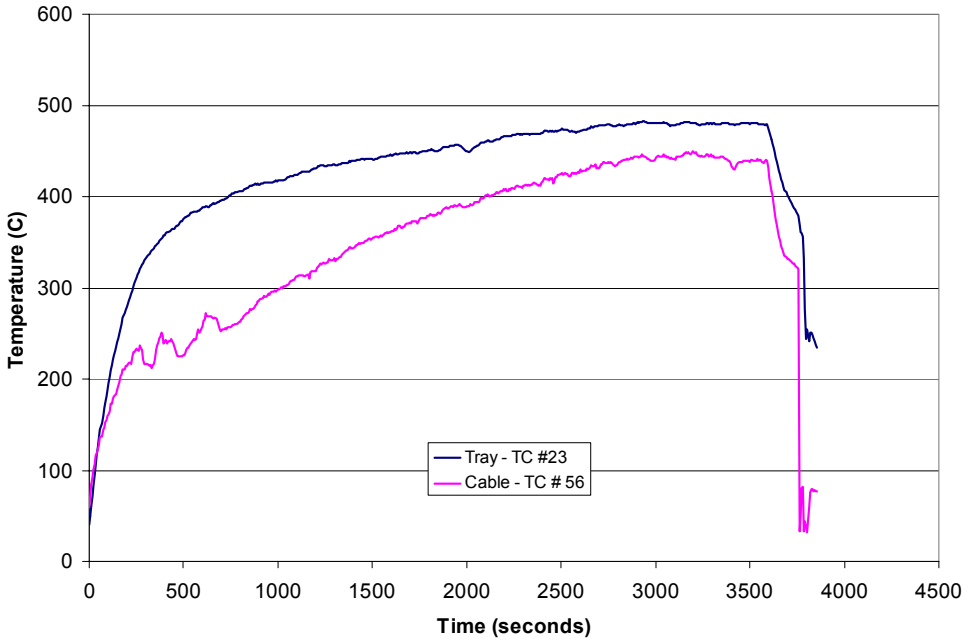

Figure 5-62. Representative tray and TC-4 cable temperatures recorded during Test 17.

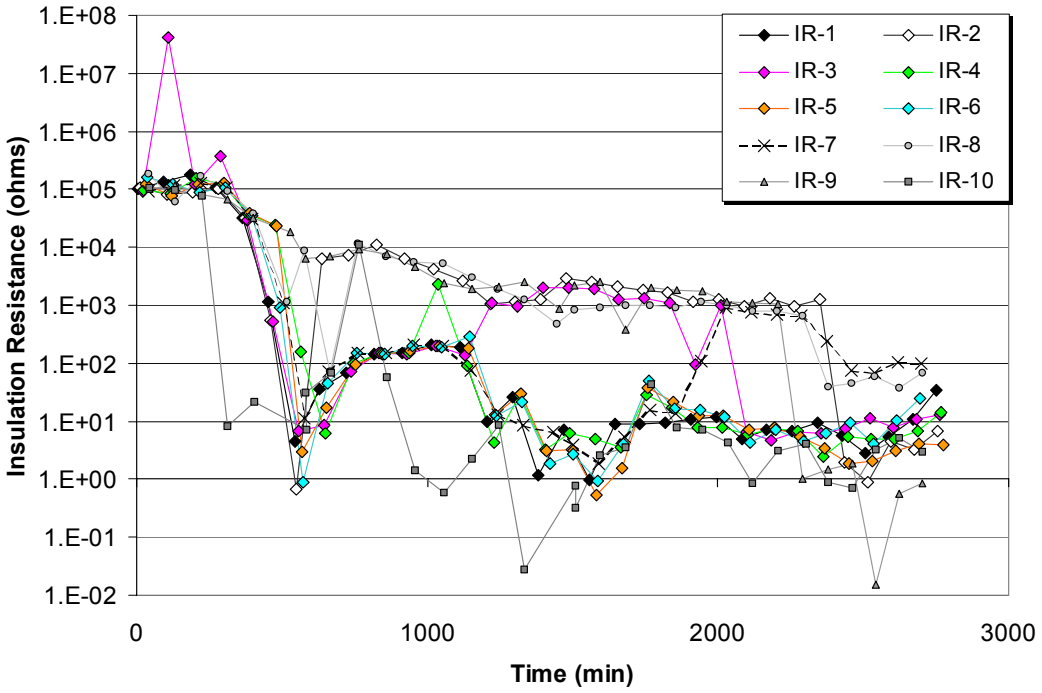

Figure 5-63. Total IR of each conductor recorded during Test 17.

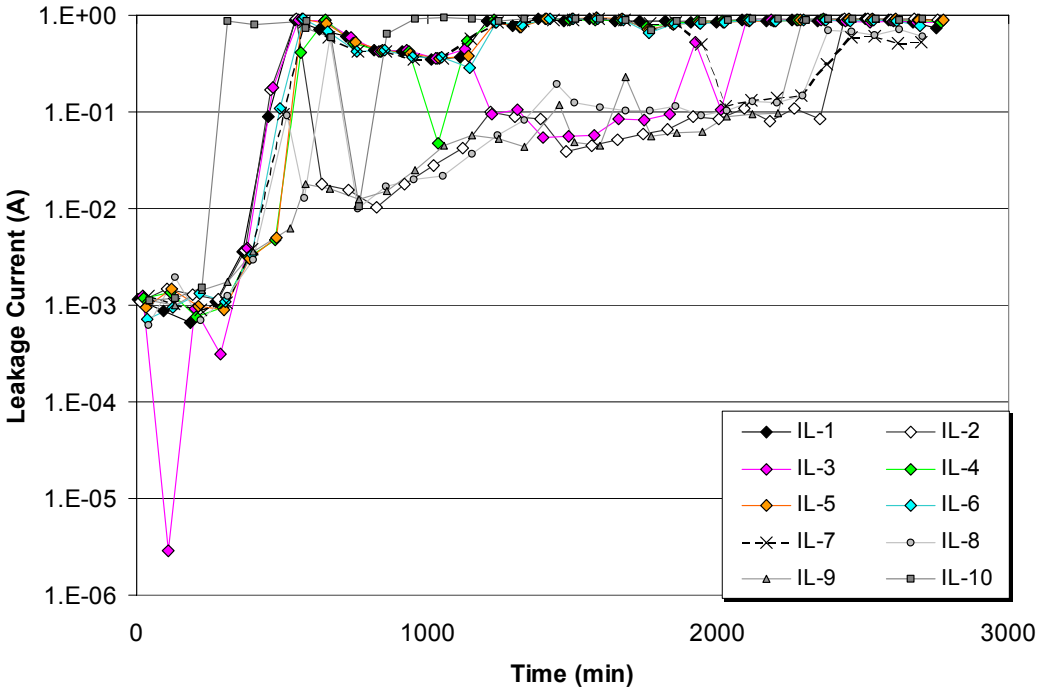

Figure 5-64. Total leakage currents resulting from IR changes for each conductor during Test 17.

Table 5-9. Summary of Cable Behavior during Test 17

Time (s)	Observations
~ 315	Conductor 10 IR decreases to ~10 Ω
~ 550–650	Conductors 1, 2, 3, 4, 5, 6, 7, and 8 IRs decrease to 1 to 10 Ω
~ 2290	Conductor 9 IR decreases to <1 Ω

5.4.6 Test 18

Test 18 was the last test conducted in the test series. It was a 250-kW heat release rate fire with the cables exposed to the hot gas layer. The burner was placed in the center of the fire test cell. The IR cable bundle consisted of three thermoset three-conductor cables secured together and routed in the horizontal conduit. A thermoset instrument cable for the current loop circuit was also placed in the conduit (see Section 6). The wiring problem with the IR Measurement system that had plagued Tests 13, 15, 16, and 17 had been diagnosed and corrected in time to allow its proper operation during this test.

No thermocouple-instrumented cable was routed in the conduit during this test; hence, there is no cable temperature data available. In addition, no direct measure of conduit temperature was made either. Failures of the IR cable bundle were identified based on the results of this test. Figure 5-65 shows a plot of the IRs between Conductor 1 and the other conductors in the IR bundle. Conductors 1 through 3 made up one of the three-conductor cables of the IR bundle, Conductors 4 through 6 were in a second cable, and Conductors 7 through 9 formed the third cable. As shown in the figure, most of the IR values drop to < 100 Ω at ~3000 seconds.

Figure 5-66 shows the IR values between each of the IR cable conductors and ground recorded during Test 18. This figure shows a relatively gradual decline in IRs to ground from ~10^6 down to ~3000 Ω over the period 1500 to 2500 seconds. The almost simultaneous failure of Conductors 1, 3, and 9 followed this. The next conductor to fail was Conductor 7 at ~ 2900 seconds, then Conductors 8 and 4 failed. Conductors 5, 2, and 6 eventually failed during the course of the test. All conductors shorted to ground before interacting with any other conductor. Table 5-10 provides a summary of the conductor failures. Figure 5-67 presents the change in leakage current for Conductors 1 and 2 occurring during Test 18.

Based solely on the results of the IR measurements made during Test 18, it appears that the IR cable experienced significant damage and could have caused blown fuses.

Table 5-10. Summary of Cable Failure Times and Modes during Test 18

Time (s)	Failure Mode Observed
~ 2730–2830	Conductors 1, 3, and 9 short to ground
~ 2930	Conductor 7 shorts to ground
~ 3200–3400	Conductors 4, 5, and 8 short to ground
~ 3580	Conductor 2 shorts to ground
~ 4300	Conductor 6 shorts to ground

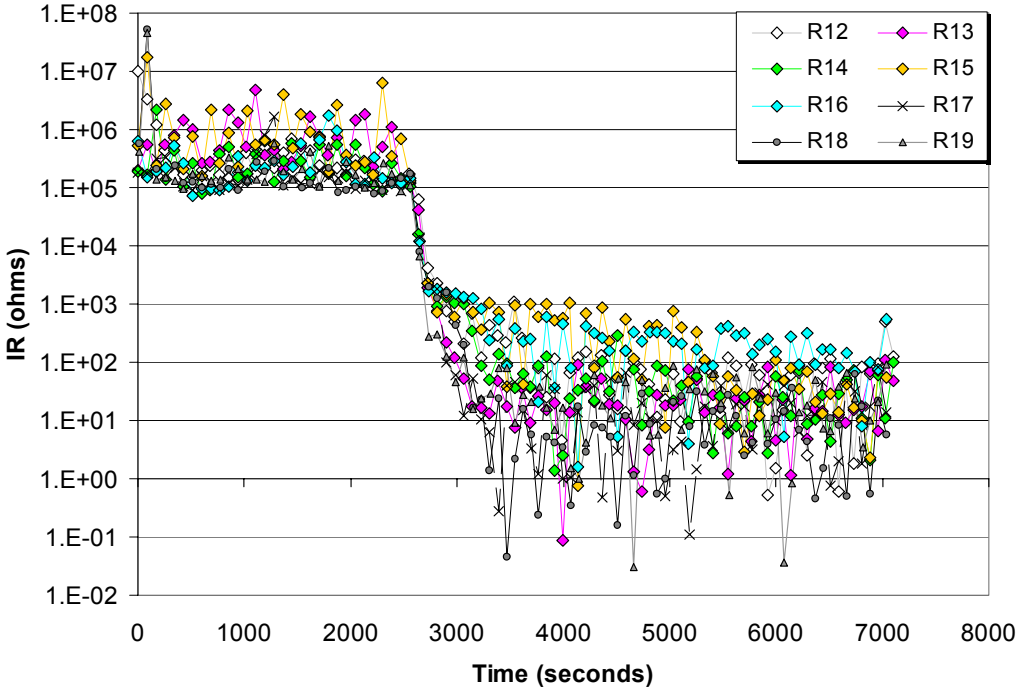

Figure 5-65. Representative conductor-to-conductor IRs obtained during Test 18. This plot shows the IR between Conductor 1 and the other eight conductors in the IR cable bundle.

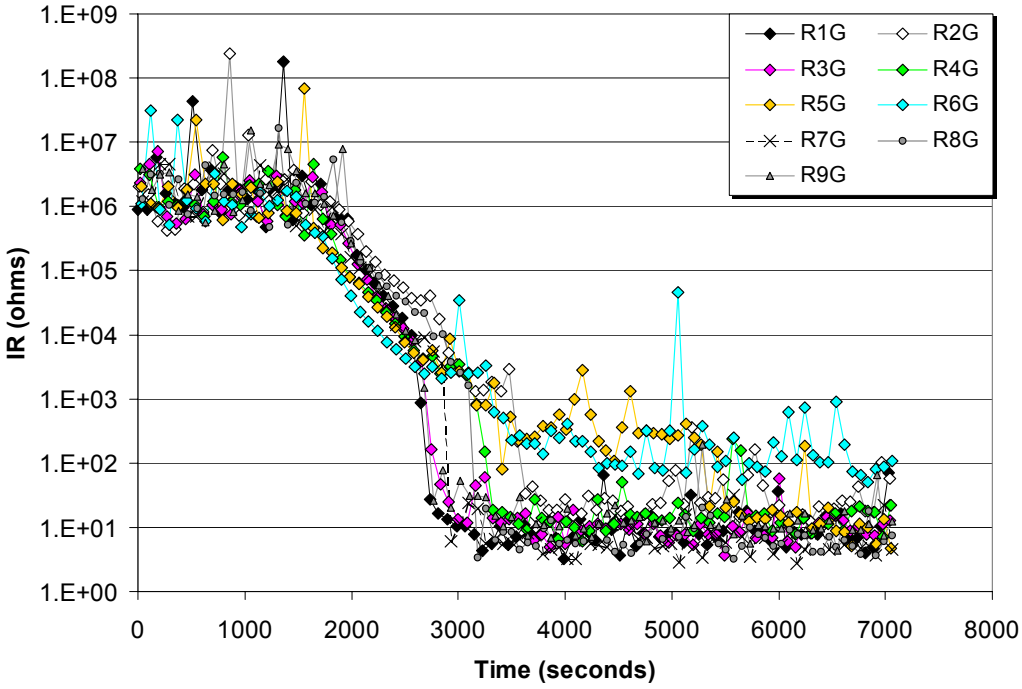

Figure 5-66. Conductor-to-ground IRs obtained during Test 18.

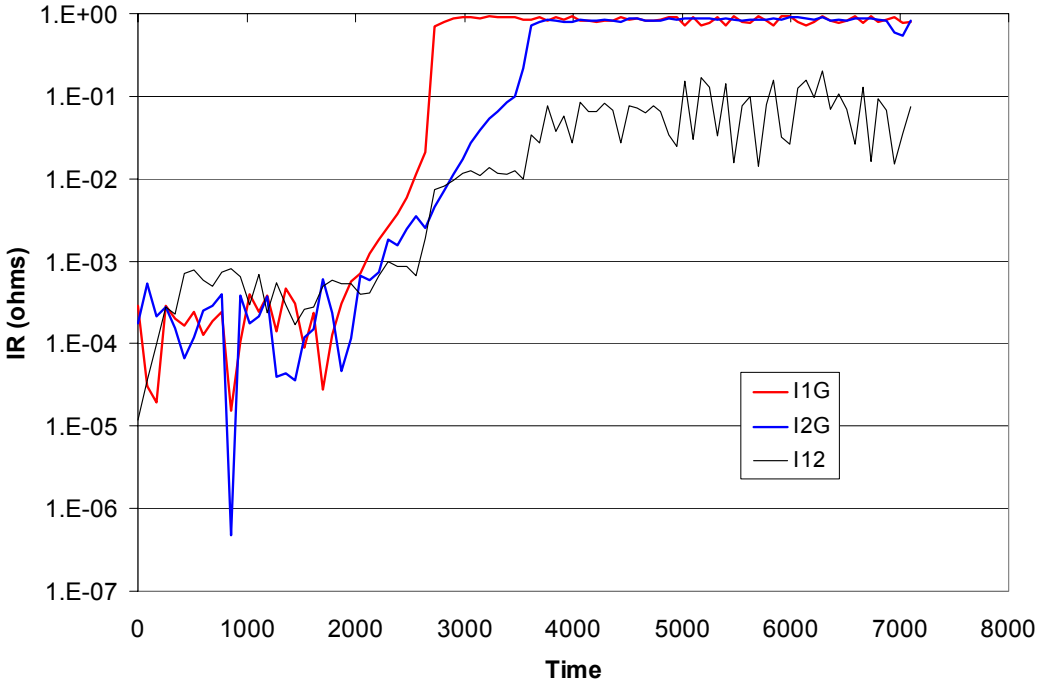

Figure 5-67. Leakage currents resulting from IR changes in Conductors 1 and 2 during Test 18.

6. CURRENT LOOP DATA AND RESULTS

During the last six tests, a mockup of an instrument circuit was added to the SNL/NRC diagnostic system. This circuit was intended to simulate the operation of a typical 4 to 20 mA instrument loop. A schematic of the instrument loop circuit used during Tests 13 through 18 is presented in Figure 6-1. The instrument loop circuit was independent and separate from the IR measurements made concurrently during the tests. However, the current loop data was gathered and stored by the same computer data acquisition system as the IR data. The cables tested using this circuit were all standard instrument cables.

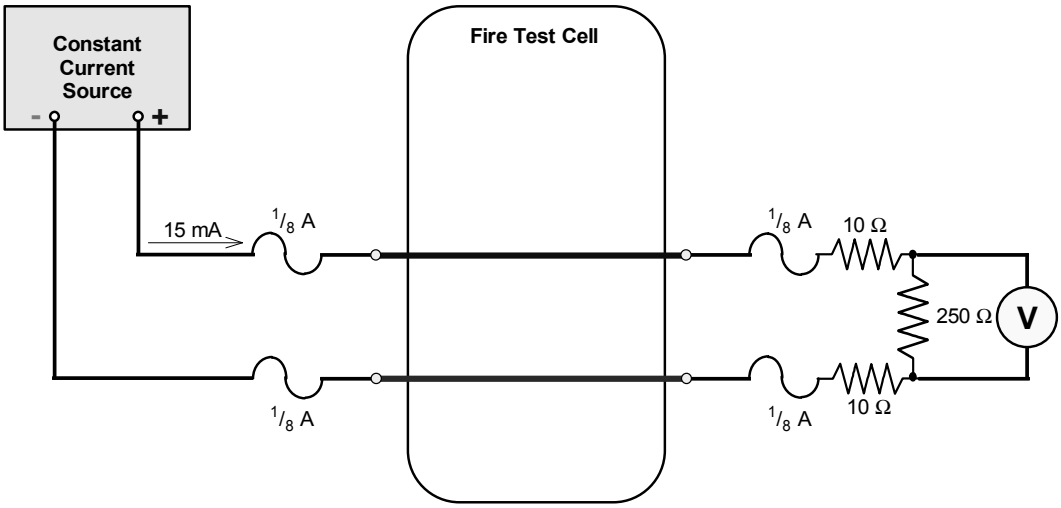

Figure 6-1. Instrument loop circuit.

The instrument loop circuit consists of a low-power current source, fuses to protect the components in the event of an unwanted voltage surge, two 10 Ω resistors to simulate a long run of instrument cable (~610 m (2000 ft) as opposed to the short length exposed during the fire test), a 250-Ω load resistor, and a voltmeter to provide the simulated readout circuit. Note that the 250-Ω load resistor is analogous to a shunt resistor in an output meter that would convert the 4 to 20 mA signal into a 1 to 5 V signal. Use of such a shunt resistor at the output device is typical of many instrumentation circuit designs.

The circuit was driven by a constant current output from the current source of 15 mA. It was anticipated that, as the fire degraded the instrument cable's IR, the apparent output signal would change. In particular, portions of the fixed current signal could leak directly from conductor to conductor bypassing the load/shunt resistor. This behavior would be reflected as an inaccurate reading at the load resistor/voltmeter assembly.

Note that in presenting the data result, the actual measured output voltage was converted to an equivalent 0 to 100% process variable scale to ease the interpretation of the results. That is, an output reading of 1 V corresponds to zero on the process variable scale, and an output reading of 5 V corresponds to 100% on the process variable scale. Given the 15 mA constant input current, a reading of about 68% on the process variable scale is expected. Also note that if the two conductors form a "hard" (or very low impedance) short, the reading would go off-scale low on the process variable scale.

6.1 Test Data and Results

6.1.1 Test 13

Figure 6-2 presents the current loop data obtained during Test 13. The cable used was a shielded two-conductor thermoset instrumentation cable exposed to the hot gas layer of a 350-kW flame. As shown in the figure, the output

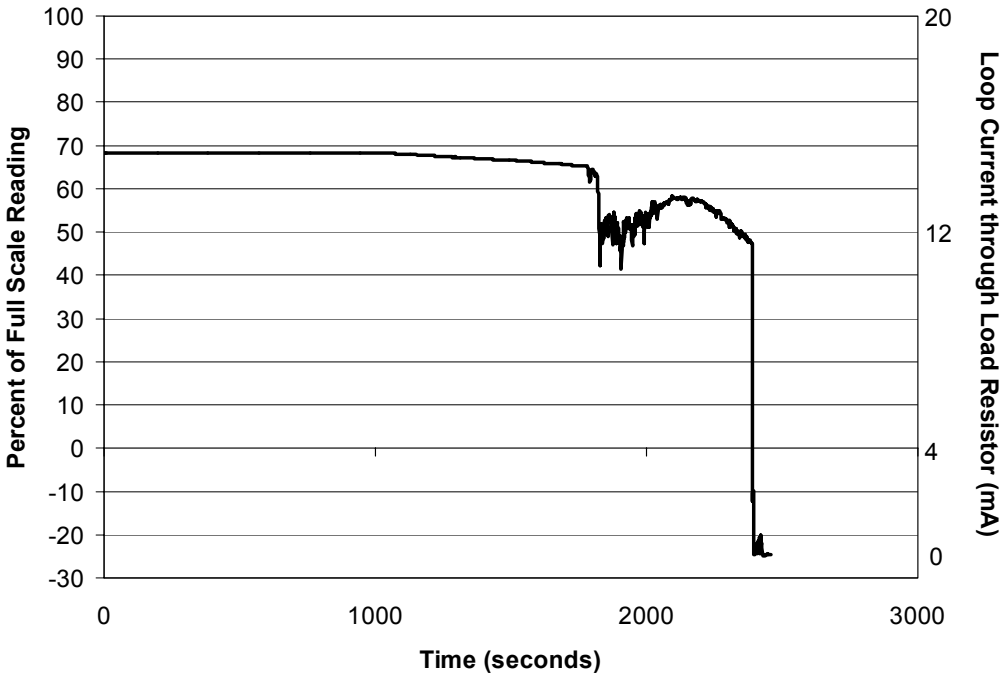

Figure 6-2. Current loop data obtained during Test 13.

signal of the circuit holds at a steady 68% (corresponding correctly to the 15 mA input signal) until ~1100 seconds. At that time, the signal begins to degrade to about 64% at ~1800 seconds. The signal then drops to ~50% and experiences several fluctuations between ~40% to ~53%. After some time, the signal climbs back up to ~57% and holds for a short time. The signal then decays to about 47% and is lost at ~2390 seconds.

This sort of behavior in an instrument circuit could provide an operator with misleading information. The operator would not be able to readily determine if the readout was an accurate indication of plant status or if it was the result of a fire. This is particularly true in this case, since the change in signal output varies rather slowly, and depending on the filtering on the input side of the readout device, the fluctuations occurring from 1800 to 2200 seconds may be damped so that the readout would remain stable. As noted below, a prolonged transition from "good signal" to obviously failed proved to be typical of the thermoset cables tested.

6.1.2 Test 14

Figure 6-3 presents the current loop data obtained during Test 14. The cable used was a two-conductor thermoplastic instrumentation cable routed in conduit and exposed to the plume of a 145-kW flame. As shown in the figure, the output signal remains at 68% until ~2225 seconds, whereupon the signal is abruptly lost. The signal briefly recovers to ~67% and is lost again for the remainder of the test.

Unlike the previous case, this sort of extremely rapid loss of signal would be an obvious indication that the instrument circuit had failed and was an unreliable source of plant information. As noted below, this abrupt failure behavior proved to be typical of the thermoplastic cables tested.

6.1.3 Test 15

Figure 6-4 presents the current loop data obtained during Test 15. The cable used was a shielded two-conductor thermoset instrumentation cable with a drain wire included. The cable was routed in a horizontal cable tray and exposed to a variable intensity flame (350/200/450 kW) during the test. As shown in the figure, the 68% output signal remains constant until ~1100 seconds. It then begins a slow decline to ~36% over the next 400 seconds. At this time, the signal is lost completely and remains so for the duration of the test.

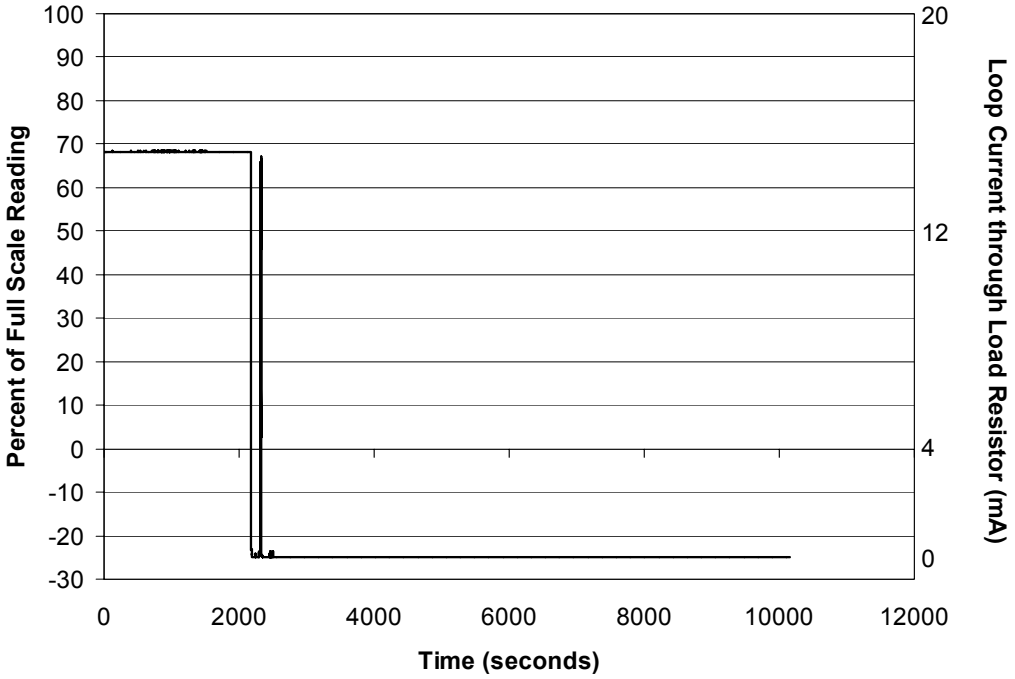

Figure 6-3. Current loop data obtained during Test 14.

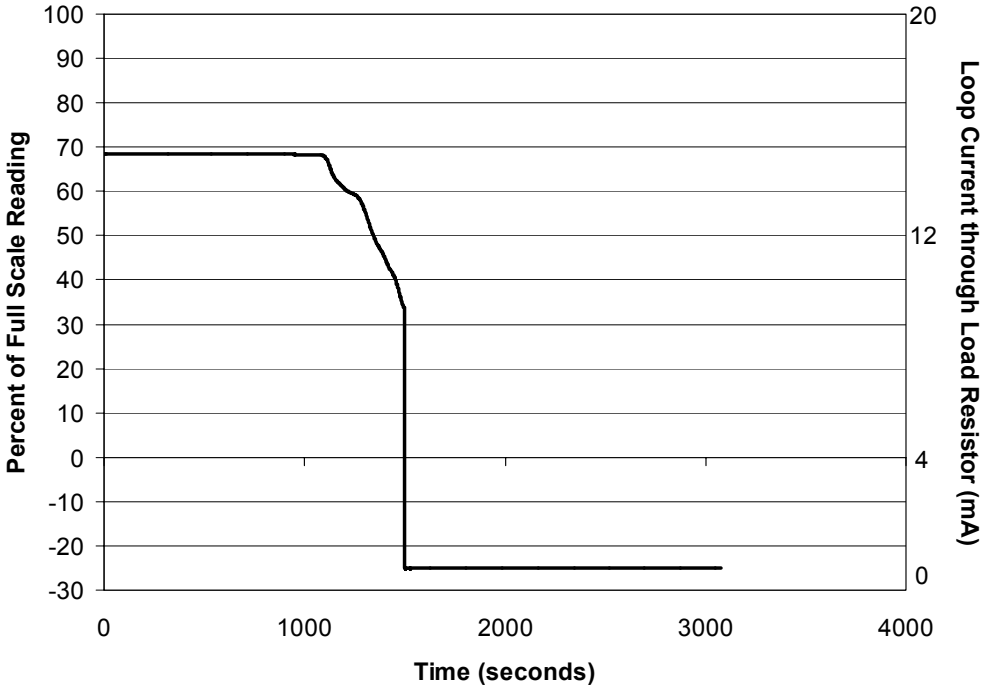

Figure 6-4. Current loop data obtained during Test 15.

Here again, as discussed above for Test 13, because of the rather slow, monotonic decay of the output signal, an operator may be misled into thinking that plant conditions are changing rather than that the instrument is being adversely affected by the fire.

6.1.4 Test 16

Figure 6-5 presents the current loop data obtained during Test 16. The cable used was a three-pair thermoplastic instrumentation cable with shield and drain wire. Only one pair of conductors was employed during this test. The instrument loop cable was routed in the cable tray and exposed to the plume of a 145 kW fire. As shown in the figure, this cable only lasted ~100 seconds before succumbing to damage and loosing the signal for the rest of the run.

As was the case for Test 14, above, this sort of extremely rapid loss of signal would make the operator realize that the instrument had been affected by the fire and was an unreliable source of plant information.

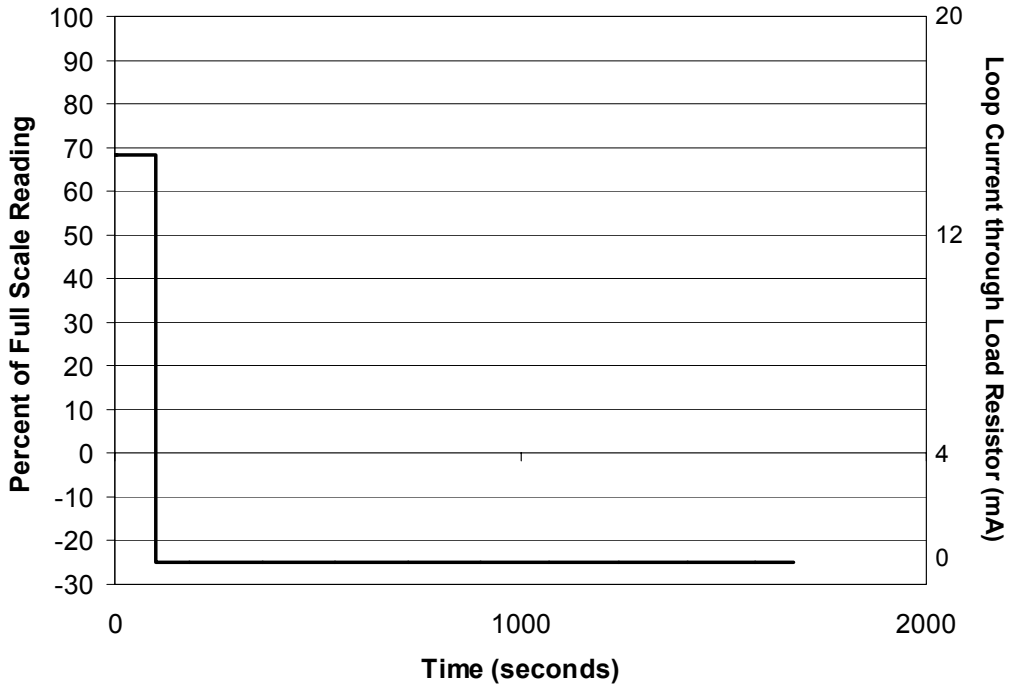

Figure 6-5. Current loop data obtained during Test 16.

6.1.5 Test 17

Figure 6-6 presents the current loop data obtained during Test 17. A two-conductor thermoset instrumentation cable was routed in a vertical cable tray and exposed to the hot gas layer and radiant heat from a 200-kW flame. As shown in the figure, the signal remains at a constant 68% until ~930 seconds when it degrades slightly to 67% at ~1420 seconds. The signal fluctuates very wildly over the period of 1420 to 1500 seconds, and then fluctuates again during the period of 1530 to 1600 seconds. The signal is then lost for the rest of the test.

This sort of extreme fluctuation and rapid loss of signal would make the operator realize that the instrument had been affected by the fire and was an unreliable source of plant information.

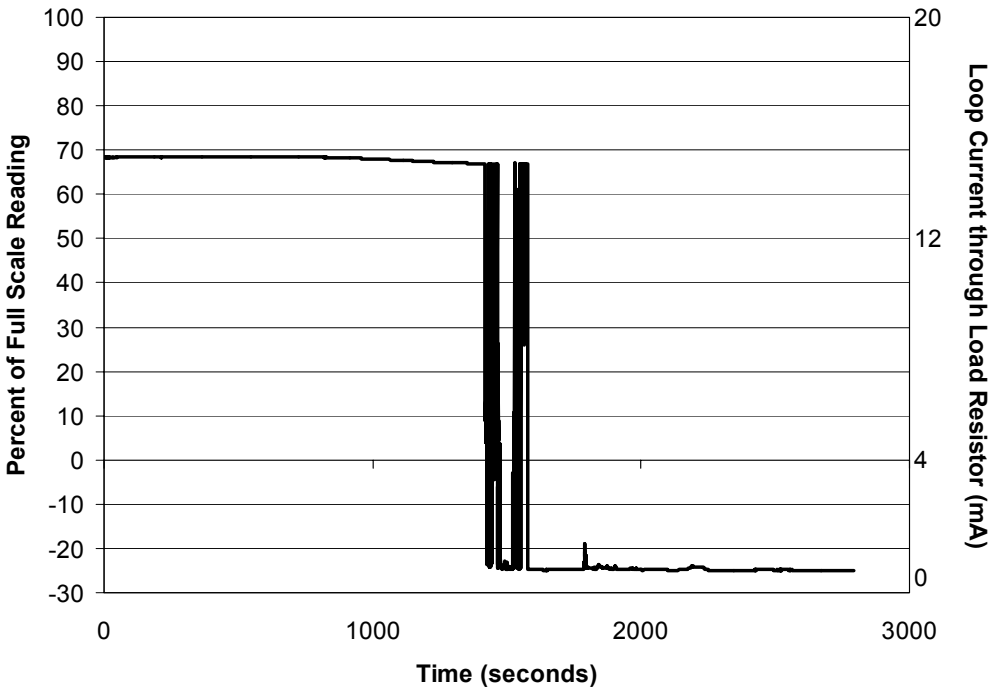

Figure 6-6. Current loop data obtained during Test 17.

6.1.6 Test 18

Figure 6-7 presents the current loop data obtained during Test 18. A two-conductor thermoset instrumentation cable was routed in the conduit. A 250-kW hot gas layer exposure fire was employed during this test. As shown in the figure, the current loop circuit output signal remains relatively constant at 68% until ~1140 seconds. The signal then decays down to ~40% at 1325 seconds. Afterwards, the signal fluctuates briefly and is ultimately lost for the duration of the test.

In this case, the signal degradation has some of the same "gentle" sloping characteristics of the other thermoset cables tested, giving rise to the concern about whether or not the operator would interpret the change as a change in plant status or as the effect of the fire.

6.2 Observations

The instrument loop cables failed at some time during each of these six tests. The most notable result of these tests is the pronounced behavioral differences observed between the failure of the thermoplastic cables and that of the thermoset cables. Thermoplastic cables generally displayed no characteristics of signal degradation prior to the complete loss of signal. On the other hand, the thermoset cables usually displayed some substantial amount of signal degradation for a relatively prolonged time period prior to the total loss of signal.

Table 6-1 presents the times for onset of signal degradation and complete loss of signal for each of the instrument cables tested.

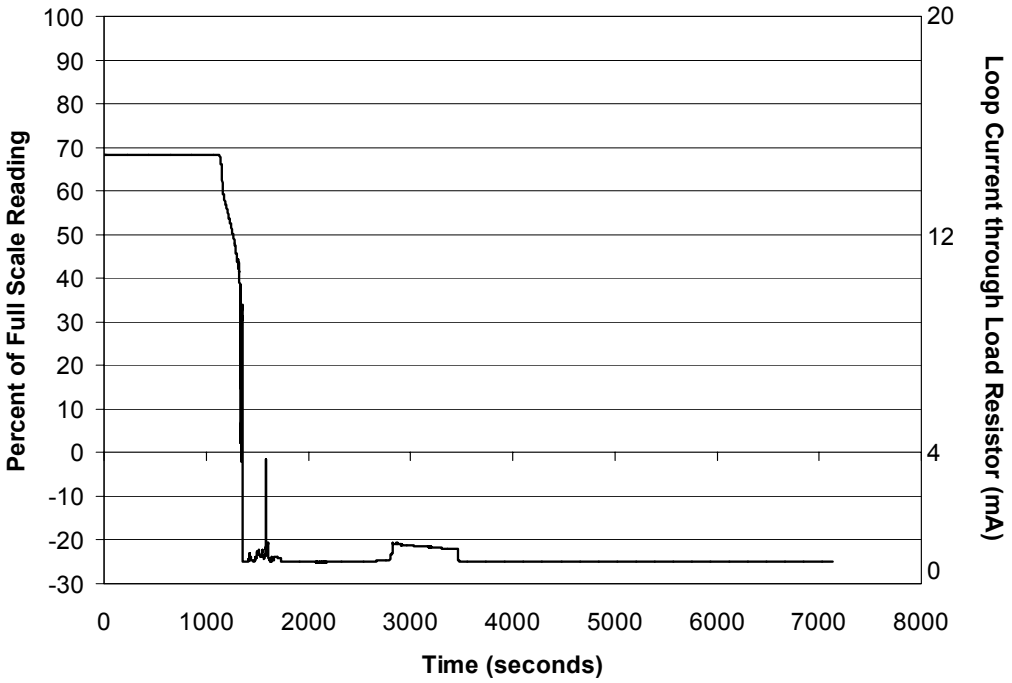

Figure 6-7. Current loop data obtained during Test 18.

Table 6-1. Current Loop Test Data

Test Number	Cable Material	Raceway Type	Time of Signal Degradation (s)	Time of Signal Loss (s)
13	Thermoset	Horiz. Tray	1100	2390
14	Thermoplastic	Conduit	—	2225
15	Thermoset	Horiz. Tray	1100	1500
16	Thermoplastic	Horiz. Tray	—	100
17	Thermoset	Vert. Tray	930	1600
18	Thermoset	Conduit	1140	1325

7. CONCLUSIONS

7.1 Insulation Resistance-Based Cable Failure Mode Results

Failures were observed in 12 of the 18 tests conducted. Tests 3, 4, and 6 through 9, 12, 13, and 15 through 18 all showed indications of cable failure based on the IR data collected. Of these 12 cases, the mode of initial failure can be discerned in seven cases (Tests 3, 4, 6 through 8, 12, and 18). The exceptions are as follows:

- Test 9 involved an ungrounded DC power source that made the IR system unable to detect shorts to ground. In total, three of the IR tests were run in the ungrounded DC power mode (Tests 9 through 11). (No failures were observed in Tests 10 and 11.) Inclusion of the failures observed during Test 9 in the overall statistics regarding failure mode would inappropriately bias the answer towards conductor-to-conductor hot shorts since conductor-to-ground shorts could not be detected. This is reflected in the "n/a" entries for Test 9 in Table 7-1.

- Tests 13 and 15 through 17 were impacted by a wiring fault in the IR system such that the approximate time of cable failure can be determined, but the mode of failure cannot. Hence, these tests also do not contribute to the failure mode statistics.

Most of the tested cable bundles involved a multiconductor cable surrounded by three single conductor cables. It has been concluded that independent treatment of the internal behavior of the multiconductor cables (intracable conductor-to-conductor hot shorts versus shorts to ground) versus the external single-conductor cables relative to each other and to the multiconductor cable (intercable conductor-to-conductor hot shorts versus shorts-to-ground) is appropriate. As discussed below, the multiconductor cables tended to display initial failures involving intracable hot shorts, which transitioned to shorts to ground at some later time. In contrast, the external single-conductor cables tended to short to ground first. These were clear distinctions in this regard; hence, the data have been parsed accordingly.

It should also be noted that in creating the IR cable bundles, three single-conductor cables typically would be bundled with one multiconductor cable using single wraps of fiberglass tape at approximately 30- to 46-cm (12- to 18-in.) intervals along the length of the bundle. This created a level of contact between the cables that may not be fully representative of in-plant conditions for all cases. Hence, some bias towards cable-to-cable shorts involving the single-conductor cables and the multiconductor cable is anticipated.

The failure modes observed in each of the 18 tests are summarized in Table 7-1. For the multiconductor cables, four of the seven observed failures involved intracable conductor-to-conductor hot shorts as the initial mode of failure (Tests 3, 4, 6, and 7). All four of these cases involved cables in a cable tray. In the fifth case involving a cable bundle in a cable tray (Test 12), the multiconductor cable displayed a short to ground as the initial failure mode. The cable bundle used in Test 12 was the same seven-conductor and three single-conductor cables configuration as used in Tests 3, 4, 6, and 7. The IR cable bundle in Test 12 was also routed in a horizontal cable tray. However, it alone of the tests employing this set of conditions exhibited shorting-to-ground failures. This is the only test conducted using the grounded DC power source. It is not clear whether or not the use of a DC source impacted the failure mode since there are no other comparable failure cases. The question of AC versus DC circuit behavior may, therefore, warrant further investigation.

The observed intracable conductor-to-conductor hot shorts involved a range of conductor combinations. In some cases, individual pairs shorted together. In others, rather complex failure transitions were observed involving progressively more conductors as the test progressed. In some cases, conductors shorted in independent groupings (e.g., four conductors shorting together and two other conductors forming an independent short circuit). In one case, all seven conductors became involved in a simultaneous hot short before a short to ground was observed. In all cases where failures were observed, the conductors did ultimately short to ground. The duration of the hot shorts observed ranged from a few seconds to four minutes. It is not clear what might have happened to the cables (e.g., whether or not a short-to-ground transition would still have been observed) had the fire been put out before such transitions occurred, as no such cases were observed during this test program (all the fires continued beyond such transitions).

Table 7-1. Summary of Observed Initial Failure Modes for Conductors in the Multiconductor Cables and the Single-Conductor Cables. Failures are based on drop in conductor-to-conductor or conductor-to-ground IR to 100 Ω or less. The notation used indicates the number of cables failing in the mode defined by the column heading to the total number of cables involved in the test.

Test #	Multiconductor Cable			Single-Conductor Cables		
	Short to Ground	Conductor-to-Conductor	No Failure	Short to Ground	Cable-to-Cable	No Failure
1[(1)×]	–	–	1/1	n/a	n/a	n/a
2	–	–	1/1	–	–	3/3
3	–	1/1	–	2/3	1/3	–
4	–	1/1	–	1/3	2/3	–
5	–	–	1/1	–	–	3/3
6	–	1/1[(6)]	–	2/3	1/3[(6)]	–
7	–	1/1	–	3/3	–	–
8[(2)]	1/2	–	1/2	n/a	n/a	n/a
9[(3)]	n/a	n/a	n/a	n/a	n/a	n/a
10	–	–	1/1	–	–	1/1
11[(4)]	n/a	n/a	n/a	n/a	n/a	n/a
12	1/1			1/1[(8)]		
13[(5)]	n/a	n/a	n/a	n/a	n/a	n/a
14[(7)]			3/3	n/a	n/a	n/a
15[(5)]	n/a	n/a	n/a	n/a	n/a	n/a
16[(5)]	n/a	n/a	n/a	n/a	n/a	n/a
17[(5)]	n/a	n/a	n/a	n/a	n/a	n/a
18[(7)]	3/3			n/a	n/a	n/a
Totals:	5/17	4/17	8/17	9/20	4/20	7/20

Notes:
1 One armored cable only, no single-conductor cables
2 Two five-conductor cables (not collocated), no single conductors
3 Ungrounded DC configuration could not detect shorts to ground
4 Instrument cable not suitable for this comparison
5 IR system miswired and unable to distinguish failure modes
6 Both of these failures are indicative of the same occurrence in Test 6
7 Three three-conductor cables bundled together, no single-conductor cables, routed in conduit
8 Three single-conductor cables electrically ganged together.

Two of seven multiconductor cable failures involved cables inside a conduit (Tests 8 and 18). In both of these particular cases, the multiconductor cables initially shorted to ground. These cases were also somewhat unique in that the cables monitored were a single five-conductor cable in one test (Test 8) and a bundled group of three three-conductor cables in the second (Test 18). This is compared to the seven-conductor with three single-conductor cable bundle configurations used in all of the other tests exhibiting failures. Overall, these results point to a pronounced difference in behavior for cables in conduits versus cables in cable trays. Cables in conduits appear more likely to display shorts to ground as the initial failure mode.

With regard to intercable conductor-to-conductor shorting behavior, there were six tests with a cable bundle of more than one cable where failures were observed and where the mode of failure could be discerned. Five of these six cases involved a seven-conductor cable surrounded by three single-conductor cables in a cable tray. In four of these

five tests, there were three independently-monitored opportunities for failure (a total of 12 failure cases). Test 12 involved three external single-conductor cables electrically ganged together; thus, it is considered as only one external conductor and only one additional opportunity for an intercable failure. Of these 13 failure cases, four involved initial failures between a single-conductor cable and one or more conductors within the multiconductor cable. The remaining nine cases all involved initial shorts to ground.

The last case involving potential intercable interactions was Test 18. This test involved three three-conductor cables place in a conduit. As noted above, all of the individual conductors displayed shorts to ground as the initial fault mode. This is the only such case available for a conduit, but again, it appears to indicate a significant difference in behavior compared to cables in a tray.

No cases involving open circuit cable failures were observed. These results are consistent with the findings of the SNL Letter Report[3] in that open circuit failures have only been observed in cases involving cables energized with a high-energy (voltage and/or current) power source, and then only after repeated short-to-ground failures and arcing. The IR tests utilized a substantial voltage (i.e., 120 VAC or 100 VDC) but a very modest maximum current (<1 A). Hence, open circuit faults were not expected, and indeed were not observed.

The SNL Letter Report also reviewed the then-existing literature relating to cable failure modes observed in fire tests. It was found that the majority (at least 72%) of cable failures observed during various past fire tests where the mode of cable failure could be discerned involved initial intracable conductor-to-conductor shorts. That is, for multiconductor cables, the initial failure mode observed in about 72% (or more) of the past cases involved a short circuit between two (or more) conductors while less than one-third (28% or less) of the identified failures involved initial shorts-to-ground. (Note that one data set in particular dominated this analysis, and for that data set, all of the indeterminate cases were counted as shorts to ground.) Again, no cases of open circuit failures as the initial failure mode were found.

If the data from the cables routed in conduit are excluded (Tests 8 and 18), the IR data results are roughly consistent with these earlier findings and, in general, indicate a high likelihood that, if failure occurs, multiconductor cables will short internally before shorting to an external ground.

The data provides strong indications that the routing of cables in conduit tends to substantially reduce the likelihood of hot shorts (either intra- or intercable). During both tests where cable in conduit failures were observed, the multiconductor cables all shorted to ground as the initial failure mode. This is discussed further in Section 6.2.2.1.

7.2 Insulation Resistance Measurement Results Compared to SNL Influence Factors

In the SNL Letter Report, the authors speculated that a number of parameters related to a particular cable, its routing, and the exposure to which it was subjected, may impact the conditional probability that given a cable failure, a specific failure mode (i.e., conductor-to-conductor hot short, short-to-ground, or open circuit) might be observed. These parameters were identified as potential "influence factors." The SNL Letter Report also provided tentative assessments of each factor's potential significance and likely impact based on then-current knowledge and the author's judgment. The influence factors identified by SNL were grouped into four broad categories, each including a number of associated cable parameters. For convenience, the list of those influence factors is repeated here:

[3] Note that in the NEI tests, it is difficult to separate exposure mode (plume versus hot layer) from Exposure Intensity and Relative Fire Elevation. Once the Exposure Intensity (the fire heat release rate) was determined, the Exposure Mode and Relative Fire Elevation was also determined for these tests. For example, if the test involved a 200-kW or greater flame intensity, the exposure mode was set up as a hot gas layer exposure and the relative height of the horizontal cable tray was set at 2.1 m (7 ft). For heat release rates of less than 200 kW, the exposure mode was always in the fire plume and the trays were set at 1.8 m (6 ft) above the gas burner. In the discussion that follows, the effects are combined under the headings of Exposure Mode and Exposure Intensity, but Relative Elevation is not separately discussed.

Cable physical properties and configuration factors:

- Insulation/jacket composition
- Number of conductors in a multiconductor cable
- Armoring
- Shielding of conductor pairs
- Presence of an uninsulated ground conductor
- Aging condition
- Cable size
- Cable qualification status

Routing factors:

- Cable tray types versus conduits
- Overall raceway fill
- Maintained spacing installations
- Protective coatings
- Raceway orientation
- Bundling of cables

Electrical function factors:

- Circuit function (instrumentation, indication, power, or control)
- Cable ampacity load for power cables
- Circuit voltage

Fire exposure condition factors:

- Exposure mode (flame impingement, thermal radiation, or convection)
- Exposure intensity and duration
- Application of suppressants
- Relative fire elevation

Of these 21 influence factors, eight were addressed to some extent in the industry's test program. (Note that, by design, only a subset of the identified influence factors was addressed by this test program.) These eight factors are: Insulation/Jacket Composition, Number of Conductors, Armoring, Cable Tray versus Conduit, Raceway Fill, Raceway Orientation, Exposure Mode, and Exposure Intensity. The following subsections discuss the IR test results and the insights they lend to these seven influence factors and their significance with regard to the cable failure mode probability.

7.2.1 Cable Physical Properties and Configuration Factors

7.2.1.1 Insulation/Jacket Composition

Table 7-2 indicates the general types of cable insulation materials tested. With the exception of the armor cable in Tests 1 and 13 and the two five-conductor cables in Test 8, all of the others were composed of multiconductor cables bundled with one or more external cables (refer to Section 3.2.8). The thermoplastic multiconductor cables most often failed by initially shorting conductor-to-conductor, whereas the thermoplastic external cables were evenly split between cable-to-cable shorts and shorts to ground. Thermoset cables tended to short to ground first.

Table 7-2. Composition of Cables Tested Using the IR Measurement System

Test No.	Cable Insulation	No. of Cable Bundles	Configuration
1, 13	Armored	One in each test	One 8/c armored cable
2, 3, 5, 7, 9, 12, and 15	Thermoset	One in each test	One 7/c cable with 3-1/c external cables
4, 6	Thermoplastic	One in each test	One 7/c cable with 3-1/c external cables
8	Thermoset	Two	One 5/c cable in tray, one 5/c cable in conduit
10	Thermoset	One	One 7/c cable with 1-1/c external cable
11	Thermoset	Two	One 2/c instrument cable and one with three pairs (6/c) instrument cable
14, 18	Thermoset	One in each test	Three 3/c cables bundled together
16, 17	Thermoset	One in each test	One 9/c cable with 3-1/c external cables

A direct comparison can be made between Tests 4 and 6, involving thermoplastic cables, and Tests 3, 7, and 12, involving similar configurations of thermoset cables. Each of these five tests saw the failure of both the seven-conductor cable and all three of the single-conductor cables. With regard to the multiconductor cables, in four of the five cases, the initial mode of failure was internal conductor-to-conductor shorting. This nominally indicates a high probability of initial conductor-to-conductor failures for both materials, but provides little basis for distinction between materials.

With the single-conductor cables, there were a total of six failures for the thermoplastic cables and seven failures for the thermoset. In the case of the thermoplastic cables, half (three) of the initial failures involved cable-to-cable shorts and half (three) involved shorts to ground. For the thermoset cables, only one failure involved initial cable-to-cable shorts (in Test 3) and the other six failures were initial shorts to ground. These results indicate a potential bias toward shorts to ground for the thermoset materials as compared to the thermoplastic materials.

The SNL Letter Report ranked Insulation Composition as a 'Likely Weak' influence factor, especially in cases where the cables were of a common insulation type. For the internal failures of the multiconductor cables versus shorts to ground, this ranking appears to have been nominally borne out. However, based on the results obtained from the IR measurement system, it appears that the material type may be of more importance when the cable-to-cable shorting behavior is considered. Thermoset cables tended to short to ground more frequently than the thermoplastic cables.

7.2.1.2 Number of Conductors in a Multiconductor Cable

The types of multiconductor cables tested using the IR system included two five-conductor cables in Test 8; one seven-conductor cable in each of the Tests 2, 3, 4, 5, 6, 7, 10, and 12; one eight-conductor armored cable in Tests 1 and 13, and three three-conductor cables each in Tests 14 and 18. However, the configurations for the tests in which failures were observed are quite different, making an assessment of the conductor count effects difficult.

One of the two five-conductor cables tested did not fail. The other five-conductor cable was a cable in conduit, which may have impacted the results more than the conductor count. Similarly, of the three-conductor cables tested, one bundle exhibited no failures and the one that failed by shorting to ground was also routed in conduit. The eight-conductor cables were armored and did not show signs of IR failure during the two tests in which they were used. Hence, these results provide little or no insight into this influence factor as related to multiconductor cables.

One interesting, though perhaps expected, result appears when comparing the number and types of failures experienced by the external single-conductor cables to the failures of all the multiconductor cables. As noted in Sec-

tion 7.1, multiconductor cables showed a high likelihood of internal conductor-to-conductor failures, whereas single-conductor cables tended to favor shorts to ground over cable-to-cable shorts.

The number of conductors in a cable was ranked in the SNL Letter Report as "significant" on the basis that the conductors in a multiconductor cable would tend to short to each other more readily than short to ground. Based on the results of the IR measurement system obtained during these tests, when failures occurred, multiconductor cables tended to short internally more often than by other failure modes; however, there is not sufficient evidence to suggest that the probability of such failure modes happening depended on the specific number of conductors in a cable.

7.2.1.3 Armoring

The results of the IR tests indicate that the armored cable used in Test 1 did not fail. Although the IR system could only determine the change in total IR during Test 13, the data obtained strongly hint at a short-to-ground failure. Unfortunately, this assessment is based more on experience with the indications of cable failures from other tests than on direct evidence available from Test 13. Hence, given no failures, it is not possible to assess the impact of the armor on the mode of failure.

Armoring of cable was ranked as a significant influence factor in the SNL Letter Report. The IR results are inconclusive about this factor. The armored cables monitored by the IR measurement system during the tests did not fail or could not indicate the actual initial failure mode, so the preferred failure mode for this type of cable is uncertain.

7.2.2 Routing Factors

7.2.2.1 Cable Tray Types Versus Conduits

The SNL Letter Report ranked Raceway Type as a "likely significant" influence factor. One particular aspect of the question was the impact of a tray configuration versus a conduit configuration on the hot-short probability. The authors speculated that there were two competing effects that would likely influence the failure mode. One effect was the presence of a more prevalent ground plane in a metal conduit, as compared to the rungs of a cable tray, which might enhance the probability for shorts to ground. The second effect was the potential that the more uniform weight support provided for a cable in a conduit might promote internal shorting, as compared to a cable tray where the rungs of the tray impose periodic sharp loading points on the cables.

Five of the seven cable failure cases were observed for seven-conductor cables in cable trays (Tests 3, 4, 6, 7, and 12). All of the cable trays used during these tests had a standard ladder-back design. Conduit effects were investigated using the IR system during Tests 8 and 18. In these tests, the IR measurement system detected failures in a five-conductor cable and the bundle of three three-conductor cables placed in a length of conduit.

The IR test results for Test 8 show that the cable in the conduit shorted to ground first (a sporadic short to ground on two of the five conductors) rather than displaying conductor-to-conductor hot shorts as the initial failure mode. All of the conductors eventually shorted to ground as the fire test progressed. (Note that there were no external conductors bundled with the IR measurement cable in this test.) In Test 18, the IR data shows that all nine conductors in the cable bundle shorted to ground before interacting with another conductor. In contrast, four of five multiconductor cables routed in the cable tray were observed to initially fail by internal conductor-to-conductor shorts. The remaining multiconductor cable routed in a tray did, however, initially fail by shorting to ground.

The IR results obtained during the fire tests provide limited evidence relevant to the tray versus conduit question. Nominally, it would appear that the conduit does introduce a greater likelihood of shorts to ground as the initial failure mode of a multiconductor cable. However, the data are somewhat sparse.

7.2.2.2 Overall Raceway Fill

The IR results were inconclusive. Most tray tests were run with two rows of cable fill. One test, Test 8, contained three rows of cables but the IR cable was located in the top row, had no external cables bundled with it, and did not

fail in any case. The cable bundle in Test 12 was part of a single-row filled tray and experienced a short to ground failure. In Tests 3, 4, 6, and 7, the cable bundles were part of a two-row filled tray condition and all experienced internal conductor-to-conductor or, in the case of Test 6, cable-to-cable shorts first.

The SNL Letter Report ranked tray fill as a significant influence factor. The IR results indicate that tray fill is a significant factor, but this is based on a very limited variety of tray fill cases.

7.2.2.3 Raceway Orientation

Although Tests 10 and 17 consisted of cables installed in vertical trays, the results of these test cannot be compared directly to the results from tests conducted using horizontal trays because the IR system was set up for the un-grounded DC input operation in Test 10 and was unable to determine any specific failure mode in Test 17. Thus, this influence factor cannot be evaluated based on the results of these tests.

7.2.3 Fire Exposure Condition Factors

As previously mentioned, three of the influence factors in this category were intimately connected in the conduct of the industry's cable tests. Once an exposure mode was selected, both the flame intensity and the relative height of the cable tray above the floor were also determined. Plume exposures were only made at 145-kW heat release rates and with the tray elevated 1.8 m (6 ft) above the test cell floor. Hot gas layer exposures were used for heat release rates greater than or equal to 200 kW and the trays were located at 2.1 m (7 ft) above the floor for these cases.

7.2.3.1 Exposure Mode (flame impingement, thermal radiation, or convection)

Two primary exposure modes were exercised in the NEI tests; namely, plume and hot gas layer exposures. One test (Test 10) involved a vertical tray exposed to both the hot gas layer and radiant heating, but no failures were observed. None of the NEI tests involved direct flame exposures. Hence, insights relating to exposure mode are somewhat limited.

A comparison can be made between Tests 3, 4, and 12 (plume exposures) and Tests 6 and 7 (hot gas layer). The multiconductor cable showed that in four of the five tests, the initial failure modes involved conductor-to-conductor shorts. The failure mode experienced by the multiconductor cable in Test 12 was shorting to ground. For the single conductor cables, the plume exposure cases were nearly evenly split – three involved initial cable-to-cable faults and four involved conductor-to-ground shorts. For the two hot gas layer tests, only one cable-to-cable short occurred, compared to five conductor-to-ground faults. These results are rather sparse, especially given that the cable type also changed in these four tests. However, it appears that the more intense plume exposures nominally favored hot shorts in comparison to the slower hot gas layer exposures.

The SNL Letter Report characterized Exposure Mode as a "likely significant" influence factor in their circuit analysis report. From the IR results obtained during the industry tests, only two modes of exposure were assessed, and even then the results were rather sparse. Overall, it appears that exposure mode between plume and hot gas layer exposures is present but relatively weak as an influence factor. Direct flame impingement was not evaluated.

7.2.3.2 Exposure Intensity and Duration

The exposure intensity and duration clearly had an impact on the overall likelihood that some failure would be observed. For example, no cable failures were identified during Test 2 at the 70-kW heat release rate. However, the tests are inconclusive regarding fire intensity and exposure duration as influence factors associated with failure mode. There is simply not enough variety in this parameter, and the variety that is provided is inextricably linked with other influence factors (e.g., cable type, plume versus hot gas layer, tray orientation, etc.).

Flame Intensity was ranked in the SNL Letter Report as "likely significant." The relative significance of this factor cannot be clearly discerned from the IR results obtained during the industry tests.

8. REFERENCES

8.1 J. LaChance, S. Nowlen, F. Wyant, V. Dandini, "Circuit Analysis—Failure Mode and Likelihood Analysis," A Letter Report to the NRC, Sandia National Laboratories, May 8, 2000. This letter report is available through the NRC Public Document Room under a NRC cover memorandum from T. L. King, NRC/RES/DRAA to G. M. Halogen, NRC/NRR/DSSA and M.E. Mayfield, NRC/RES/DET, dated June 13, 2000.

8.2 S. Nowlen, "Ampacity Derating and Cable Functionality for Raceway Fire Barriers," SAND2000-1825, NUREG/CR-6681, Sandia National Laboratories, August 2000.

USNRC Internal Distribution:

Name		Mail Stop	
C.	Antonescu	T-10L1	
S.	Bahadur	T-2E26	
P.	Baranowski	T-9C4	
R.	Barrett	O-10H4	
R.	Bernhard	Region II	
S.	Burgess	Region III	
J.	Calvert	T-10L1	
M.	Cheok	O-10H4	
N.	Chokshi	T-10E10	
E.	Cobey	O-7H6	
E.	Connell	O-11A11	
M.	Cunningham	T-10E50	
M.	Dey	T-10E50	(5 copies)
M.	Drouin	T-10E50	
T.	Eaton	O-11A11	
F.	Eltawila	T-10E32	
M.	Fields	O-7E1	
J.	Flack	T-10F13A	
E.	Hackett	T-10E10	
J.	Hannon	O-11A11	
G.	Holahan	0-10A1	
J.	Houghton	T-9C4	
J.S.	Hyslop	T-10E50	
R.	Jenkins	O-9D5	
K.	Kennedy	Region IV	
E.	Leeds	T-8A33	
J.	Linville	Region I	
C.	Lui	T-8A23	
D.	Matthews	O-12E5	
M.	Mayfield	T-10D20	
S.	Mays	T-9C4	
S.	Newberry	T-10E50	
P.	O'Reilly	T-9B3	
M.	Parker	Region III	
G.	Parry	O-10A1	
T.	Pruett	Region IV	
P.	Qualls	O-11A11	
W.	Rogers	Region II	
J.	Rosenthal	T-10K8	
A.	Rubin	T-10E50	
M.	Salley	O-11A11	
J.	Singh	T-10E50	
N.	Siu	T-10E50	
N.	Stablein	T-7J8	
S.	Steele	T-8A33	
A.	Thadani	T-10F12	
J.	Trapp	Region I	
M.	Virgilio	T-8A23	
J.	Vora	T-10E10	
M.	Weber	T-8A33	
E.	Weiss	O-11A11	
L.	Whitney	O-11A11	
P.	Wilson	O-10H4	
S.	Wong	O-10H4	
H.	Woods	T-10E50	(20 copies)
R.	Zimmerman	T-10F12	

External Distribution (U.S.):

Amir Afzali
Scientech Inc.
11140 Rockville Pike, Suite 500
Rockville, MD 20852

Ali Azarm
Brookhaven National Laboratory
P.O. Box 5000
Upton, NY 11973

Vytenis Babrauskas
Fire Science and Technology Inc.
9000 300th Place SE
Issaquah WA 98027-8832

Dr. Craig Beyler
Technical Director
Hughes Associates, Inc.
Suite 902
2730 University Boulevard West
Wheaton, MD 20902

Dennis C. Bley
Buttonwood Consulting, Inc.
11738 English Mill Ct.
Oakton, VA 22124-2253

Doug Brandies
Duke Energy
Mail Code EC09H
PO Box 1006
Charlotte, NC 28201-1006

Robert J. Budnitz
Future Resources Associates, Inc.
2039 Shattuck Ave., Suite 402
Berkeley, CA 94704

Charles E. Burke
PP&L, Inc.
Susquehanna Steam Electric Station
P.O. Box 467 (NUCSA2)
Berwick, PA 18603-0467

Francis T. Cann
Fire Protection Program Manager
PO Box 63
Lycoming, NY 13093

Douglas Carpenter
Combustion Science & Engineering
Suite B1
9160 Rumsey Road
Columbia, MD 21045-1997

David J. Conti
North Atlantic Energy Service Corp.
P.O. Box 300
Seabrook, NH 03874

Louis E. Eichelberger III
Perry Nuclear Power Plant
10 Center Road
Perry, Ohio 44081

D. M. Eissenberg
Oak Ridge National Laboratory
PO Box 2009
Oak Ridge, TN 37831-8059

Fred Emerson
Nuclear Energy Institute
Suite 400
1776 I Street, NW
Washington, DC 20006-3708

Jeff Ertman
Duane Arnold Energy Center
3313 DAEC Road
Palo, IA 52324-9646

Daniel Funk
EDAN Engineering Corp.
Suite 830
900 Washington St.
Vancouver, WA 98660

Anthony Hamins
NIST
Mail Stop 8653
100 Bureau Drive
Gaithersburg, MD 20899-8653

William Gross Handler, Chief
Fire Research Division NIST
Building 224, Stop 8660
Gaithersburg, MD 20899-8660

Vincent S. Ho
PLG Inc.
4590 MacArthur Blvd., Ste. 400
Newport Beach, CA 92660-2027

A. B. Johnson
Battelle - PNL
MS P8-10
PO Box 999
Richland, WA 99352

David Johnson
PLG Co.
4590 MacArthur Blvd., Suite 400
Newport Beach, CA 92660-2027

Walter Jones
NIST
Mail Stop 8653
100 Bureau Drive
Gaithersburg, MD 20899-8653

Robert Kalantari
Engineering Planning and Management, Inc.
20 Speen St.
Framingham, MA 01701

Robert Kasawara
Electric Power Research Institute
PO Box 10412
Palo Alto, CA 94303

Dr. Mardy Kazarians
Kazarians and Associates
Suite 545
425 East Colorado St.
Glendale, CA 91205

Elizabeth Kleinsorg
The Kleinsorg Group
526 Maple Street
Aptos, CA 95003

John Lambright
Lambright Technical Assoc., Inc.
9009 Lagrima de Oro NE
Albuquerque, NM 87111

James C. Lin
ABS Consulting
300 Commerce Dr., Suite 200
Irvine, CA 92602

Wee Tee Loh
ABS Consulting / EQE International
300, Commerce Drive Suite 200
Irvine, CA 92602-1300

Christopher E. Marrion
Arup Fire
155 Avenue of the Americas
New York, NY 10013

Dave McAfee
Fire Protection Program Manager
Harris Nuclear Plant
Carolina Power and Light
PO Box 165
New Hill, NC 27562-5904

Kevin McGrattan
NIST
Mail Stop 8653
100 Bureau Drive
Gaithersburg, MD 20899-8653

Andrew Minister
PNNL
902 Battelle Boulevard
Richland, WA 99352

M. Modarres
Materials and Nuclear Engineering
Rm. 2100E, Marie Mount Hall
College Park, MD 20742-2115

Ali Mosleh
Materials & Nuclear Engineering
Rm.2100AH, Marie Mount Hall.
University of Maryland
College Park, Maryland 20742-2115

Frederick Mowrer
Room 0151, Engineering Classroom Bld.
Dept. of Fire Protection Engineering
University of Maryland
College Park, MD 20742-3031

Bijan Najafi
Data Systems & Solutions, LLC
4920 El Camino Real
Los Altos, CA 94022

Cliff Naylor
WS Atkins
Suite 263-E Expo Mart
105 Mall Boulevard
Monroeville, PA 15146

Jeff Newman
Factory Mutual Research Corp.
1151 Boston-Providence Turnpike
Norwood, MA 02062

Hossein P. Nourbakhsh, Pres.
Energy and Environmental Science,
25 East Loop Road
Stony Brook, New York, 11790-3350

James R. Perry
Fire Protection System Engineer
10 Center Rd #A250
Perry, Ohio 44081

Deggary Priest
Omega Point Laboratories
16015 Shady Falls Rd.
Elmendorf, TX 78063

Andrew Ratchford
Ratchford Diversified Services
908 Camino Ricardo
Moraga, CA 94556

Ronald D. Rispoli
ANO1 Entergy Operations, Inc.
1488 S.R. 333
Russellville, AR 72801

Marty Sattison
INEEL
P.O. Box 1625
Idaho Falls, ID 83415

George Stramback
GE Nuclear Energy
175 Curtner Ave., M/C 747
San Jose, CA 95125

Ken Sullivan
Bld. 750
Brookhaven National Laboratory
PO Box 5000
Upton, NY 11973-5000

Woody Walker
Entergy Operations, Inc.
Arkansas Nuclear One
1448 S.R. 333
Russellville, AR 72801

Robert Youngblood
Scientech, Inc. Suite 500
11140 Rockville Pike
Rockville, MD 20852

Professor Robert G. Zalosh
Fire Protection Engineering
Worcester Polytechnic Inst.
100 Institute Rd.
Worcester, MA 01609-2280

External Distribution (Foreign):

Petra Andersson
SP - Swedish National Testing and
Research Institute
Brinellgatan 4, Box 857
S-501 15 Borås
Sweden

Dr. Remy Bertrand
IPSN CEA B.P. 6
92265 Fontenay-Aux-Roses CEDEX
France

Jouni Björkman
Research Scientist
Kivimiehentie 4, Espoo
P.O. Box 1803
FIN-02044 VTT
Finland

David Charters
Arup Fire Ove Arup & Partners
Admiral House Rose Wharf
78 East Street Leeds, London
ENGLAND

Geoff Cox
Fire Research Station
Building Research Establishment
Garston, Watford
Hertfordshire WD2 7JR
UK

Mamoru Fukuda
INS/NPEC
Fujita Kanko Bld, 7F 17-3
3-Chome Toranomon Minato-Ku
Tokyo 105
JAPAN

Bernard Gautier
Electricité de France
6 Quai Watier
78401 Chatou CEDEX
France

Fredrik Jörud
Nuclear Power Technology
SYCON Energikonsult
S-205 09 Malmö
SWEDEN

Maurice Kaercher
EdF - SEPTEN
12-14 Avenue Dutriévoz
69628 Vileurbanne CEDEX
FRANCE

Barry Kaufer
Nuclear Safety Div.
OECD Nuclear Energy Agency
Le Seine Saint Germain - Bât. B
12, boulevard des Iles
92130 Issy-les-Moulineaux
FRANCE

Dr. Tsu-Mu Kao
INER.ROCAEC
1000 Wenhua Road
Chiaan Village, Lungtan Taoyuan
Taiwan, 325
REPUBLIC OF CHINA

Olavi Keski-Rahkonen
VTT Technical Research Centre of Finland
Fire Technology Laboratory
PO Box 109 (Kivimiehentie 4)
SF-02151 Espoo
Finland

Matti Lehto
Fortum Engineering Ltd.
PO Box 10
00048 FORTUM
Finland

Henry C.W. Leung
Atomic Energy of Canada Limited
2251 Speakman Dr.
Mississauga, Ontario
Canada, L5K 1B2

Jouko Marttila
Nuclear Reactor Regulation
STUK
PO Box 14, FIN-00881
Helsinki
FINLAND

Takeshi Matsuoka
Ship Research Institute
Ministry of Transportation
6-38-1 Shinkawa
Mitaka Tokyo 181
JAPAN

Samuel Netanel, Pres.
S. Netanel Engineers Consultants
12, Hahoma St.
Rishon Le Zion 75655
ISRAEL

Toni Quant
16th Floor
Ontario Hydro
700 University Ave.
Toronto, Ontario
Canada, M5G1X6

Peter Rew
WS Atkins Fire
Woodcote Grove Ashley Rd.
Epsom Surrey KT18 5BW
England

Dr. Marina Röwekamp
Operational Behavior Division
GRS
Schwernergasse 1
D-50667 Köln
Germany

Jean-Marc Such
IPSN - CEA Cadarache
13108 Saint Paul lez Durance CEDEX
France

Osami Sugawa
Center for Fire Science and Tech.
Science University of Tokyo
2641 Yamasaki
NODA-SHI, 278
Japan

Hiroko Tezuka
International Atomic Energy Agency
Wagramer Strasse 5
PO Box 100
A-1400 Vienna
Austria

Tsuyoshi Uchida
Institute of Nuclear Safety
NUPEC
Fujita Kanko Toranomon Bld. 7F
17-1, 3-Chome Toranomon
Minato-Ku, Tokyo 105
Japan

Reino Virolainen
STUK
P.O. Box 14
FIN-00881 Helsinki
FINLAND

NRC FORM 335
(2-89)
NRCM 1102,
3201, 3202

U.S. NUCLEAR REGULATORY COMMISSION

BIBLIOGRAPHIC DATA SHEET

(See instructions on the reverse)

1. REPORT NUMBER
(Assigned by NRC, Add Vol., Supp.. Rev., and Addendum Numbers, if any)
NUREG/CR-SAND2002-0447P

2. TITLE AND SUBTITLE

Cable Insulation Resistance Measurements Made During Cable Fire Tests

3. DATE REPORT PUBLISHED

MONTH	YEAR

4. FIN OR GRANT NUMBER

Y6037

5. AUTHOR(S)

Francis J. Wyant
Steven P. Nowlen

6. TYPE OF REPORT

Technical

7. PERIOD COVERED *(inclusive Dates)*

8. PERFORMING ORGANIZATION – NAME AND ADDRESS *(If NRC, provide Division, Office or Region, U.S. Nuclear Regulatory Commission, and mailing address; if contractor, provide name and mailing address.)*

Sandia National Laboratories
P.O. Box 5800
Albuquerque, NM 87185-0744

9. SPONSORING ORGANIZATION – NAME AND ADDRESS *(If NRC, type "Same as above", if contractor, provide NRC Division, Office or Region, U.S. Nuclear Regulatory Commission, and mailing address.)*

Division of Risk Analysis and Applications
Office of Nuclear Regulatory Research
U.S. Nuclear Regulatory Commission
Washington, DC 20555-0001

10. SUPPLEMENTARY NOTES
H. W. Woods, NRC Project Manager

11. ABSTRACT *(200 words or less)*

An insulation resistance diagnostic system was recently developed and exercised during a series of cable fire tests. This insulation resistance measurement system was able to identify and quantify the changes in insulation resistance occurring between the separate conductors and the conductors to ground in cable bundles as they were being exposed to fires. Eighteen separate fire tests were conducted and included a variety of cable and fire exposure conditions. The insulation resistance measurement system was operated at 120 VAC for 14 of those test runs and at 100 VDC for three of the runs. One test was run with the insulation resistance measurement system providing 24 VDC to two separate instrument cables being exposed to the fire. The results obtained by the insulation resistance measurement system during these tests showed that cables will fail during a fire in one of three ways: by internal shorting of the conductors in a multiconductor cable, by shorting of the conductors in different cables bundled together, or by individual conductors shorting to ground. A mockup of a simple 4 to 20 mA DC current loop instrument circuit was included in six of the later tests.

12. KEY WORDS/DESCRIPTORS *(List words or phrases that will assist researchers in locating the report.)*

Electric Cables, Electrical Faults, Electrical Insulation, Electrical Testing, Failure Mode Analysis, Fires

13. AVAILABILITY STATEMENT
Unlimited

14. SECURITY CLASSIFICATION
(This Page)
Unclassified
(This Report)
Unclassified

15. NUMBER OF PAGES

16. PRICE